

# NAVAL POSTGRADUATE SCHOOL

## Monterey, California



## THESIS

### ANALYSIS OF DIGITAL COMMUNICATION SIGNALS AND EXTRACTION OF PARAMETERS

by

Anwar Al-Jowder

December 1994

Thesis Advisor:  
Thesis Co-Advisor:

Ralph Hippenstiel  
Donald V. Z. Wadsworth

Approved for public release, distribution is unlimited.

19950531 014

DTIC QUALITY INSPECTED

REPORT DOCUMENTATION PAGE			Form Approved OMB No. 0704-0188	
<small>Public reporting burden for this collection of information is estimated to average 1 hour per response, including the time for reviewing instructions, searching existing data sources, gathering and maintaining the data needed, and completing and reviewing the collection of information. Send comments regarding this burden estimate or any other aspect of this collection of information, including suggestions for reducing this burden, to Washington Headquarters Services, Directorate for Information Operations and Reports, 1215 Jefferson Davis Highway, Suite 1204, Arlington, VA 22202-4302, and to the Office of Management and Budget, Paperwork Reduction Project (0704-0188), Washington, DC 20503.</small>				
1. AGENCY USE ONLY (Leave blank)		2. REPORT DATE December 1994		3. REPORT TYPE AND DATES COVERED Master's Thesis
4. TITLE AND SUBTITLE ANALYSIS OF DIGITAL COMMUNICATION SIGNALS AND EXTRACTION OF PARAMETERS				5. FUNDING NUMBERS
6. AUTHOR(S) Al-Jowder, Anwar				
7. PERFORMING ORGANIZATION NAME(S) AND ADDRESS(ES) Naval Postgraduate School Monterey, CA 93943-5000				8. PERFORMING ORGANIZATION REPORT NUMBER
9. SPONSORING / MONITORING AGENCY NAME(S) AND ADDRESS(ES)				10. SPONSORING / MONITORING AGENCY REPORT NUMBER
11. SUPPLEMENTARY NOTES The views expressed in this thesis are those of the author and do not reflect the official policy or position of the Department of Defense or the United States Government.				
12a. DISTRIBUTION / AVAILABILITY STATEMENT Approved for public release; distribution unlimited.				12b. DISTRIBUTION CODE
13. ABSTRACT (Maximum 200 words) The signal classification performance of four types of Electronics Support Measure (ESM) Communications detection systems is compared from the standpoint of the unintended receiver (interceptor). Typical digital communication signals considered include Binary Phase Shift Keying (BPSK), Quadrature Phase Shift Keying (QPSK), Frequency Shift Keying (FSK), and On-Off Keying (OOK). The analysis emphasizes the use of available signal processing software. Detection methods compared include broadband energy detection, FFT-based narrowband energy detection, and two correlation methods which employ the Fast Fourier Transform (FFT). The correlation methods utilize modified time-frequency distributions, where one of these is based on the Wigner-Ville Distribution (WVD). Gaussian white noise is added to the signal to simulate various signal-to-noise ratios (SNRs).				
14. SUBJECT TERMS signal generation, energy detector, FFT detector, Fourier transform of lagged products, detection methods				15. NUMBER OF PAGES 123
				16. PRICE CODE
17. SECURITY CLASSIFICATION OF REPORT Unclassified	18. SECURITY CLASSIFICATION OF THIS PAGE Unclassified	19. SECURITY CLASSIFICATION OF ABSTRACT Unclassified	20. LIMITATION OF ABSTRACT UL	



Approved for public release; distribution is unlimited

# ANALYSIS OF DIGITAL COMMUNICATION SIGNALS AND EXTRACTION OF PARAMETERS

by

Anwar Al-Jowder  
Lieutenant Commander, Bahrain Navy  
B.S.E.E., Ned University of Engineering & Technology, 1980

Submitted in partial fulfillment of the  
requirements for the degree of

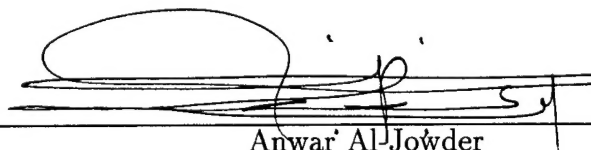
**MASTER OF SCIENCE IN ELECTRICAL ENGINEERING**

from the

**NAVAL POSTGRADUATE SCHOOL**

December 1994

Author:



Anwar Al-Jowder

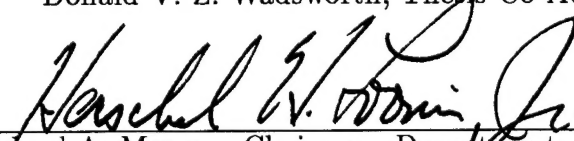
Approved by:



Ralph Hippenstiel, Thesis Advisor



Donald V. Z. Wadsworth, Thesis Co-Advisor



for Michael A. Morgan, Chairman, Department of Electrical  
and Computer Engineering





## ABSTRACT

The signal classification performance of four types of Electronics Support Measure (ESM) communications detection systems is compared from the standpoint of the unintended receiver (interceptor). Typical digital communication signals considered include Binary Phase Shift Keying (BPSK), Quadrature Phase Shift Keying (QPSK), Frequency Shift Keying (FSK), and On-Off Keying (OOK). The analysis emphasizes the use of available signal processing software. Detection methods compared include broadband energy detection, FFT-based narrowband energy detection, and two correlation methods which employ the Fast Fourier Transform (FFT). The correlation methods utilize modified time-frequency distributions, where one of these is based on the Wigner-Ville Distribution (WVD). Gaussian white noise is added to the signal to simulate various signal-to-noise ratios (SNRs).

Accession For	
NTIS (GAI)	<input checked="checked" type="checkbox"/>
NTIC <del>XXX</del>	<input type="checkbox"/>
Unannounced	<input type="checkbox"/>
Justification	
By	
Distribution/	
Availability Codes	
Dist	Avail and/or Special
A-1	



## TABLE OF CONTENTS

I.	INTRODUCTION . . . . .	1
II.	SIGNAL GENERATION . . . . .	5
	A. INTRODUCTION . . . . .	5
	B. SIGNAL GENERATION . . . . .	5
	1. Binary Phase Shift Keying (BPSK) . . . . .	5
	2. On-Off Keying (OOK) . . . . .	8
	3. Quadrature Phase Shift Keying (QPSK) . . . . .	8
	4. Frequency Shift Keying (FSK) . . . . .	8
III.	SIGNAL INTERCEPT DETECTION . . . . .	15
	A. INTRODUCTION . . . . .	15
	B. BROADBAND ENERGY DETECTOR . . . . .	16
	C. FAST FOURIER TRANSFORM (FFT) DETECTION . . . . .	16
	D. MODIFIED TIME-FREQUENCY DISTRIBUTION METHODS .	17
	1. Method-1 . . . . .	17
	2. Method-2 . . . . .	18
IV.	EXPERIMENTAL PERFORMANCE RESULTS . . . . .	21
	A. BASIC CONCEPTS . . . . .	21
	B. BROADBAND ENERGY DETECTION . . . . .	21
	C. FFT BASED DETECTION . . . . .	25
	1. BPSK . . . . .	27
	2. OOK . . . . .	31
	3. FSK . . . . .	37
	4. QPSK . . . . .	42
	D. TIME-FREQUENCY DISTRIBUTION METHODS . . . . .	42
	1. Method-1 . . . . .	42
	a. BPSK . . . . .	47
	b. OOK . . . . .	52
	c. FSK . . . . .	57
	d. QPSK . . . . .	57
	2. Method-2 . . . . .	63

a.	BPSK . . . . .	67
b.	OOK . . . . .	72
c.	FSK . . . . .	72
d.	QPSK . . . . .	78
V.	SUMMARY AND CONCLUSION . . . . .	87
	APPENDIX . . . . .	93
	LIST OF REFERENCES . . . . .	103
	INITIAL DISTRIBUTION LIST . . . . .	105

## LIST OF TABLES

1	Confusion Matrix . . . . .	89
2	Parameters Extracted from the Modulations after Identification . . . . .	90



## LIST OF FIGURES

1	Overall Schematic . . . . .	3
2	Modulating signal and BPSK signal . . . . .	6
3	BPSK signal: (a) 10-dB SNR; (b) 0-dB SNR . . . . .	7
4	Modulation signal and OOK signal . . . . .	9
5	OOK signal: (a) 10-dB SNR; (b) 0-dB SNR . . . . .	10
6	Modulation signal and QPSK signal . . . . .	11
7	QPSK signal: (a) 10-dB SNR; (b) 0-dB SNR . . . . .	12
8	Modulation signal and FSK signal . . . . .	13
9	FSK signal: (a) 10-dB SNR; (b) 0-dB SNR . . . . .	14
10	Output of energy detector for OOK, no noise. . . . .	23
11	Output of energy detector for OOK with 10-dB SNR. . . . .	24
12	Output of energy detector for OOK with 0-dB SNR. . . . .	26
13	Output of FFT detector for BPSK signal, no noise; 75% overlap . . .	28
14	Output of FFT detector for BPSK signal with 10-dB SNR; 75% overlap	29
15	Output of FFT detector for BPSK signal, 0-dB SNR; 75% overlap . .	30
16	Averaged output of FFT detector for BPSK signal at all SNR levels .	32
17	Output of FFT detector for OOK signal, no noise; 75% overlap . . .	33
18	Output of FFT detector for OOK signal, 10-dB SNR; 75% overlap . .	34
19	Output of FFT detector for OOK signal, 0-dB SNR; 75% overlap . .	35
20	Averaged output of FFT detector for OOK signal at all SNR levels .	36
21	Output of FFT detector for FSK signal, no noise; 75% overlap . . .	38
22	Output of FFT detector for FSK signal, 10-dB SNR; 75% overlap . .	39
23	Output of FFT detector for FSK signal, 0-dB SNR; 75% overlap . . .	40
24	Averaged output of FFT detector for FSK signal at all SNR levels . . . . .	41
25	Output of FFT detector for QPSK signal, no noise; 75% overlap . . .	43



26	Output of FFT detector for QPSK signal, 10-dB SNR; 75% overlap .	44
27	Output of FFT detector for QPSK signal, 0-dB SNR; 75% overlap . .	45
28	Averaged output of FFT detector for QPSK signal at all SNR levels . . . . .	46
29	Output of Method-1 detector for BPSK signal, no noise . . . . .	48
30	Output of Method-1 detector for BPSK signal, 10-dB SNR . . . . .	49
31	Output of Method-1 detector for BPSK signal, 0-dB SNR . . . . .	50
32	Averaged output of Method-1 detector for BPSK signal at all SNR levels . . . . .	51
33	Output of Method-1 detector for OOK signal, no noise . . . . .	53
34	Output of Method-1 detector for OOK signal, 10-dB SNR . . . . .	54
35	Output of Method-1 detector for OOK signal, 0-dB SNR . . . . .	55
36	Averaged output of Method-1 detector for OOK signal at all SNR levels . . . . .	56
37	Output of Method-1 detector for FSK signal, no noise . . . . .	58
38	Output of Method-1 detector for FSK signal, 10-dB SNR . . . . .	59
39	Output of Method-1 detector for FSK signal, 0-dB SNR . . . . .	60
40	Averaged output of Method-1 detector for FSK signal at all SNR levels . . . . .	61
41	Output of Method-1 detector for QPSK signal, no noise . . . . .	62
42	Output of Method-1 detector for QPSK signal, 10-dB SNR . . . . .	64
43	Output of Method-1 detector for QPSK signal, 0-dB SNR . . . . .	65
44	Averaged output of Method-1 detector for QPSK signal at all SNR levels . . . . .	66
45	Output of Method-2 detector for BPSK signal, no noise . . . . .	68
46	Output of Method-2 detector for BPSK signal, 10-dB SNR . . . . .	69
47	Output of Method-2 detector for BPSK signal, 0-dB SNR . . . . .	70
48	Averaged output of Method-2 detector for BPSK signal at all SNR levels . . . . .	71
49	Output of Method-2 detector for OOK signal, no noise . . . . .	73
50	Output of Method-2 detector for OOK signal, 10-dB SNR . . . . .	74

51	Output of Method-2 detector for OOK signal, 0-dB SNR . . . . .	75
52	Averaged output of Method-2 detector for OOK signal at all SNR levels . . . . .	76
53	Output of Method-2 detector for FSK signal, no noise . . . . .	77
54	Output of Method-2 detector for FSK signal, 10-dB SNR . . . . .	79
55	Output of Method-2 detector for FSK signal, 0-dB SNR . . . . .	80
56	Averaged output of Method-2 detector for FSK signal at all SNR levels . . . . .	81
57	Output of Method-2 detector for QPSK signal, no noise . . . . .	82
58	Output of Method-2 detector for QPSK signal, 10-dB SNR . . . . .	83
59	Output of Method-2 detector for QPSK signal, 0-dB SNR . . . . .	84
60	Averaged output of Method-2 detector for QPSK signal at all SNR levels . . . . .	86
61	Method-2 block diagram . . . . .	89



## ACKNOWLEDGMENT

I wish to thank my thesis advisor Professor Ralph Hippenstiel and co-advisor Professor Donald V. Z. Wadsworth for their guidance, patience, and encouragement in this research. Also, thanks go to Mr. Jim Allen who typeset the entire work. Finally, thanks to my wife for her support and patience.



# I. INTRODUCTION

Communication signal detection and interception is an important aspect of modern Command and Control Warfare (C2W). Detection and interception techniques extract signal features such as the carrier frequency, bit rate, type of modulation, and chip rate in the case of spread spectrum signals [1, 2].

The detection problem for the unintended interceptor or receiver is more difficult than that for the intended receiver, since the interceptor may not know the carrier frequency, the type of modulation, or the message bit transition instants. The work done in this thesis provides some basic ideas on extracting unknown signal parameters or features such as modulation type, bandwidth, bit rate, and carrier frequency.

Four types of detectors are implemented: the broadband energy detector with adjustable integration time, the FFT-based detector with adjustable integration time, and two types of correlation detectors based on a modified time-frequency distribution method. The latter two are denoted as method-1, which is related to the Fourier transform of lagged products (over lag  $m$ ), and method-2 which is based on the Fourier transform of lagged products (over time  $n$ ).

These four signal detectors are compared with respect to their ability to distinguish among four types of modulations (BPSK, QPSK, FSK, OOK). The overall schematic for the systems is shown in Figure 1.

Chapter II presents the signal generation and the underlying assumptions. Chapter III describes the detectors. Chapter IV presents experiments of the detection methods for each modulation type as a function of SNR. The performance of the four detectors is summarized and recommendations for future studies are discussed in Chapter V. The MATLAB programs used for this study are listed in the Appendix.

Interception of spread spectrum signals is not included in this thesis which is limited to detectors for signals with positive SNR. The intercept problem is particularly difficult for spread spectrum signals which typically have negative SNRs. In this case techniques such as “prefilter delay and multiply” introduce nonlinear transformations which enable certain feature extractions [3].

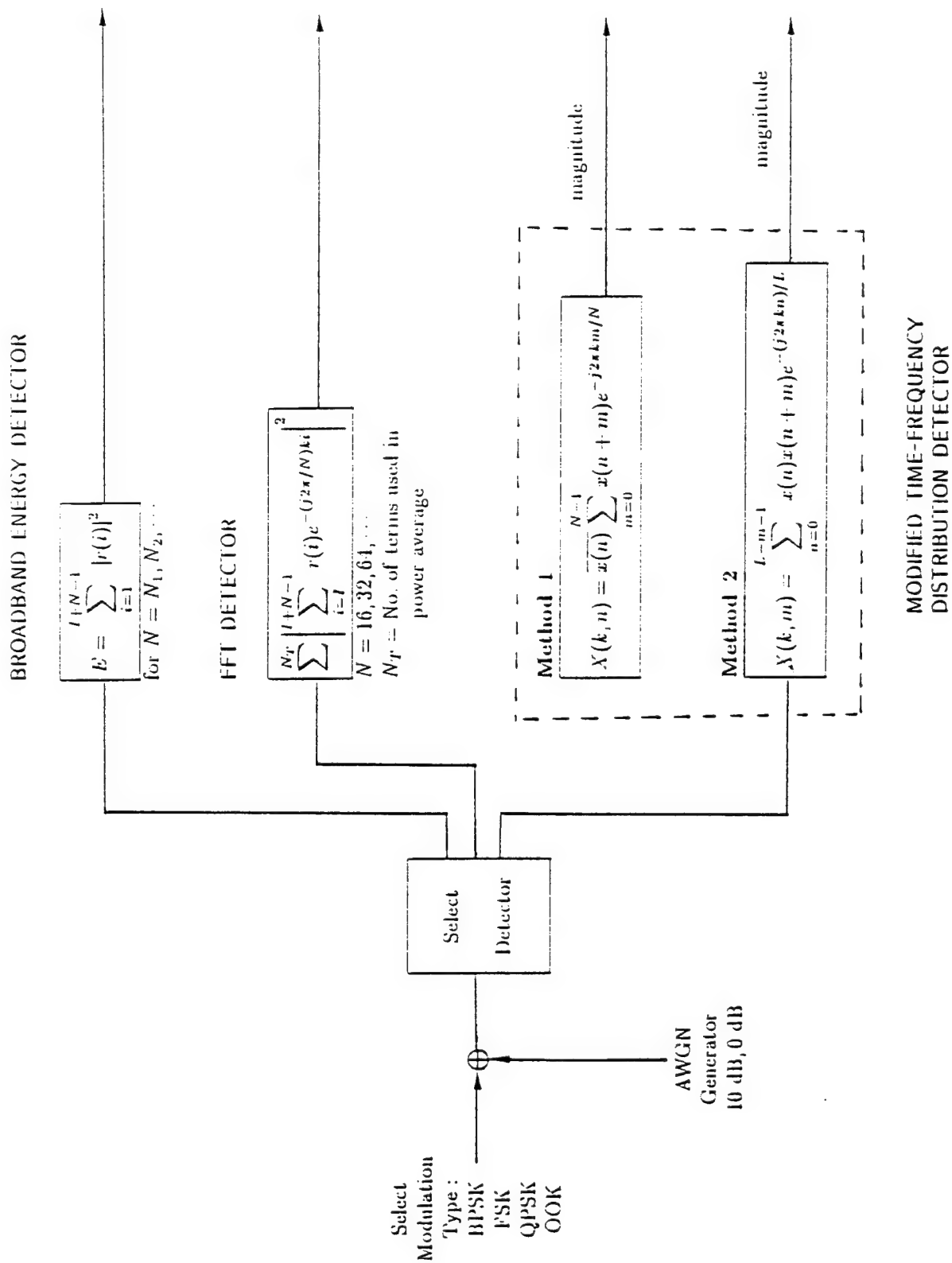


Figure 1: Overall schematic.





## II. SIGNAL GENERATION

### A. INTRODUCTION

In digital communications systems, various types of modulation techniques are employed to transmit information. Some of the more common forms of modulation are amplitude modulation (AM), frequency modulation (FM), and phase modulation (PM). In AM, FM, or PM, the amplitude, frequency, or phase, respectively, is varied by the modulating signal [4].

### B. SIGNAL GENERATION

Four types of binary modulation schemes (BPSK, OOK, FSK, QPSK) are used in the work addressed by this thesis. All messages have the same sine wave carrier and a peak amplitude of one. A common 16-bit information sequence is input to each modulator, resulting in four carrier cycles per bit. There are four sampling points per cycle, resulting in a “message” length of 256 points. These parameters remain constant throughout the simulations. To allow simulation of corrupted data, Gaussian noise is added to create 10-decibel (dB) and 0-dB SNRs.

#### 1. Binary Phase Shift Keying (BPSK)

This signal is a common example of phase modulation, where the phase of the carrier is shifted 180 degrees relative to the quiescent carrier phase during the zero of the modulating signal. In Figure 2 the binary values of +1 and 0 are represented by +1 and -1, respectively. Figure 2 shows the modulating signal and resulting BPSK signal while Figure 3a shows the BPSK signal at an SNR of 10-dB. Note that it is difficult to estimate the type of modulation. Figure 3b shows the BPSK signal at an SNR of 0-dB. Note that it is impossible to separate the signal from the noise .

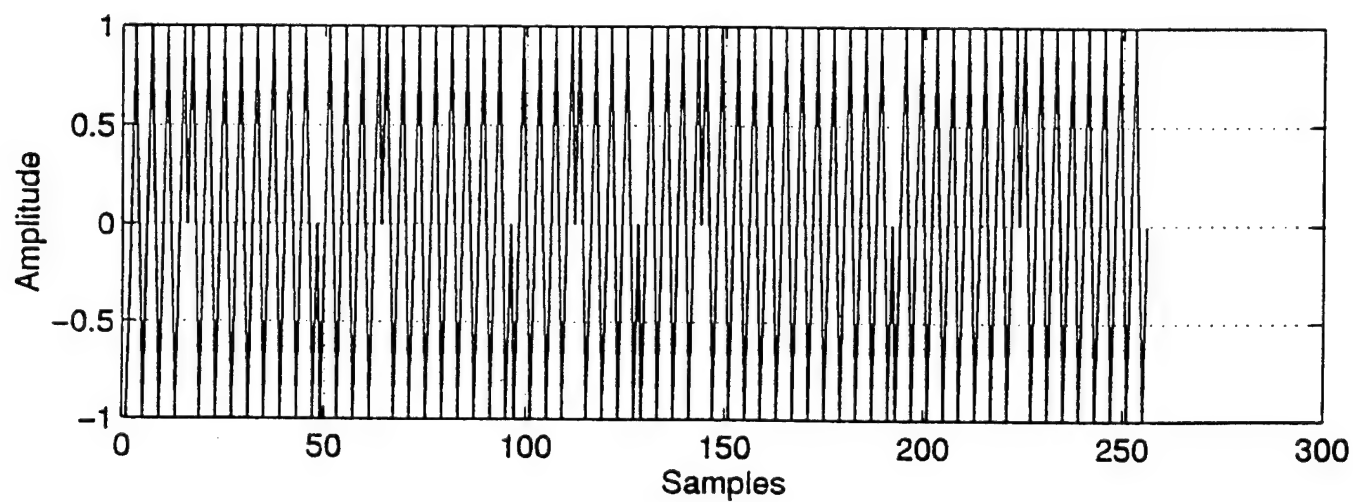
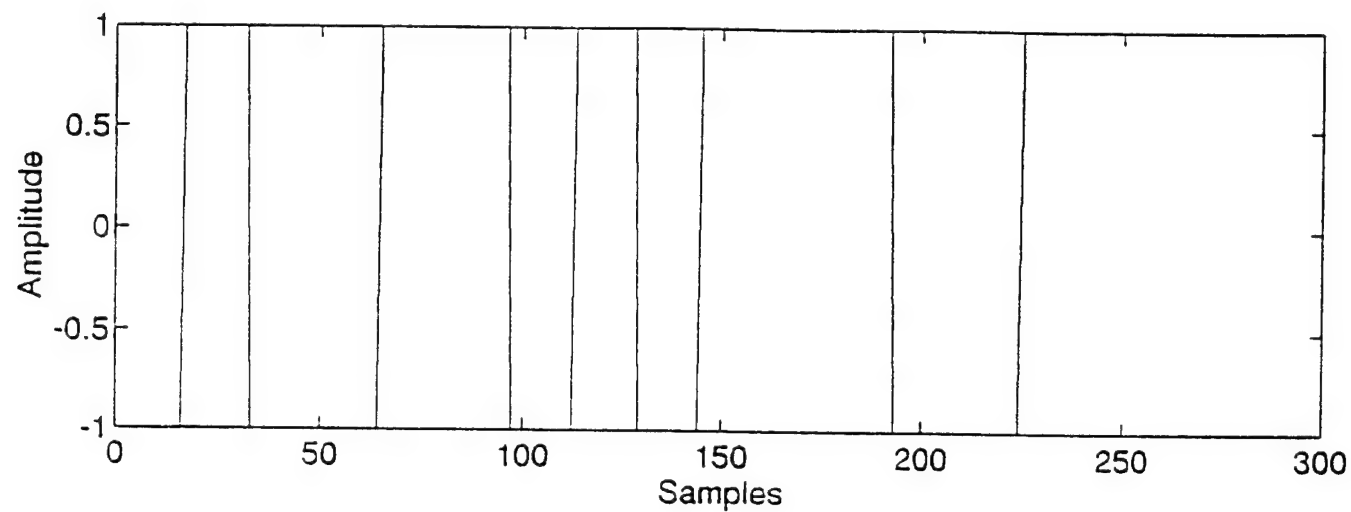
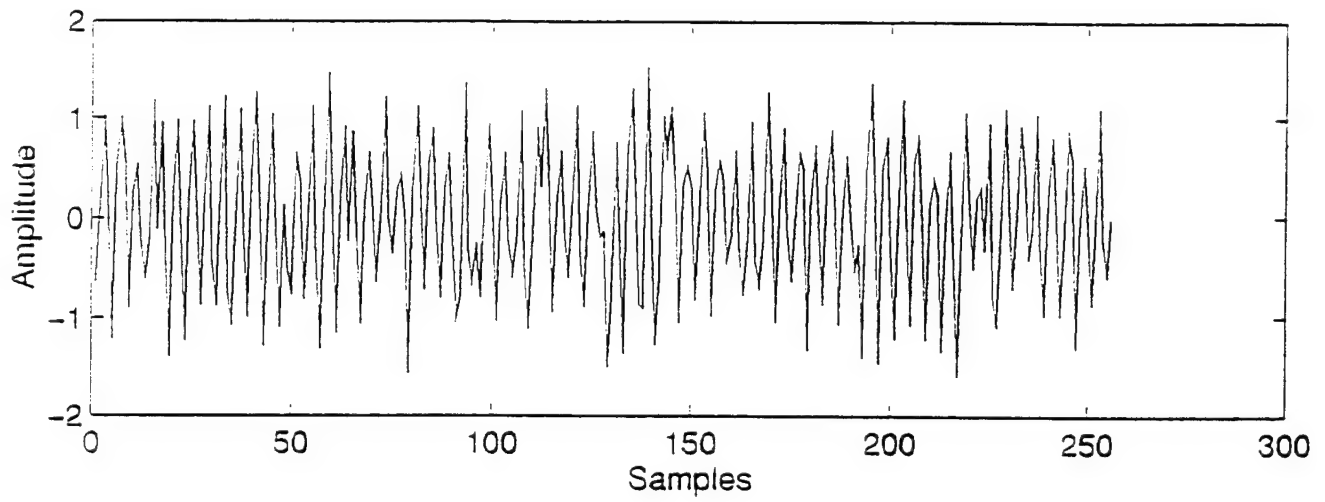
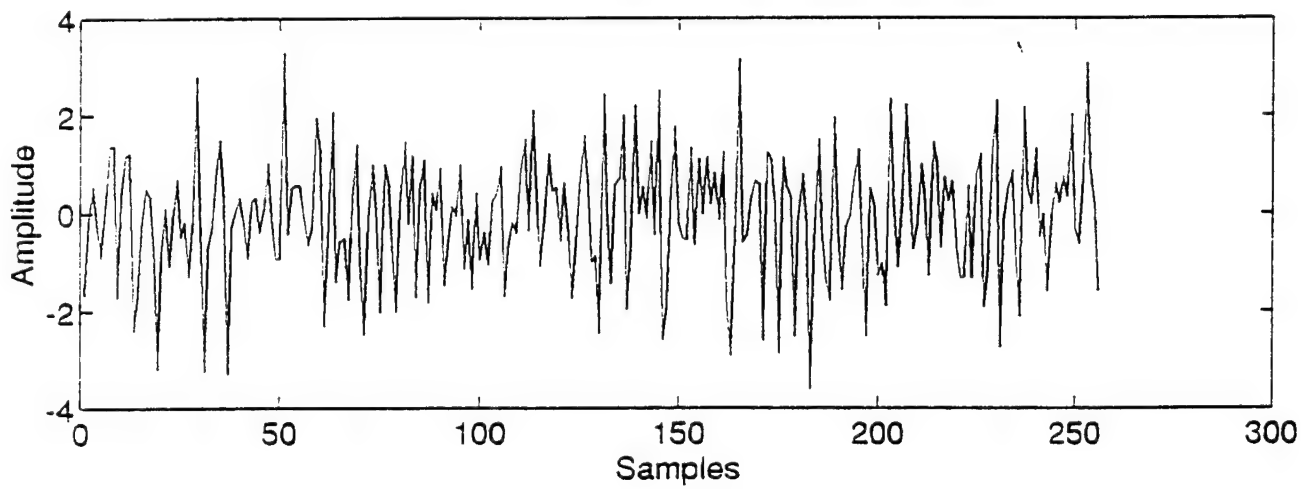


**Figure 2:** Modulating signal and BPSK signal.



(a)



(b)

Figure 3: BPSK signal: (a) 10-dB SNR; (b) 0-dB SNR.

## **2. On-Off Keying (OOK)**

This type of modulation technique is also called amplitude shift keying (ASK). It consists of keying (switching) a carrier sinusoid ON and OFF with a unipolar binary signal. It is identical to unipolar binary amplitude modulation resulting in a Double Sideband-Suppressed Carrier (DSB-SC) signal. Figure 4 shows the modulating signal and the resulting OOK signal, while Figure 5a shows the OOK signal at an SNR of 10-dB. In this figure the features of OOK modulation can be recognized. In contrast, as shown in Figure 5b, at 0-dB SNR, it is difficult to differentiate between the signal and noise.

## **3. Quadrature Phase Shift Keying (QPSK)**

This signal can be considered as two BPSK signals occupying the same channel, in a quadrature arrangement. The QPSK signals are created by 90 degrees relative phase shifts, as shown in Figure 6. The QPSK signal at an SNR of 10-dB is shown in Figure 7a. The signal can be recognized. Figure 7b shows the QPSK signal at an SNR of 0-dB, which does not allow differentiation of the signal from the noise.

## **4. Frequency Shift Keying (FSK)**

In this case, the frequency of a carrier will shift from a mark frequency (corresponding to a binary 1) to a space frequency (corresponding to a binary 0) according to the baseband modulation signal. This is illustrated in Figure 8, which shows the modulation signal and the resulting FSK signal. In the experiments, the difference between the mark frequency and space frequency is one carrier cycle per bit (i.e., the mark frequency is equal to 5 cycles and the space frequency is equal to 4 cycles per bit). The FSK signal at an SNR of 10-dB, shown in Figure 9a, can still be recognized. Figure 9b shows the FSK at an SNR of 0-dB, which does not allow differentiation of the signal from the noise.

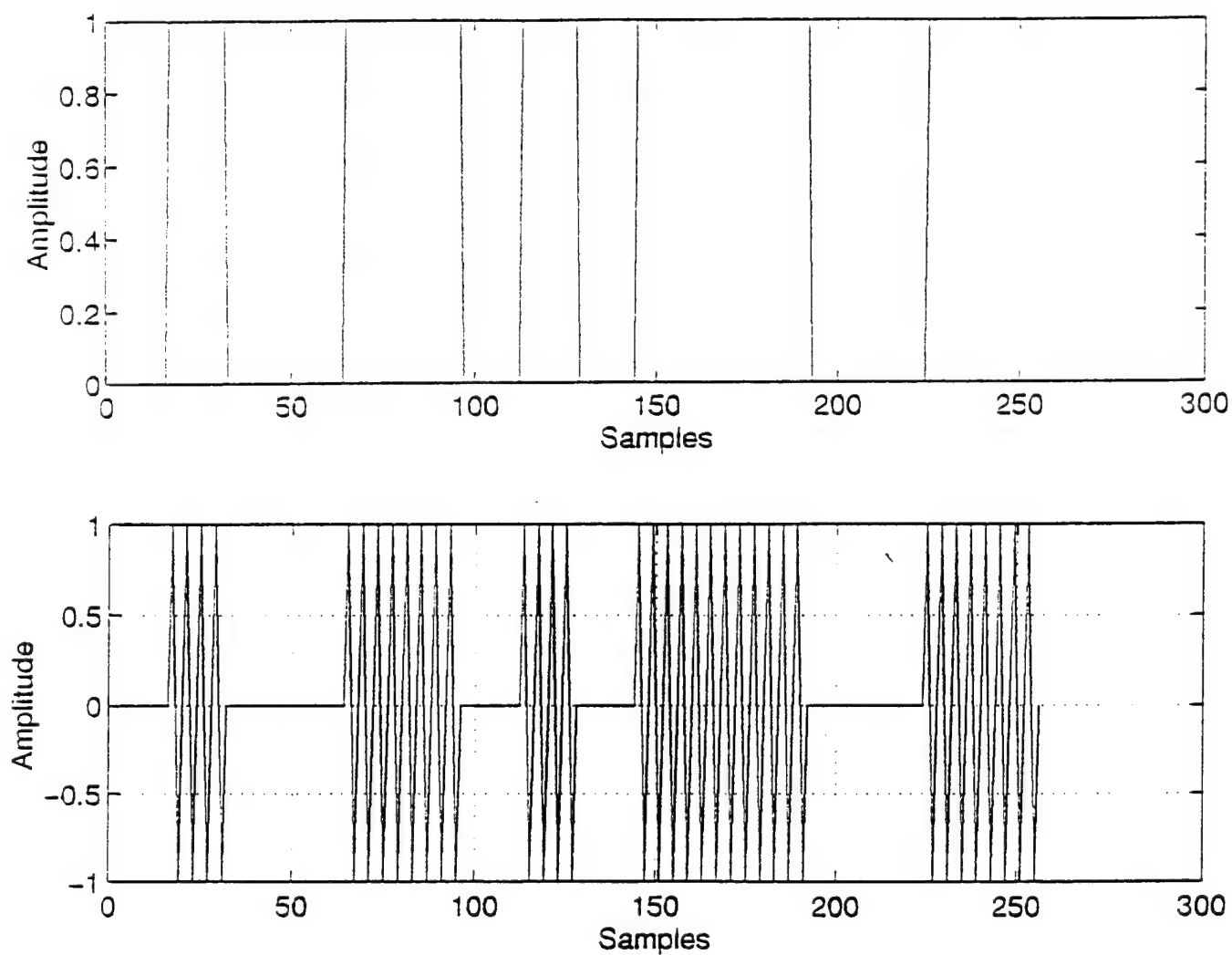
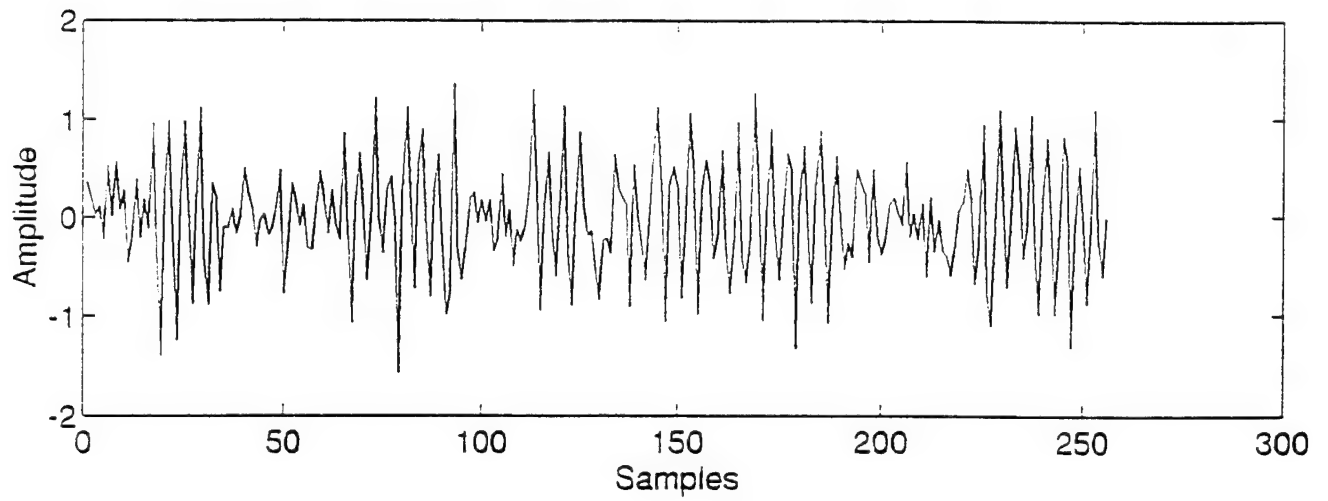
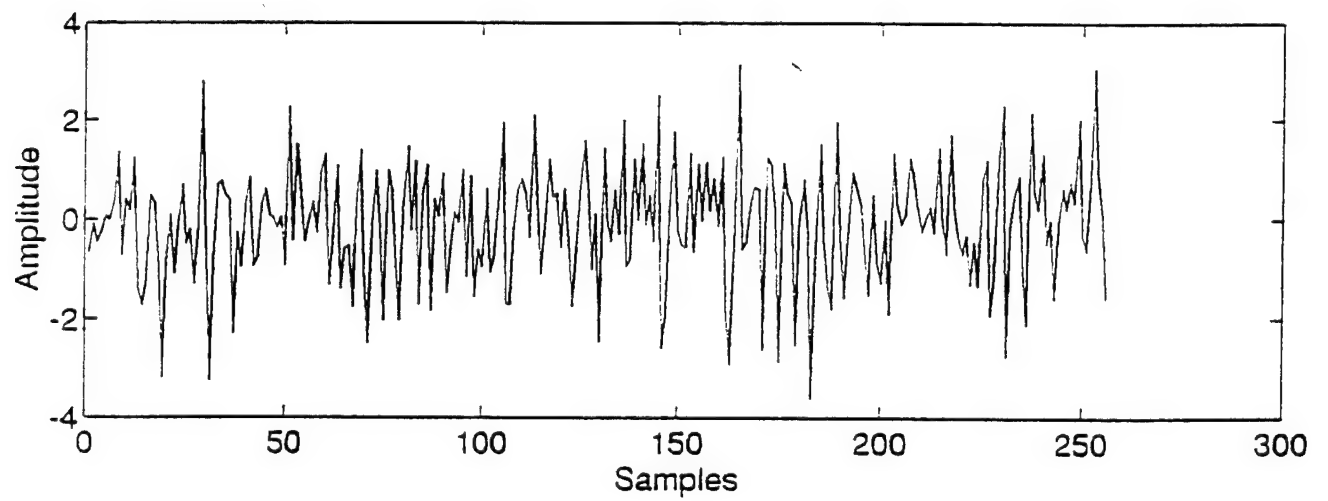


Figure 4: Modulation signal and OOK signal.



(a)



(b)

**Figure 5:** OOK signal: (a) 10-dB SNR; (b) 0-dB SNR.

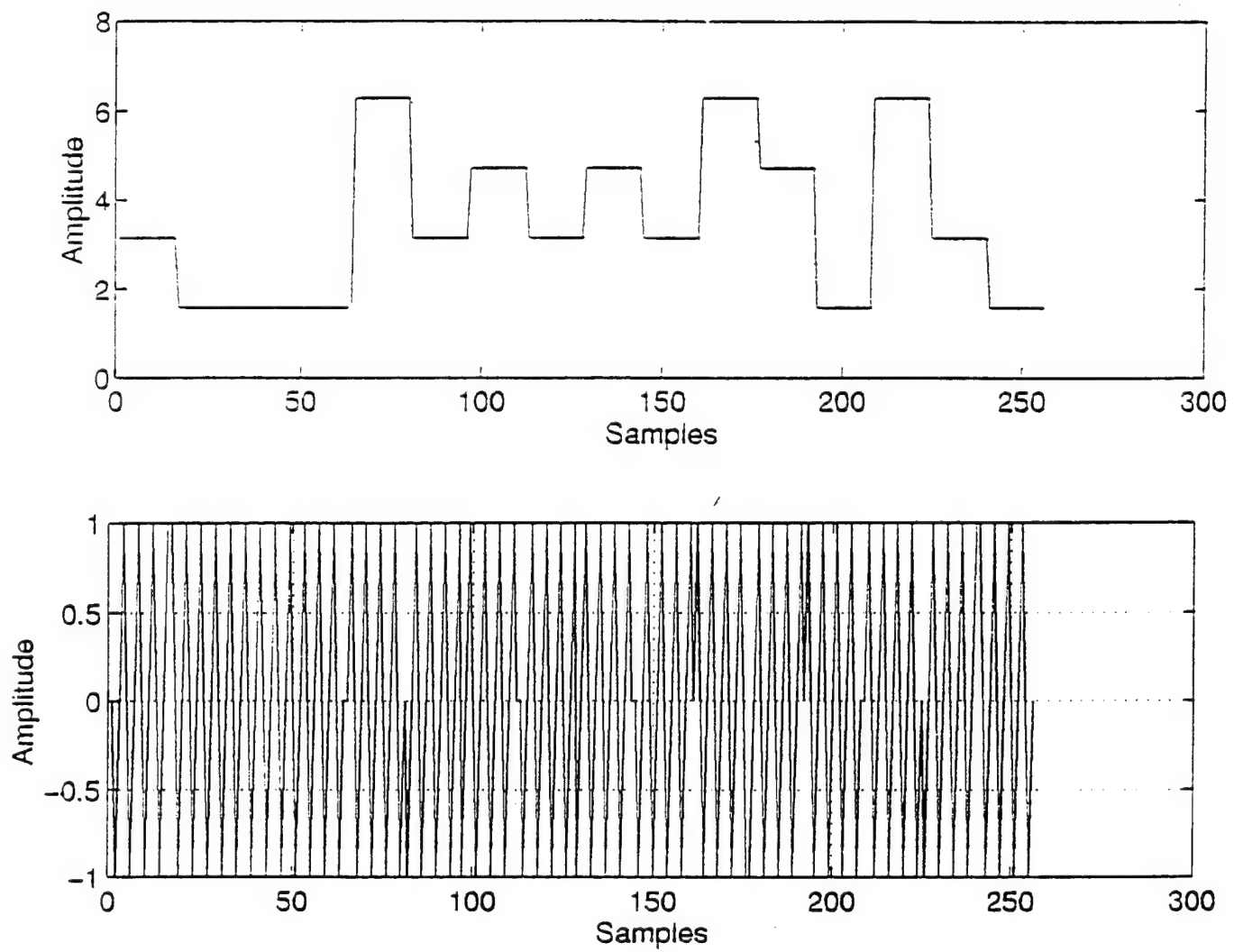
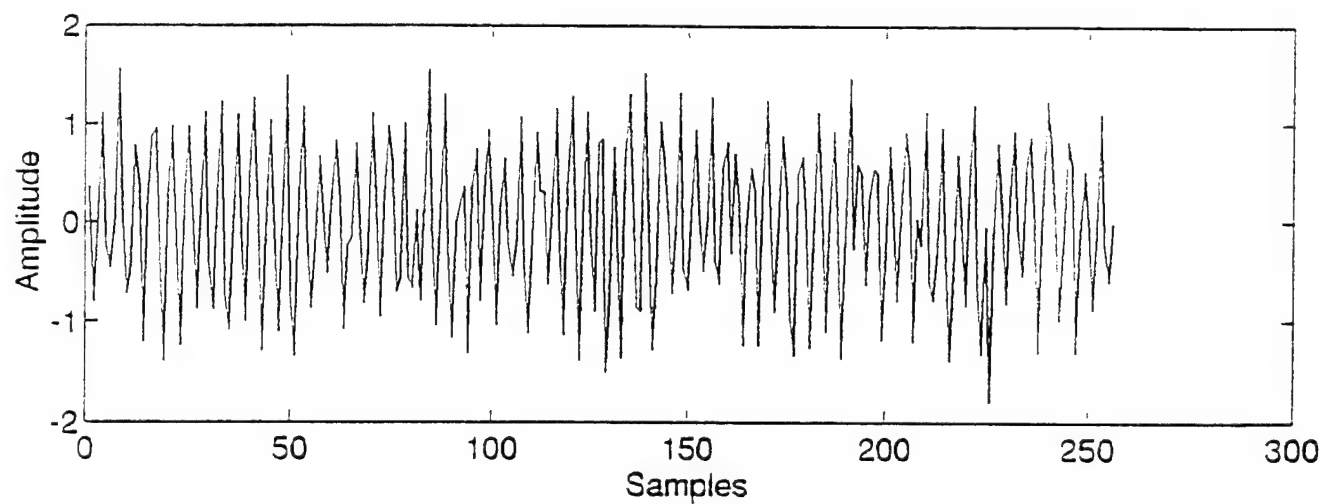
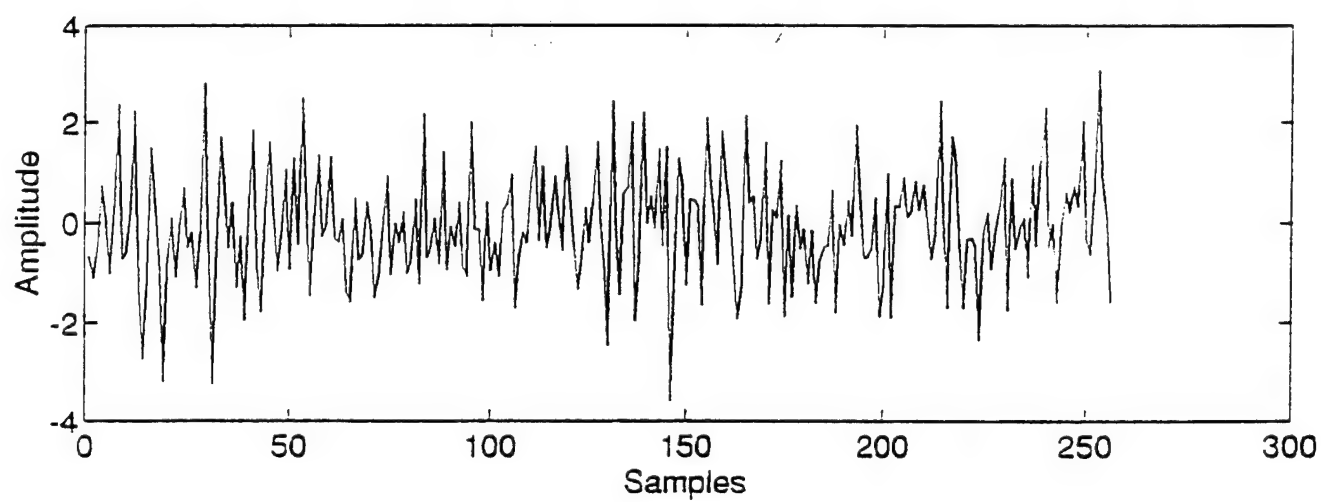


Figure 6: Modulation signal and QPSK signal.





(a)



(b)

**Figure 7:** QPSK signal: (a) 10-dB SNR; (b) 0-dB SNR.

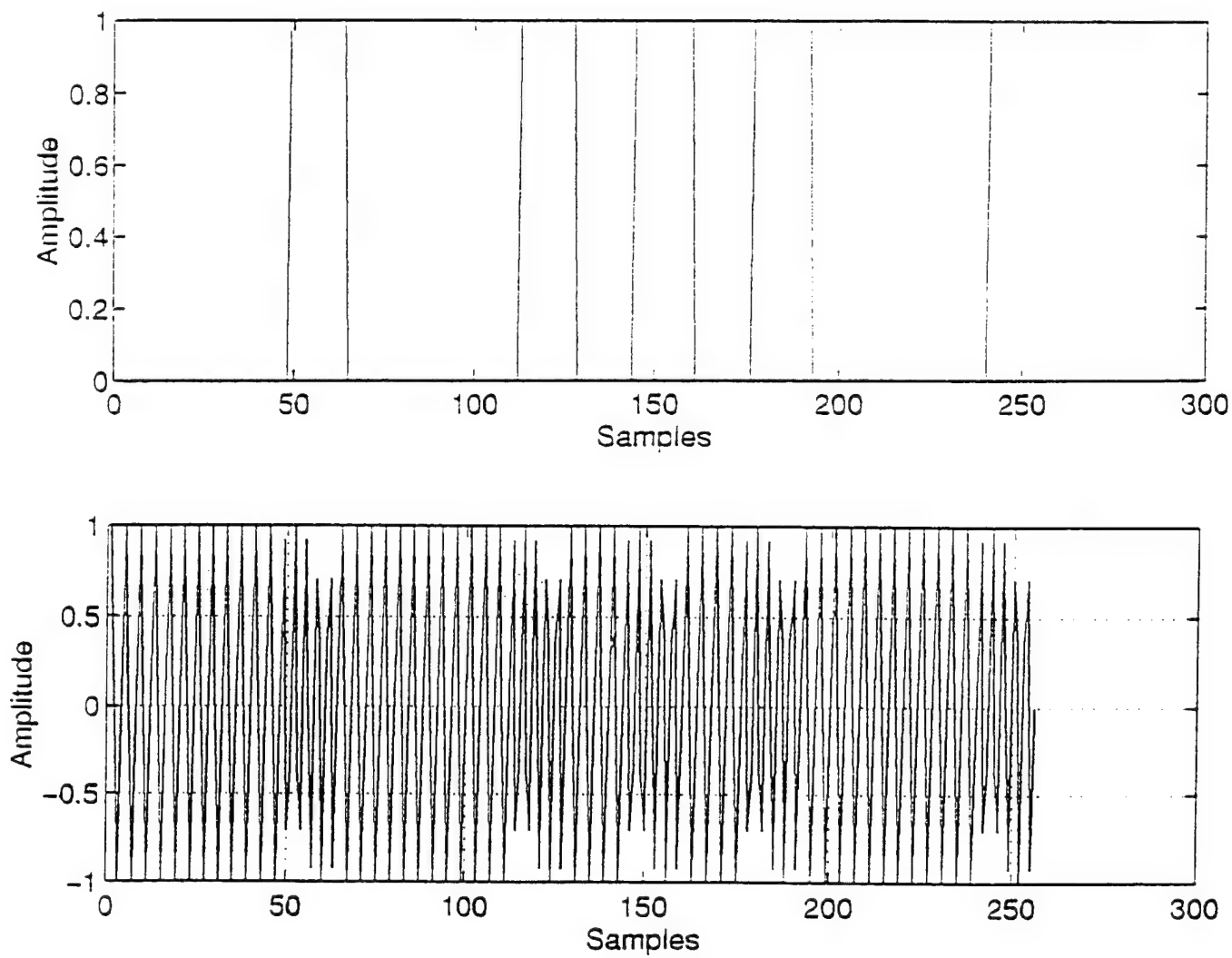
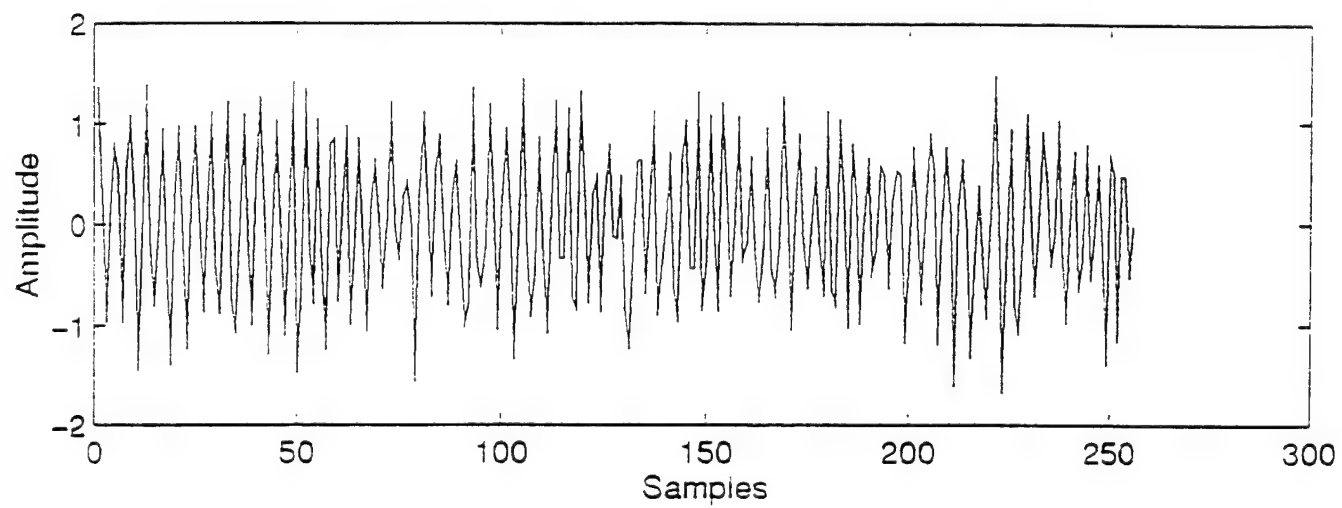
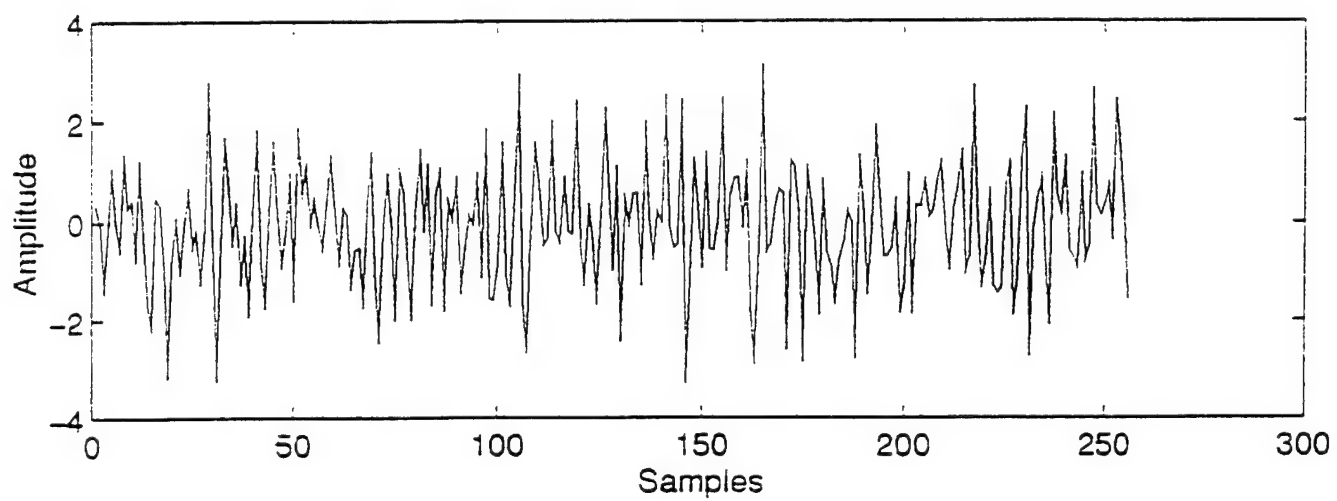


**Figure 8:** Modulation signal and FSK signal.



(a)



(b)

Figure 9: FSK signal: (a) 10-dB SNR; (b) 0-dB SNR.

### III. SIGNAL INTERCEPT DETECTION

#### A. INTRODUCTION

In the detection of signals, especially LPI (low probability of intercept) signals, the ease of detection and the methods used vary greatly, depending upon whether the receiver is the *intended* or *unintended* receiver. For the purpose of this thesis, the *intended* receiver is the person or system that receives the signal from a cooperative transmitter and has full access to the frequency and code information required for detection and recovery of the message. The *unintended* receiver, on the other hand, does not have access to the frequency and code information and is attempting to detect the presence of the signal and/or recover the message contained in the data [5].

The traditional method of signal intercept detection employed by an *unintended* receiver is the radiometer (integration of energy) detector which requires a positive SNR. In recent years this has been extended to intercept spread spectrum signals with negative SNR [3]. Negative SNR requires a long observation time and accurate estimation of the threshold set by the noise above. Only positive SNR detection is considered in this work. Four types of detectors are described in the following section: energy, FFT, method-1, and method-2. The broadband energy detector is intended to be a benchmark for comparison with the other detectors and is used for OOK only. The FFT detector is more effective than the energy detector. Methods 1 and 2 are based on time-frequency distribution. One of these methods is related to the WVD. The various detectors are illustrated in Figure 1.

## B. BROADBAND ENERGY DETECTOR

The interceptor employs the radiometer or traditional energy detector to determine the presence of a signal which may have an unknown bit rate or start time. The energy detector integrates the signal energy for a finite length of time as described by

$$E = \sum_{i=I}^{I+N-1} |r(i)|^2, \quad (1)$$

where  $E$  is the energy and  $r(i)$  is the received signal at time  $i$ . The summation is over  $N$  points, where  $N$  is the segment length, and  $I$  is the starting point. If the total energy, received over a given integration length  $N$ , is greater than some threshold value which is a function of ambient noise, then a “detection” occurs. The threshold depends on the acceptable false alarm rate and on the probability of detection. When the noise is non-stationary or strong interference signals (ISs) are present, frequently the case in practice, this method is ineffective [4, 7, 8].

The energy detector described above is used on the OOK signal modulation type. Some detection examples are shown in Chapter IV as a function of integration length  $N$ , start time  $I$ , and SNR.

## C. FAST FOURIER TRANSFORM (FFT) DETECTION

The Fast Fourier Transform (FFT) algorithm is used in the analysis of finite duration sequences. In this thesis, an attempt is made to use the FFT to extract parameters such as modulation type, bit rate, transition time, band width, etc., from the intercepted signals [7]. This method is more efficient than broadband energy detection. The FFT parameters are selected by the user to enhance the signal frequency components by using a range of likely integration times. This method is equivalent to a parallel bank of noncoherent correlation detectors in which the detection decision is based on comparing the detector outputs to the threshold. This is similar to the method used to noncoherently detect and demodulate M-ary Frequency Shift Keying

(MFSK) [2, 4, 8, 9]. The algorithm used for calculating the detector energy output level  $E(k)$  at each frequency bin  $k$  is

$$E(k) = \sum_{i=I}^{N_T} \left| \sum_{i=I}^{I+N-1} r(i) e^{-j2\pi ki/N} \right|^2, \quad (2)$$

where  $i$  is the time index,  $E(k)$  is the total output energy in the time interval and frequency interval with index  $k$ ,  $r(i)$  is the received signal at time  $i$ ,  $I$  corresponds to the integration or observation start time,  $N_T$  is the number of terms used in the power average, and  $N$  is the coherent integration length. The FFT intervals (i.e.,  $(I, I + N)$ ) are either contiguous or overlapping.

#### D. MODIFIED TIME-FREQUENCY DISTRIBUTION METHODS

One remarkable fact regarding time-frequency distribution is that many derivations and approaches have been suggested. It is important to understand the ideas and arguments that have been given, as variations and insights into them will undoubtedly lead the way to further development. These approaches will not be presented in this work, but we will refer to them for further study [10].

Two types of time-frequency distributions are presented in this work, **method-1**, which is related to the Fourier transform of lagged products (over lag  $m$ ), and **method-2**, which is based on the Fourier transform of lagged products (over time  $n$ ). The output magnitude of each method is examined to evaluate its diagnostic potential in recognizing the modulation of the signal.

##### 1. Method-1

Method-1 uses

$$X(k, n) = \sum_{m=0}^{N-1} x(n) x(n + m) e^{-j2\pi km/N}, \quad (3)$$

where  $n$  is independent of delay time  $m$ . Eq. (3) is interpreted as

$$X(k, n) = \overline{x(n)} \sum_{m=0}^{N-1} x(n + m) e^{-j2\pi km/N}, \quad (4)$$

where  $k$  is the frequency index,  $n$  the time index,  $m$  the time delay, and  $N$  the number of samples during the observation period.  $\overline{x(n)}$  is the estimated value of the mean of  $x(n)$  simply given by

$$\overline{x(n)} = \frac{1}{N} \sum_{i=n}^{n+N-1} x(i). \quad (5)$$

## 2. Method-2

The following algorithm is used to differentiate between the modulated signals

$$X(k, m) = \sum_{n=0}^{L-m-1} x(n)x(n+m)e^{-j2\pi kn/L}, \quad (6)$$

where  $k$  is the frequency index,  $n$  the time index,  $m$  is the delay, and  $L$  the number of samples used during the observation period. Even though a spectrum can be computed for every  $m$  ( $m = 0, 1, \dots$ ), we choose to compute for computational efficiency, the spectra only at evenly spaced points. That is,  $m$  might be indexed to go from  $m_0$ , to  $m_0 + \text{step}$ , to  $m_0 + 2 \text{ step}$ , and so on. The resulting time-frequency surface will be computed much faster, yet not too much information is lost if the nonstationarity of the signal and the step size are compatible.

As mentioned earlier, this method is related to WVD, which is a three-dimensional (energy vs. time and frequency) representation of a signal that is particularly well-suited for analysis of non-stationary signals. It was first introduced by Eugene Wigner and then applied to signal analysis in 1948 by J. Ville.

The WVD is a transformation of a continuous time signal into the time-frequency domain. The auto WVD is defined as [6, 10]

$$WVD_{r,r}(t, \omega) = \int_{-\infty}^{\infty} e^{-j\omega\tau} \left(t + \frac{\tau}{2}\right) r^* \left(t - \frac{\tau}{2}\right) d\tau. \quad (7)$$

In terms of the transform variables, it is

$$WVD_{r,r}(t, \omega) = \int_{-\infty}^{\infty} e^{j\theta t} R \left(\omega + \frac{\theta}{2}\right) R^* \left(\omega - \frac{\theta}{2}\right) d\theta, \quad (8)$$

where

$r(t)$  = complex valued signal in time domain

$R(\omega)$  = complex valued signal in frequency domain

$t$  = time

$\omega$  = frequency

$*$  = complex conjugate

Since the concern in this work is to detect and extract parameters from signals, there are properties of WVD which should be kept in mind when interpreting the processing results [10]:

- (1) WVD always goes to zero at the beginning and the end of a finite-duration signal, sometimes called the support properties of WVD.
- (2) In general, the Wigner distribution is not zero when the signal is zero. This causes considerable difficulty in interpretation.
- (3) According to Cohen [10], "In general, the Wigner distribution has a noisy behavior, that is, if there is a noise in a small finite time of the signal, this noise will appear for all time."





## IV. EXPERIMENTAL PERFORMANCE RESULTS

### A. BASIC CONCEPTS

The energy detector is only tested using the OOK signal modulation. The other three detection methods are tested by comparing the detector's three-dimensional output display. The ability of a human to determine signal presence, modulation type, and other signal features from the displays provides useful insights for future design of automatic digital classification algorithms. The experiment is conducted as illustrated in Figure 1. At the left-hand side, the signals (BPSK, OOK, QPSK, FSK) are generated and saved in files for input to the various detectors that are to be compared. This assures a fixed input waveform as the detector parameters (e.g., FFT window size) are varied.

The broadband energy detector is implemented with the `ENERGY.m` program and the FFT detector with `SHIFT2.m`. The time-frequency distribution method-1 and method-2 are implemented with the `CORR1.m` and `CORR2.m` programs, respectively. In all plots the frequency axis is calibrated in FFT bin numbers.

### B. BROADBAND ENERGY DETECTION

As mentioned earlier, we restrict our broadband energy detection experiments to the OOK signal because the other modulation techniques have continuous time energy, while the OOK signal has an ON-OFF energy representation. This makes OOK message identification simple, especially at high SNR. Due to the time constraints, we did not compare the outputs with signal ON and signal OFF.

For analysis purposes, the output of the energy detector, with different noise levels, will be represented by two plot types. First, an overall plot, shown in Figure 10a, 11a, and 12a displays the detector output as a function of integration time

(samples) and time. The second plot in these figures shows the detector output for selected integration time lengths superimposed on each other. This will demonstrate the effect of the integration length on the detector output, as shown in Figures 10b, 11b, and 12b. For comparison purposes, the detector input signal is shown in Figures 10c, 11c, and 12c.

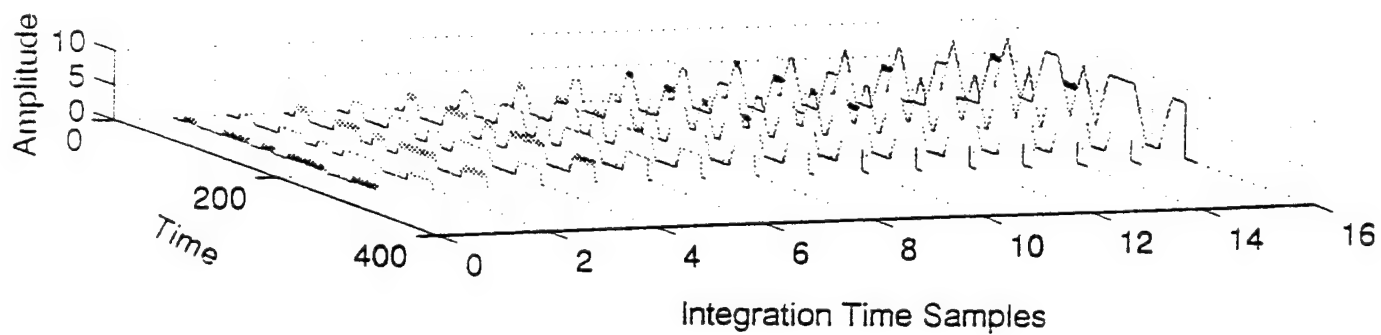
Figure 10a shows the energy detector output for the noise-free OOK signal. Note that the shorter the integration time, the steeper become the leading and the trailing edges of the output, approaching a rectangular shape. Distinct bits result in a triangular output shape when the integration time length is exactly equal to the bit length. To clarify this idea, four integration lengths are selected from Figure 10a and superimposed in Figure 10b.

Comparing Figures 10a and 10b, it is noted that the amplitude increases and the output starts earlier with increasing integration time. The amplitude increase is caused by summing more non-negative numbers as the integration time is increased.

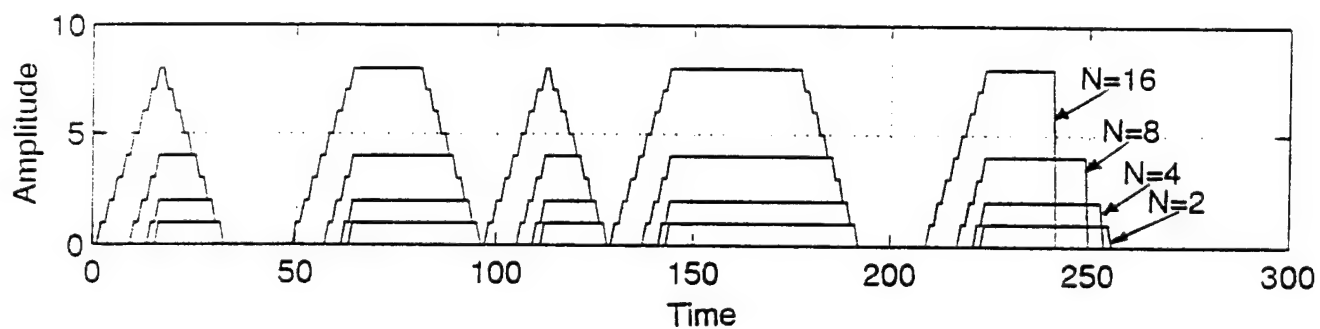
Comparing the input and the output of the energy detector, note that, for a short integration length, the output of the energy detector matches the amplitude modulated signal. Hence, under noise-free conditions, the pulse width and the bit rate can readily be estimated.

The output of the energy detector for an SNR of 10-dB as a function of different integration times is shown in Figure 11a. Note that it is difficult to detect or separate the signal from the noise at short integration lengths (integration lengths 1 through 4). Using more samples (i.e., longer integration time, say 6 through 16) makes the signal recognizable.

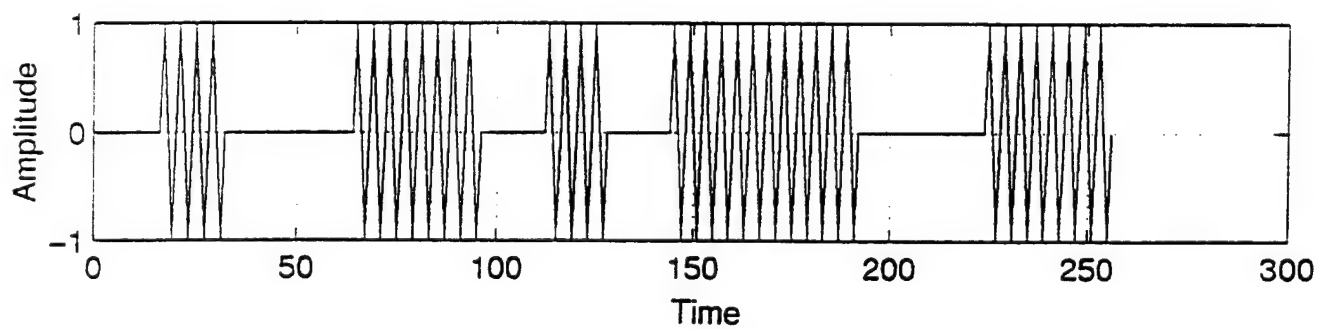
Some results for different integration times are shown in Figure 11b. Note that at lengths 8 and 16, the modulation signal can be recognized. In contrast, when using 2 or 4 samples, the signal cannot be detected.



(a)

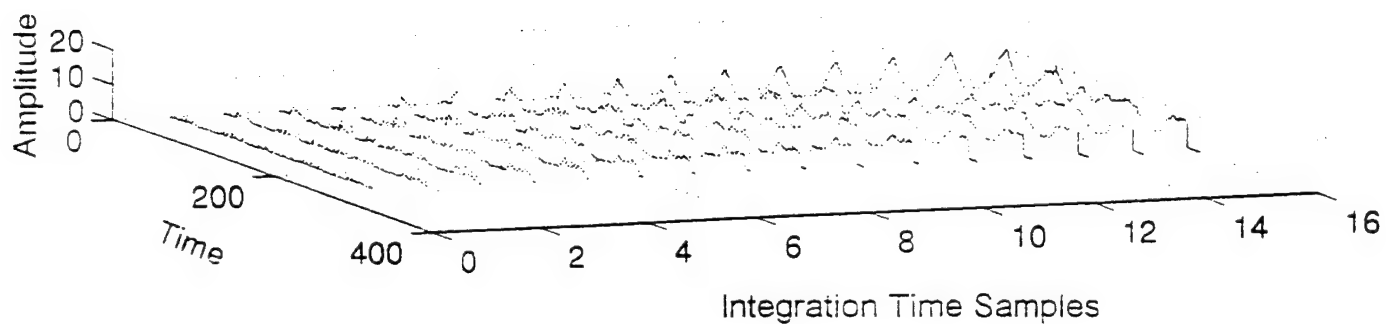


(b)

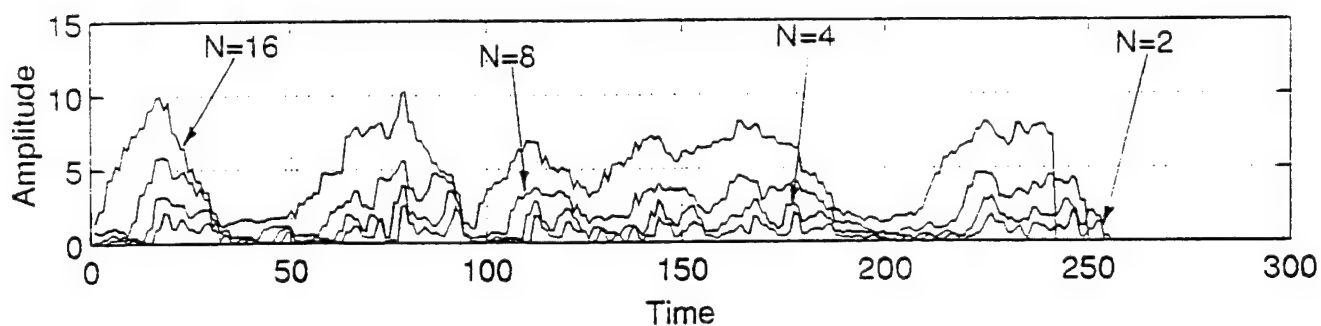


(c)

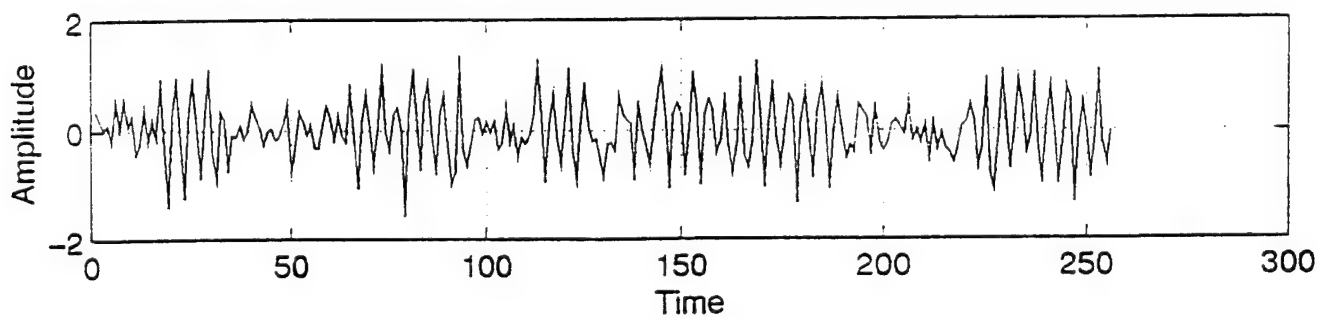
Figure 10: Output of energy detector for OOK, no noise.



(a)



(b)



(c)

**Figure 11:** Output of energy detector for OOK with 10-dB SNR.

As shown in Figures 12a and 12b, the energy detector output will have a very high level of energy, which causes the signal to be completely lost, as the level of the noise is further increased (i.e., 0-dB).

Figure 12c shows the input signal for comparison purposes. It is clear from this that the broadband energy detector can be used as a pulse-width detector at SNR levels greater or equal to 10-dB.

### C. FFT BASED DETECTION

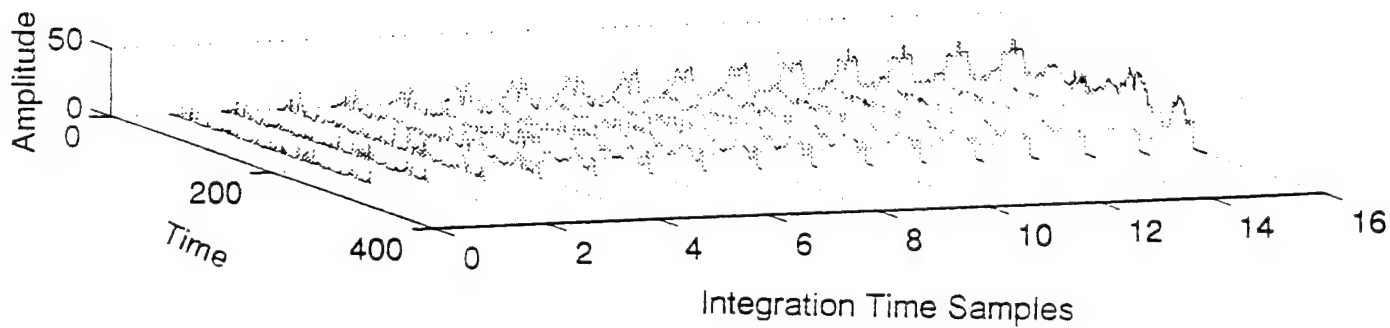
BPSK, OOK, QPSK, and FSK signals are applied to the FFT detector to detect and identify message features such as the modulation type, carrier frequency, frequency shift (if appropriate), and bit rate.

All FFT detector simulations use an integration length of 16. This length is chosen to determine which message parameters can be extracted if the FFT size equals the number of samples per message bit.

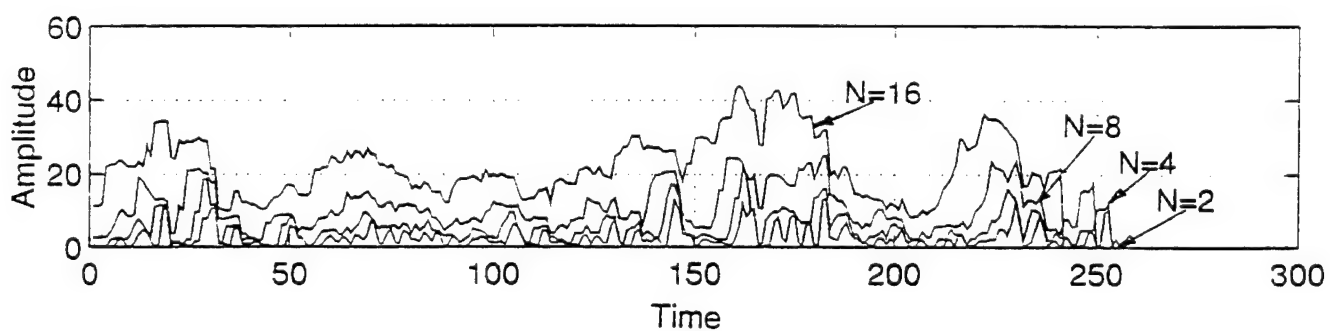
The user has the option to select an arbitrary overlap factor. A 75% overlap factor is chosen, hence a new segment will start every four points. The purpose of using an overlap is to enhance the signal frequency components along the time axis to extract more parameter information from the signal, which might be lost when using a window.

Adding noise to the message gives us a basic idea as to whether the signal can be identified in the presence of noise. The SNR selection is limited to two values, 10-dB and 0-dB. All messages are of the same length, and have the same number of points per cycle, number of cycles per bit, and number of bits per message length.

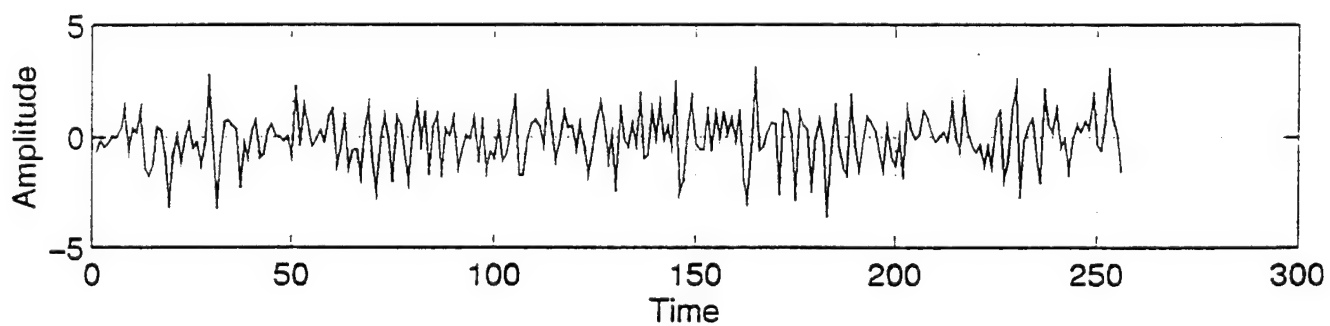
The output of the FFT detector for the modulated signals is presented in three types of plots. The three-dimensional plot of the 'a' part of Figures 13 through 15, 17 through 19, 21 through 23, and 25 through 27 represents the spectrogram of the



(a)



(b)



(c)

Figure 12: Output energy detector for OOK with 0-dB SNR.

signals. The 'b' parts of these figures are the corresponding contour plots. Figures 16, 20, 24, and 28 consist of six subplots. The first column shows the output averaged over time and the second column shows the output averaged over frequency for different levels of SNR. The time axis (samples or delay) is scaled by a factor of 4 relative to the original time series. It represents the shift of four points between the signal segments (i.e., 75% overlap at a transform length of 16).

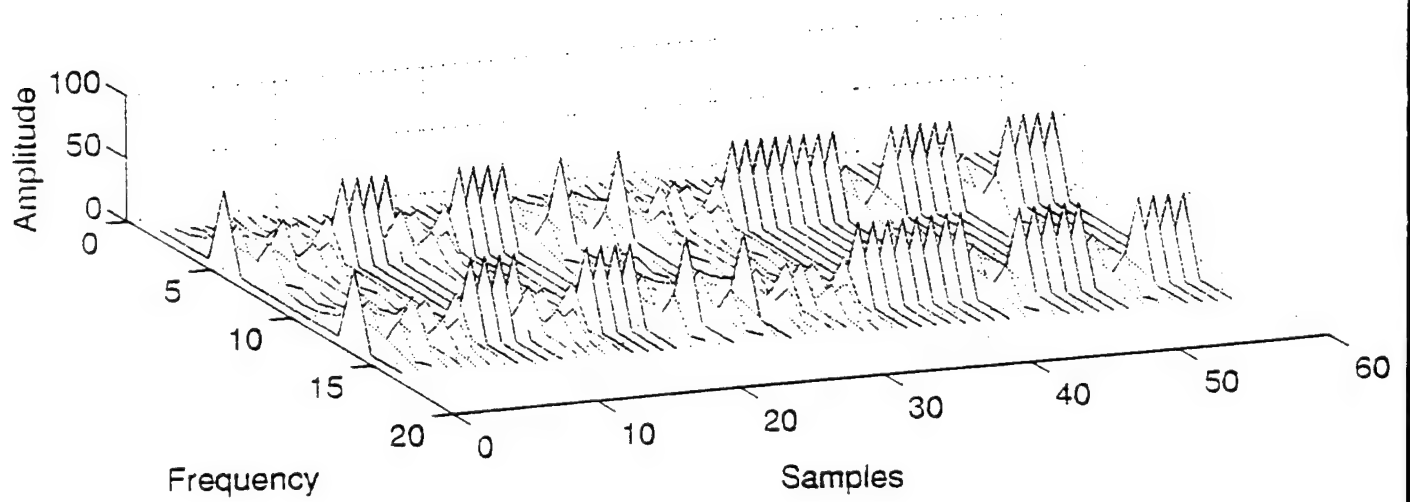
## 1. BPSK

The output of the detector driven by a noise-free BPSK signal is shown in Figure 13a. A modulated carrier is indicated. Spreading of the spectrum (over frequency) could indicate the presence of phase shift keying. Looking at Figure 13b, which shows the corresponding contour plot, we note that transition points (i.e., phase shifts) are fairly easy to identify. A modulated carrier is present at spectral locations 5 and 11. The bit rate can be estimated by measuring the minimum distance between the leading edges of two consecutive transition points. This minimum distance is properly defined if all distances between transition points (or the majority of them) are integer multiples of this minimum distance. The message, with a plus/minus sign uncertainty, can be recovered.

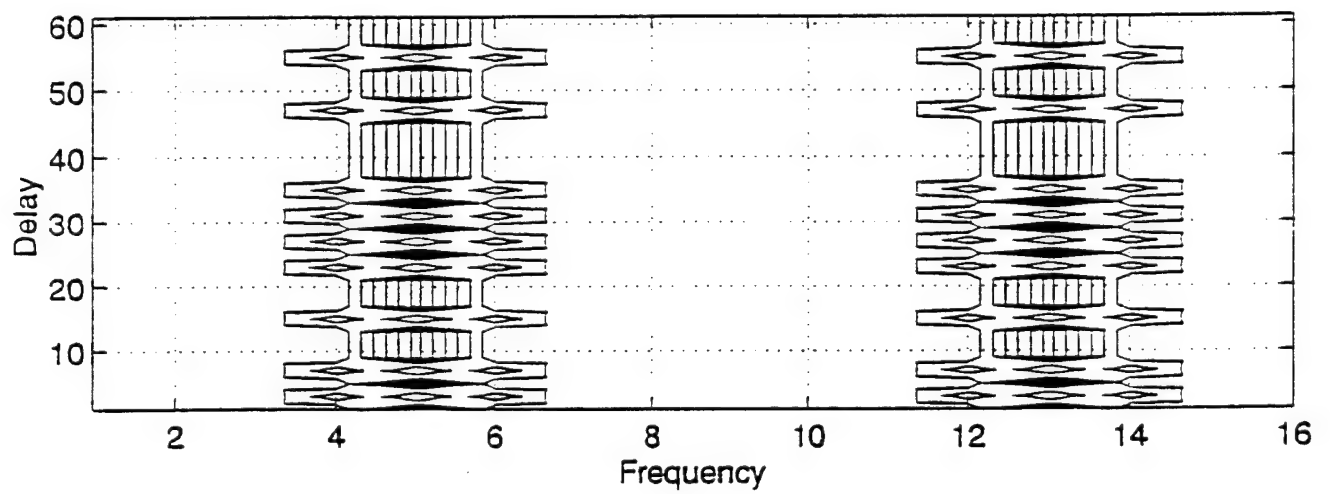
At an SNR level of 10-dB, the output of the detector still shows the modulated carrier, as shown in Figure 14a. Figure 14b is a contour plot of Figure 14a. It reveals that the modulated carrier is at spectral locations 5 and 11, the transition points can be obtained, and hence the bit rate can still be estimated.

At an SNR level of 0-dB the features of the output completely change. Figure 15a shows the output of the detector and indicates the difficulty in identifying the output (i.e., any type of modulation can cause it). Figure 15b shows the corresponding contour plot of the output. It appears that the effect of noise at this level may lead us to conclude that a FSK or OOK modulated signal is present.



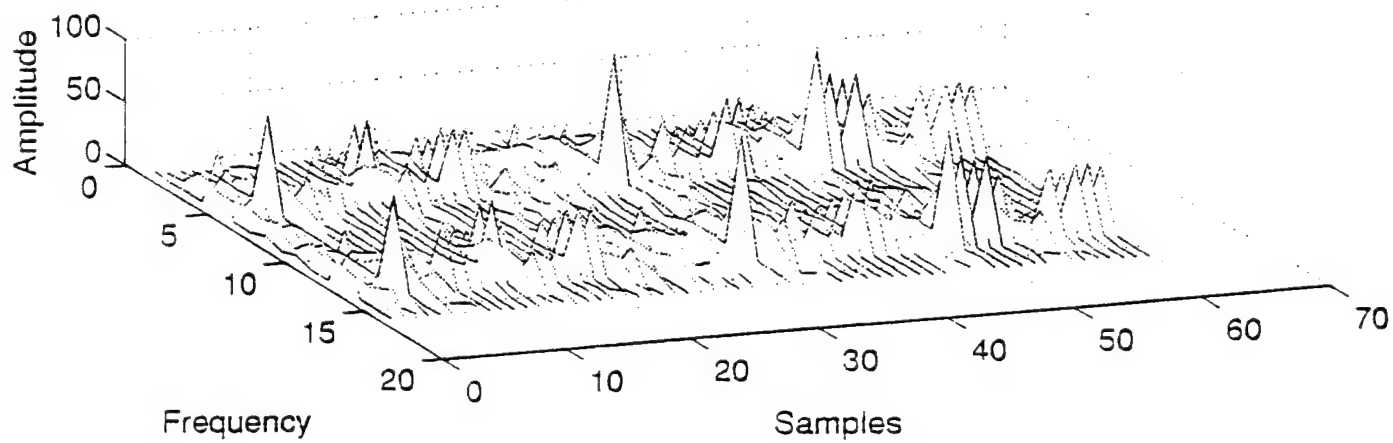


(a)

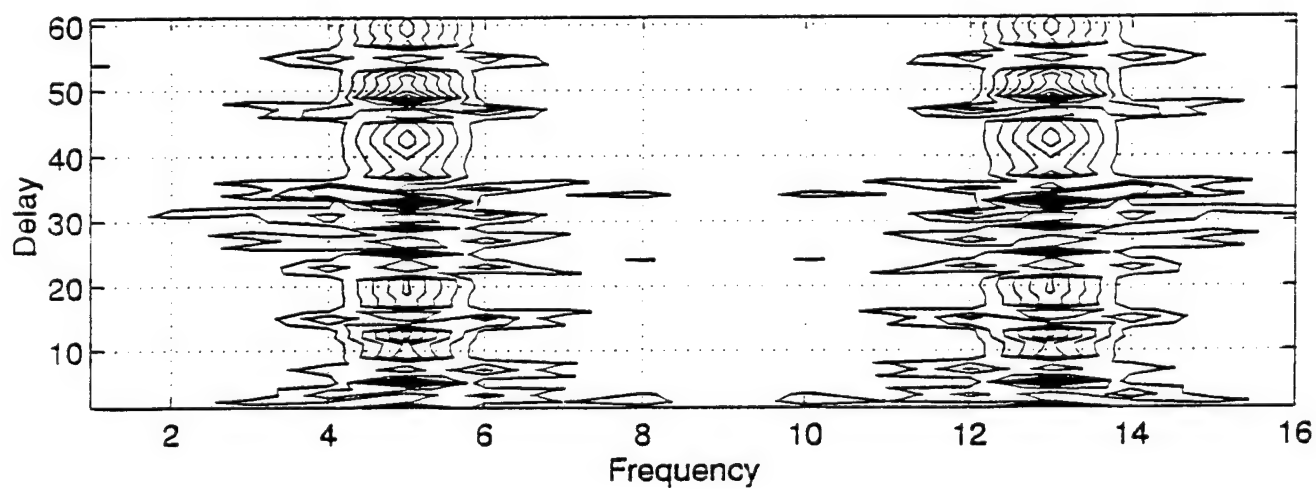


(b)

**Figure 13:** Output of FFT detector for BPSK signal, no noise; 75% overlap.

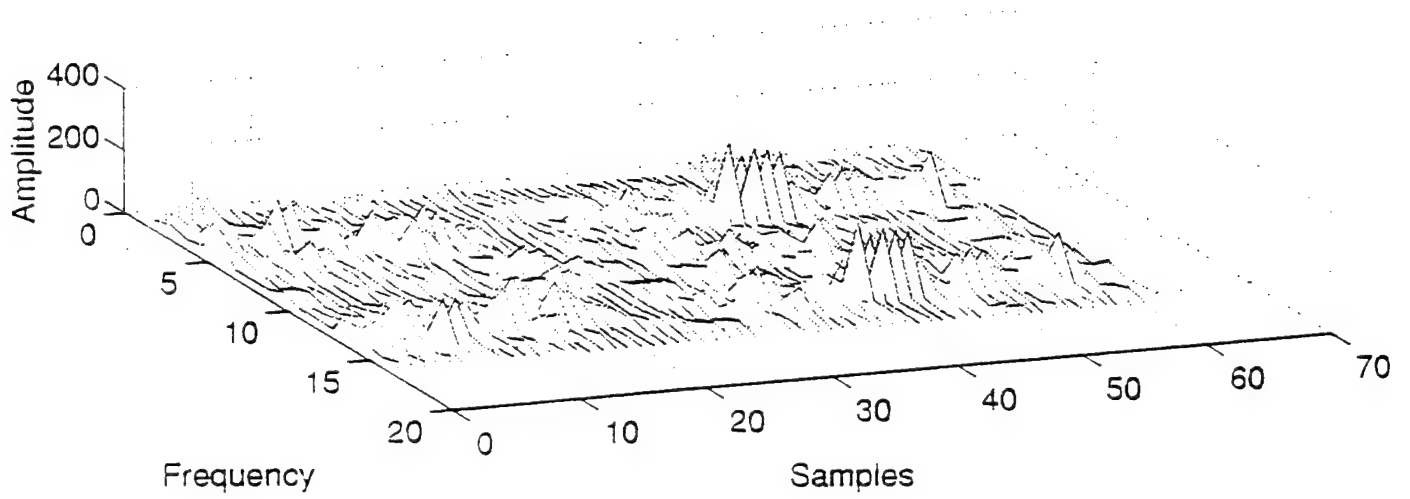


(a)

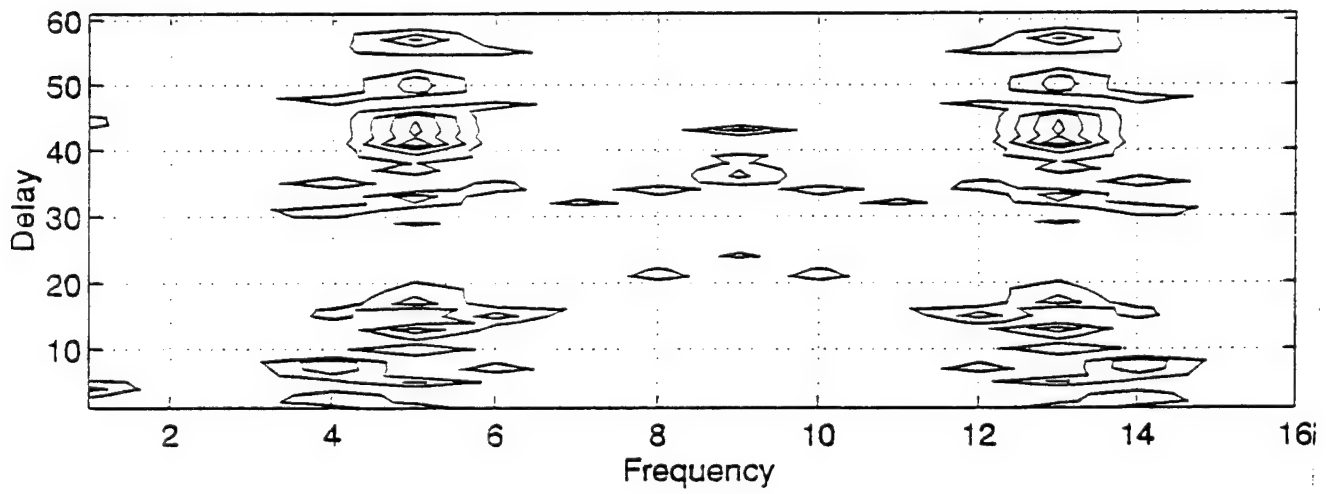


(b)

Figure 14: Output of FFT detector for BPSK signal with 10-dB SNR; 75% overlap.



(a)



(b)

**Figure 15:** Output of FFT detector for BPSK signal, 0-dB SNR; 75% overlap.

Figure 16 shows the output averaged over frequency and time. At all SNR levels, the carrier frequency and bandwidth can be estimated using the time averaged outputs (1a, 2a, 3a).

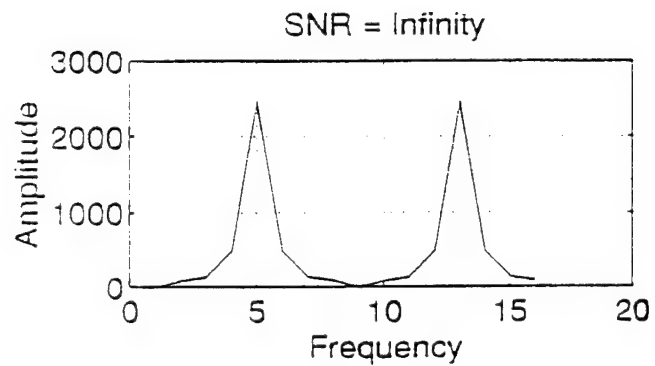
The frequency averaged output (see 1b, 2b, and 3b) provides little information. Plot 1b (no noise) shows constant energy. At 10-dB SNR (see 2b), it is difficult to estimate the presence of the BPSK and the level of the noise completely masks the signal at 0-dB SNR (see 3b).

## 2. OOK

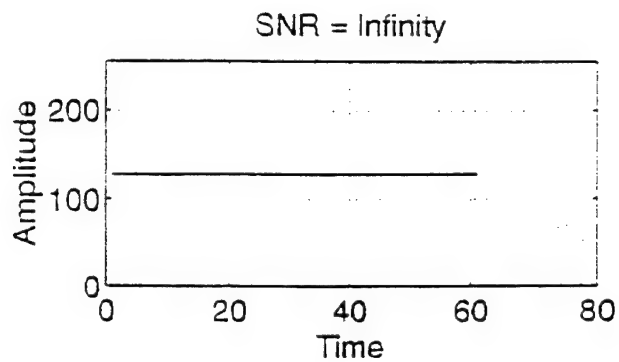
This modulation technique is much easier to identify than the other types of modulation. The output of the FFT detector driven by a noise-free OOK signal (Figure 17a) show that the modulated carrier has an ON-OFF characteristic. The bit rate and carrier frequency at spectral positions 5 and 11 can be estimated using Figure 17b. The original message (within a  $180^\circ$  phase uncertainty) can easily be recovered.

At a level of 10-dB (see Figures 18a and 18b) the noise does not have a significant effect on the output of the FFT detector. The modulating message can still be recovered (with a phase uncertainty as mentioned before). But, when the noise is increased to a level of 0-dB SNR (Figure 19a and 19b), it becomes very difficult to distinguish the signal from the noise.

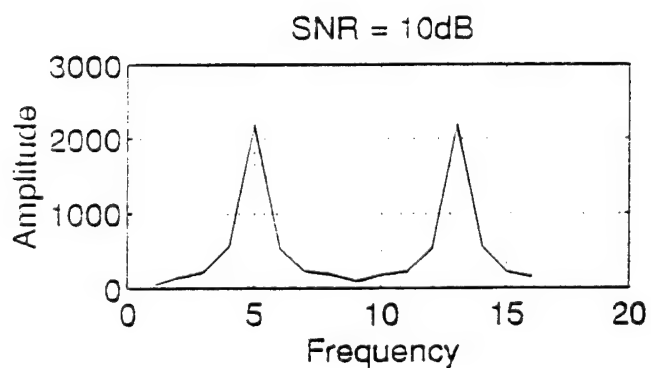
Figure 20 shows the output averaged over frequency and time. The presence of the signal can be recognized at all noise levels and the carrier frequency and bandwidth can be estimated (see 1a, 2a, and 3a). The frequency averaged output for noise-free OOK (see 1b) allows the message code to be estimated. The amplitude modulation can be recognized, and the bit rate can be obtained. But, when the SNR drops to 10-dB (see 2b), it is difficult to estimate OOK features from



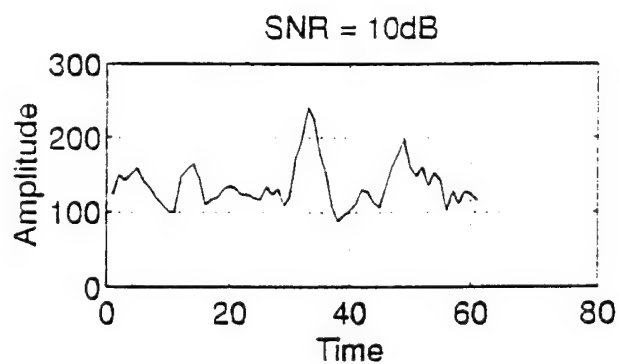
(1a)



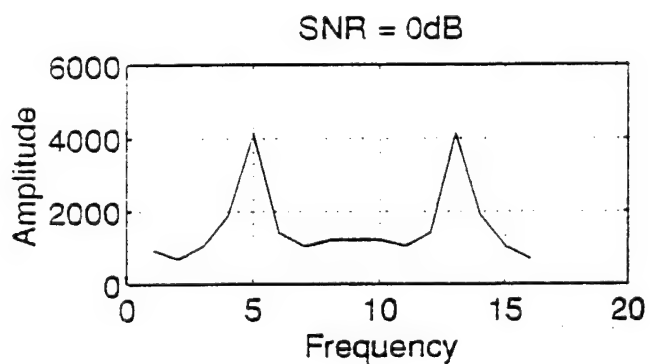
(1b)



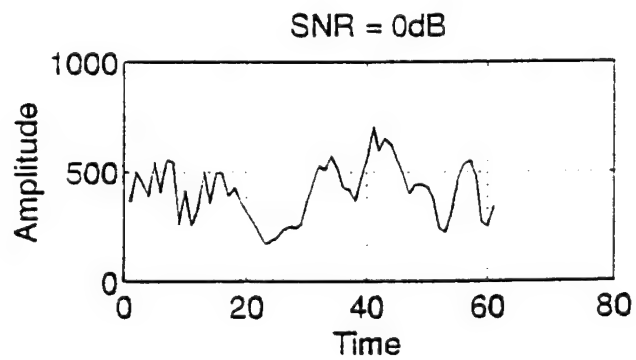
(2a)



(2b)

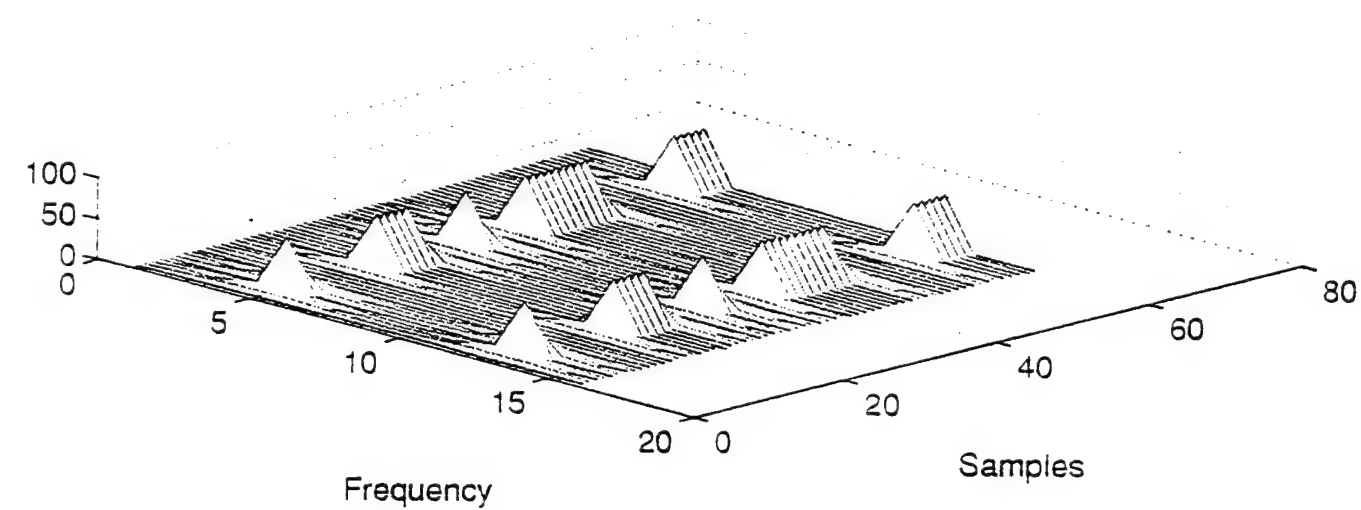


(3a)

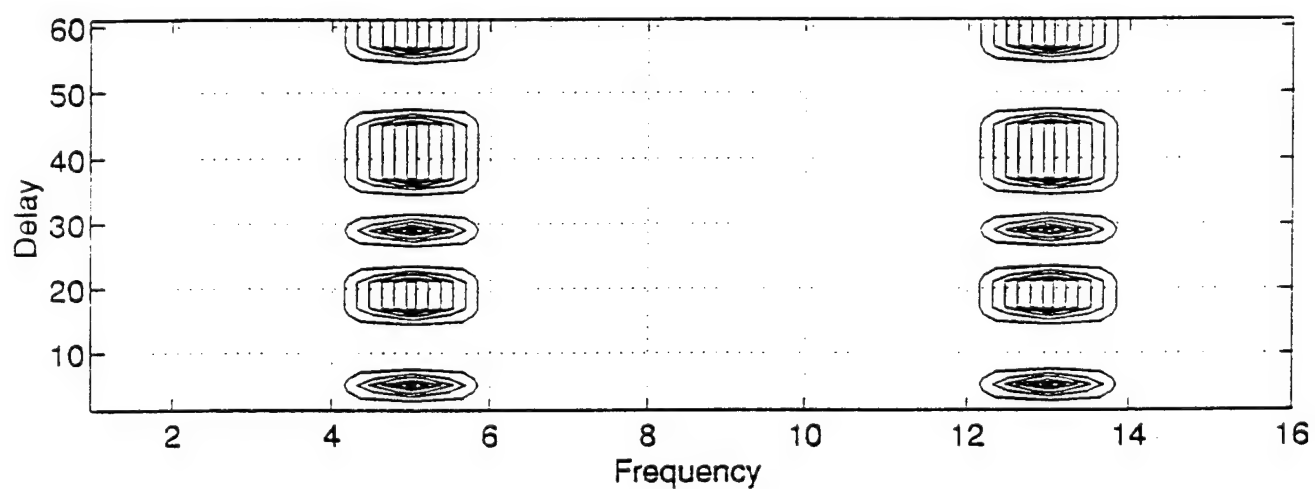


(3b)

Figure 16: Averaged output of FFT detector for BPSK signal at all SNR levels.

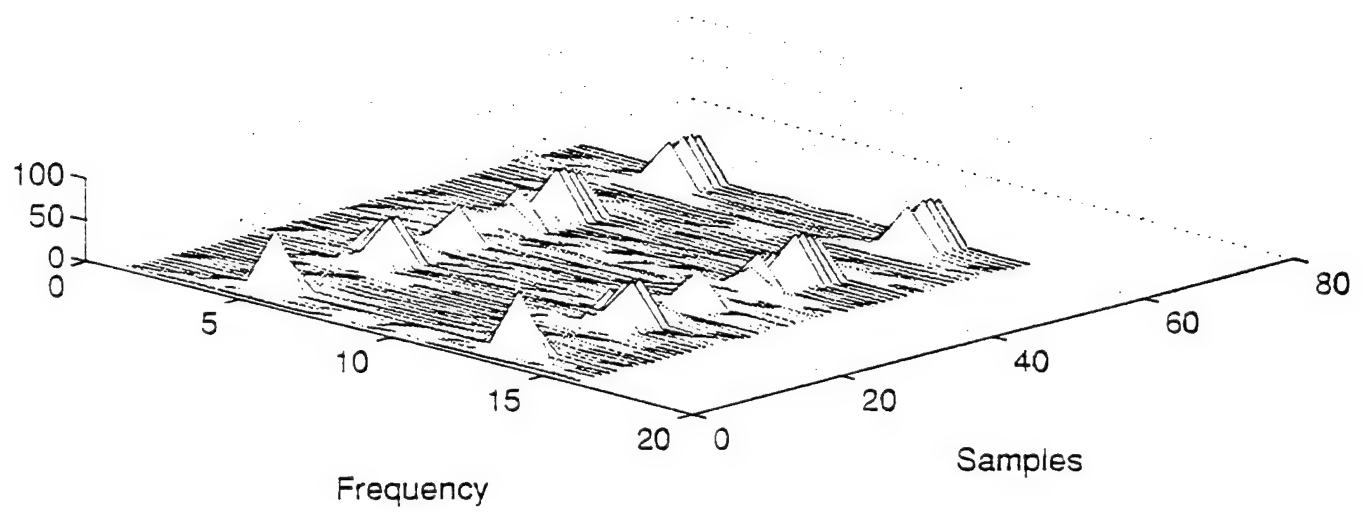


(a)

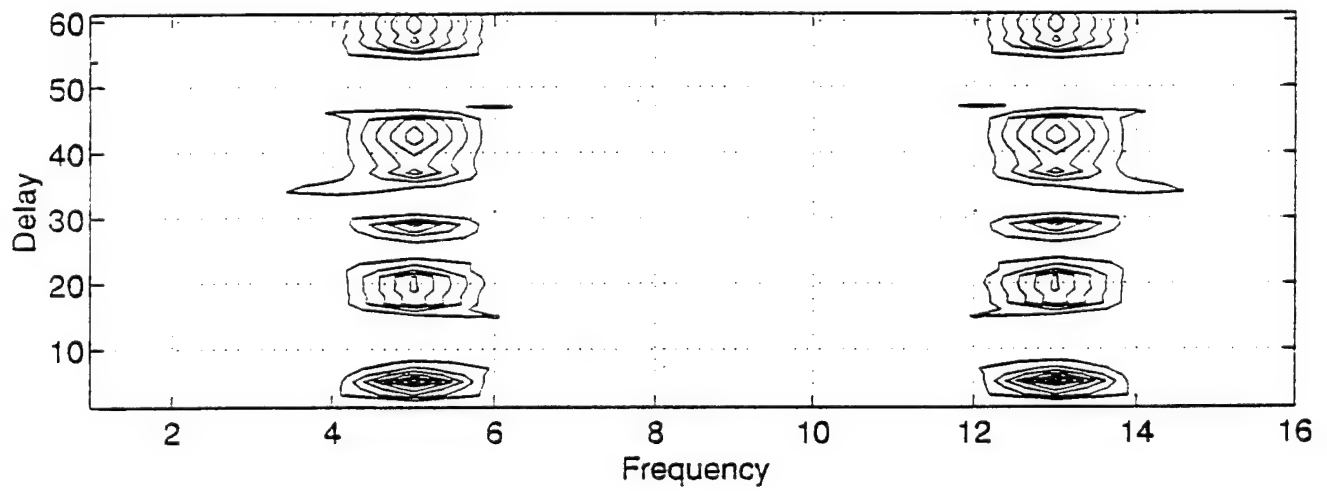


(b)

Figure 17: Output of FFT detector for OOK signal. no noise; 75% overlap.

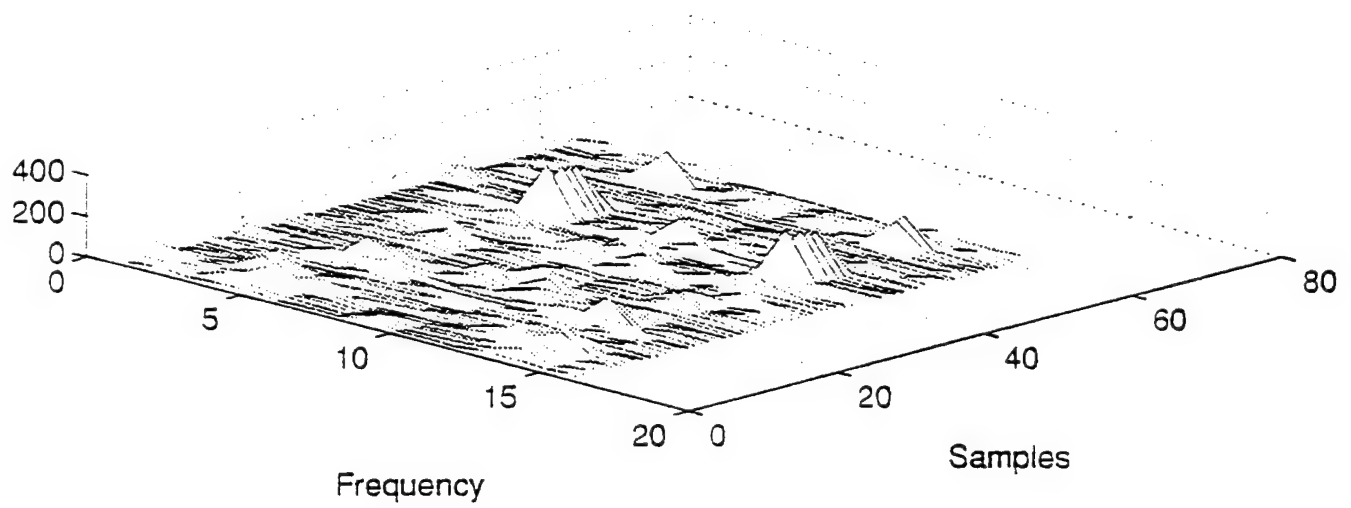


(a)

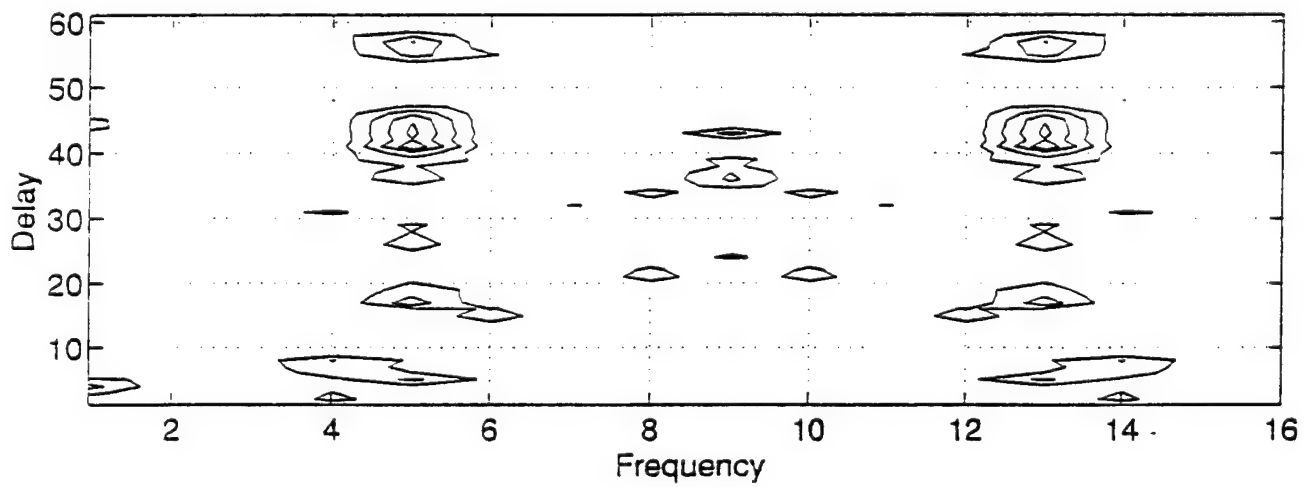


(b)

Figure 18: Output of FFT detector for OOK signal, 10-dB SNR; 75% overlap.



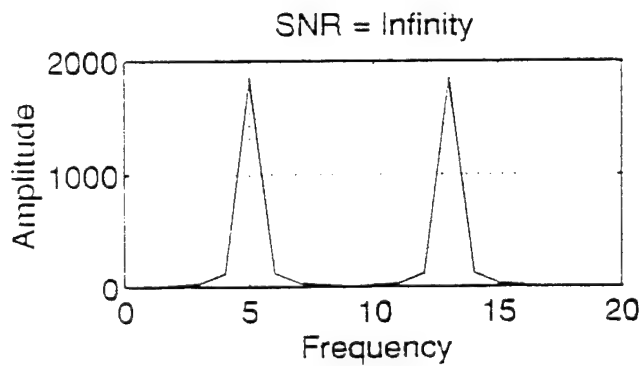
(a)



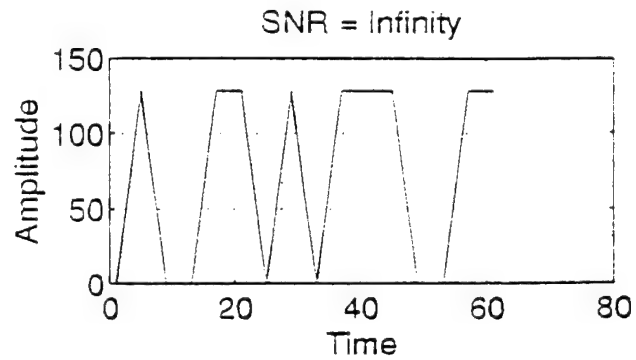
(b)

Figure 19: Output of FFT detector for OOK signal, 0-dB SNR; 75% overlap.

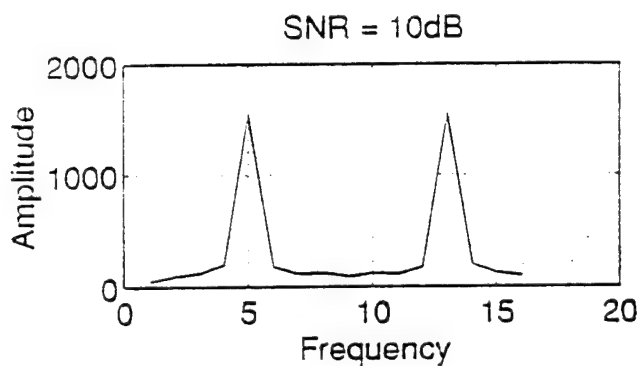




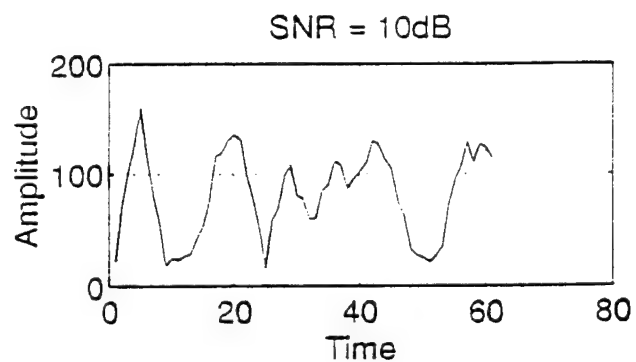
(1a)



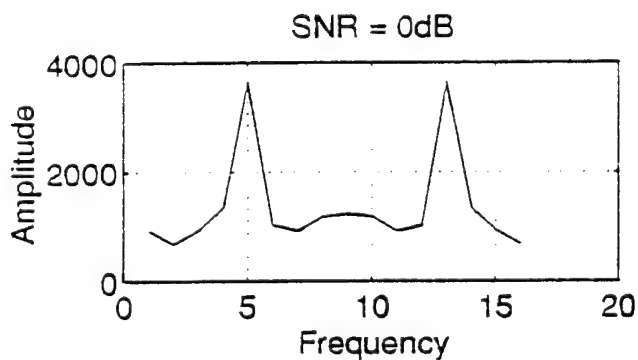
(1b)



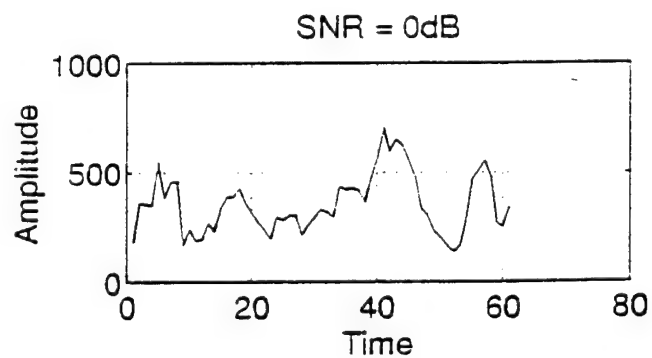
(2a)



(2b)



(3a)



(3b)

Figure 20: Averaging output of FFT detector for OOK signal at all SNR levels.

the averaged output. At an SNR level of 0-dB, the signal vanishes completely (see 3b).

### 3. FSK

The output of the detector driven by a noise-free FSK signal is shown in Figure 21a. It shows a signal having a constant amplitude and some modulation. Figure 21b shows the corresponding contour plot. It displays FSK characteristics and the bit rate can be extracted from this plot by measuring the minimum width of a single message bit. The carrier frequency and the frequency shift can also be estimated from the contour plot. The message, within a sign ( $\pm$ ) uncertainty, can be recovered.

Figure 22a shows the output for the FSK signal with an SNR level of 10-dB. Note that, even at this level of noise, we can still recognize the presence of a carrier and we note that the amplitude is not constant due to the added noise. Figure 22b allows estimation of the parameters such as the carrier frequency, the frequency shift, and the bit rate. It still permits the demodulation of the message (within a phase uncertainty of  $180^\circ$ ).

Figures 23a and 23b shows the output of the detector driven by an FSK signal with an SNR level of 0-dB. It is difficult to identify the FSK signal. The output can be interpreted as OOK at a carrier frequency of 5 and 13 (see Figure 23b).

Figure 24 shows the output averaged over frequency and time. The time averaged output (see 1a, 2a, and 3a) shows that at all SNR levels a non-symmetric spectrum is present, which is probably a result of a summation of more than one frequency component. One of the carrier frequencies can be estimated and a measure of bandwidth can be obtained. Plot 1b, 2b, and 3b show the frequency averaged output. Plot 1b (noise-free case) shows a constant amplitude carrier. No information can be obtained at 10-dB and 0-dB (see 2b and 3b).

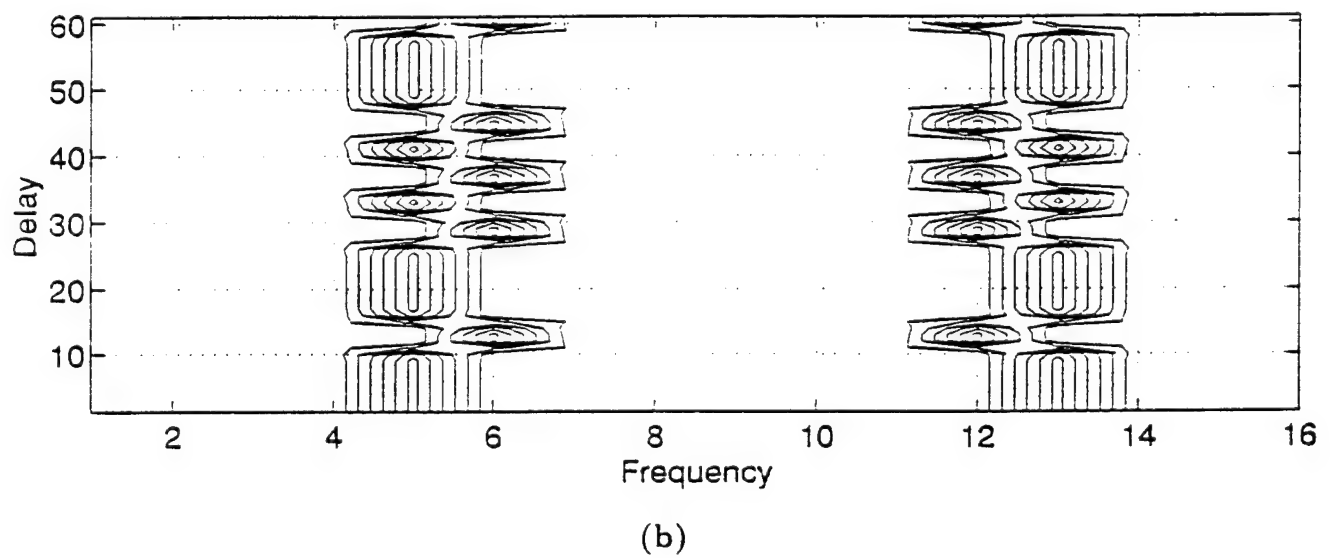
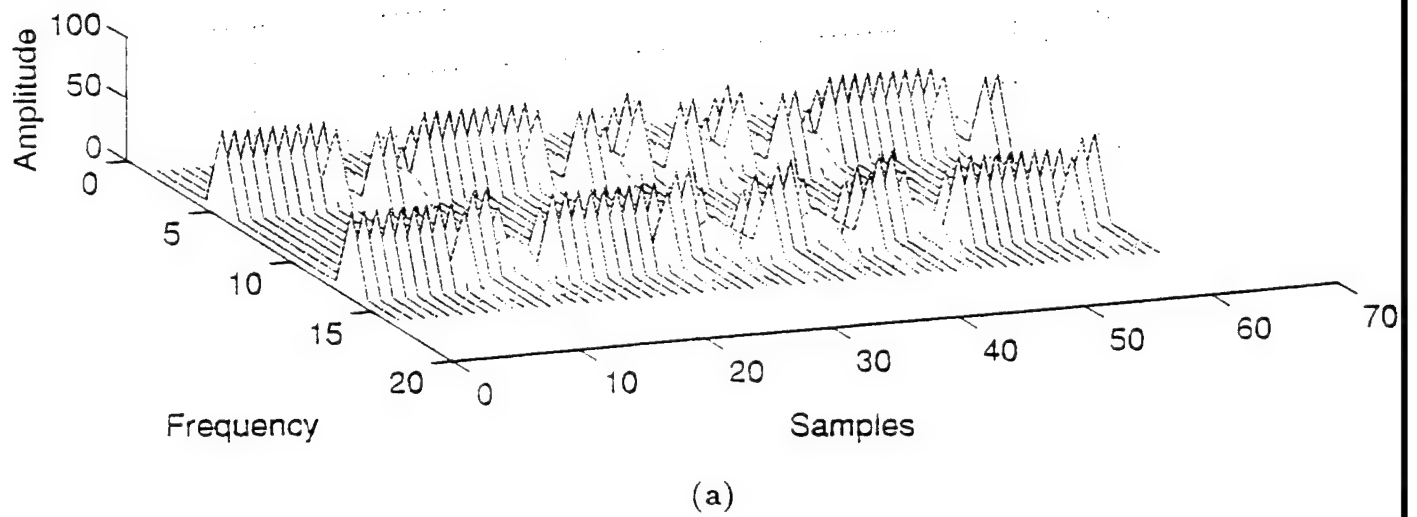
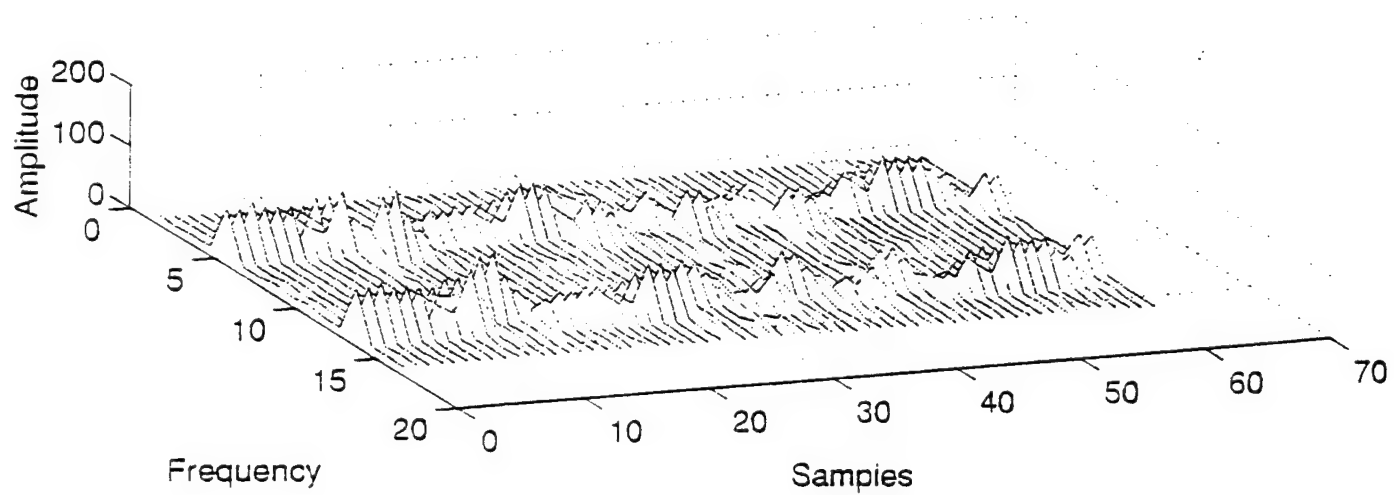
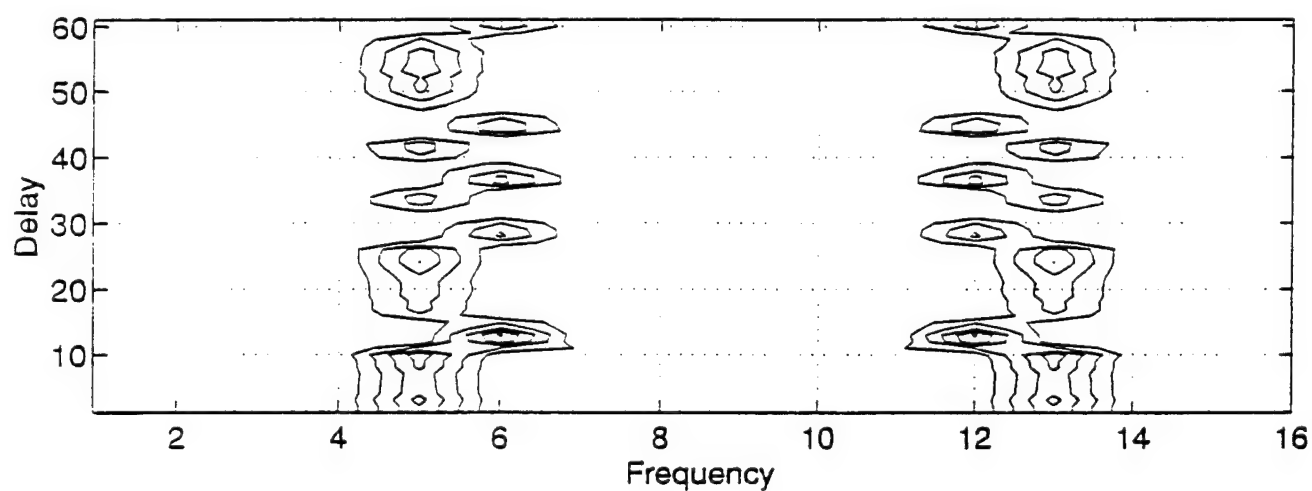


**Figure 21:** Output of FFT detector for FSK signal, no noise; 75% overlap.

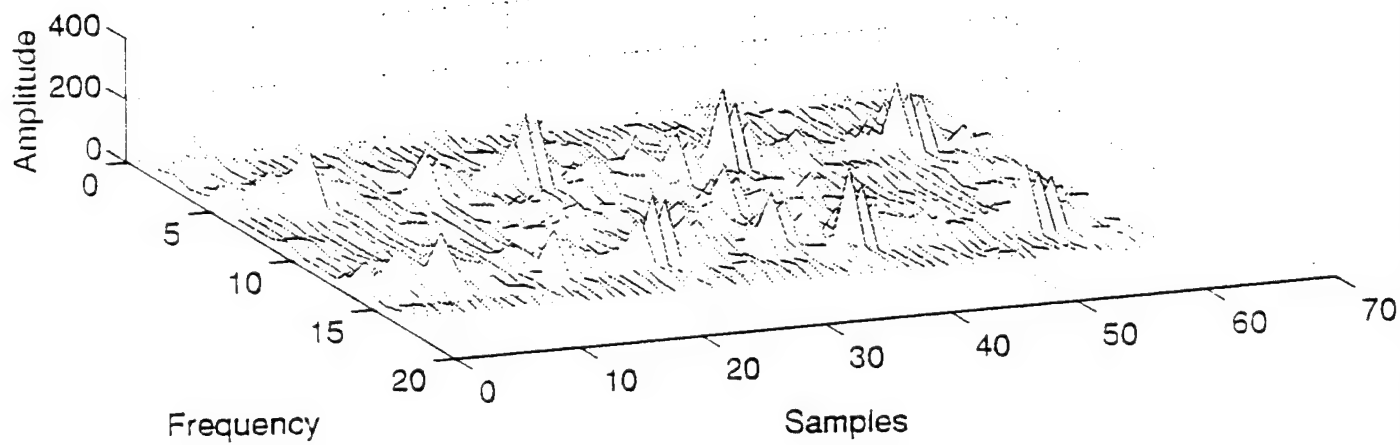


(a)

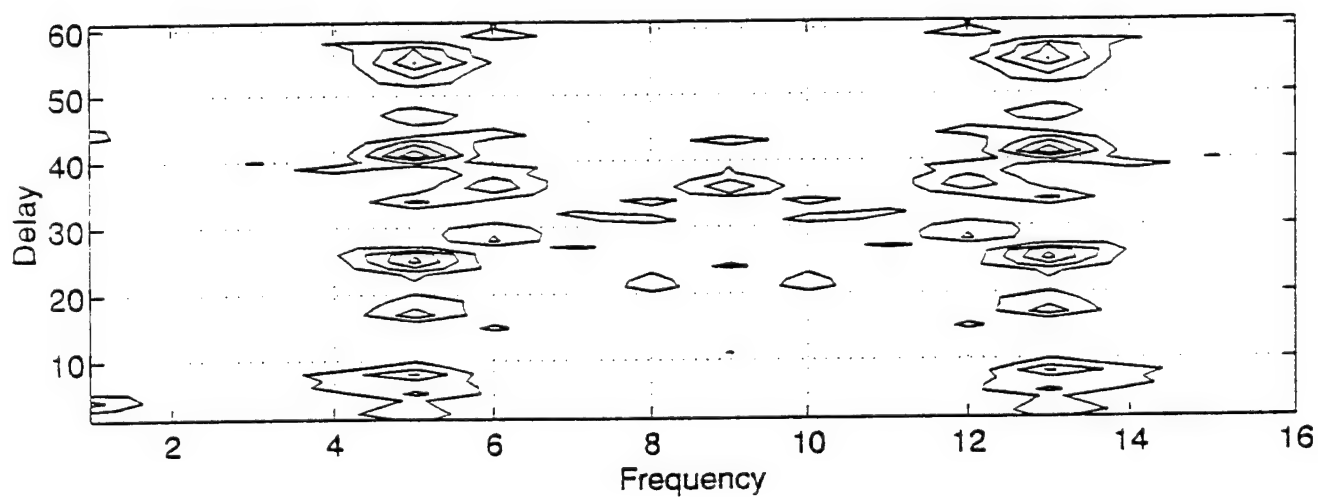


(b)

Figure 22: Output of FFT detector for FSK signal, 10-dB SNR; 75% overlap.

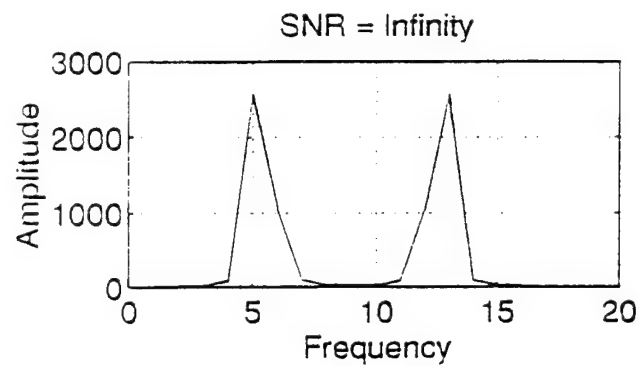


(a)

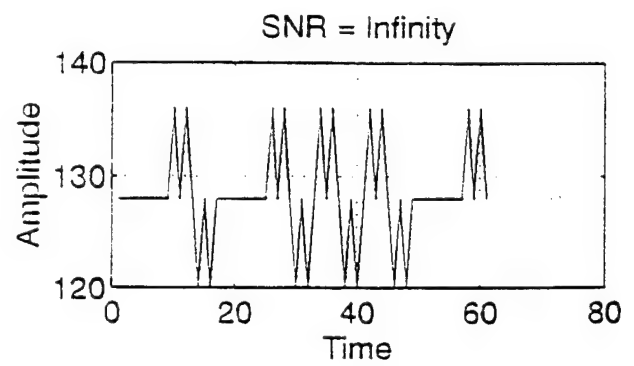


(b)

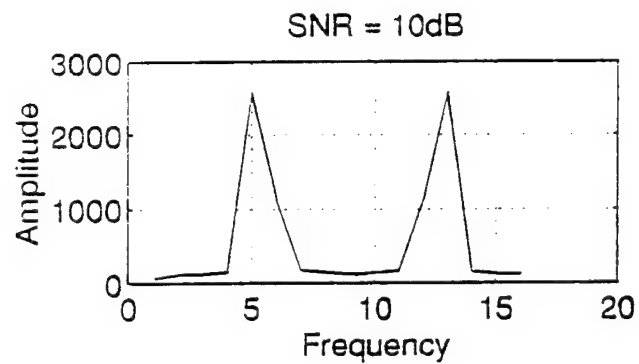
Figure 23: Output of FFT detector for FSK signal, 0-dB SNR; 75% overlap.



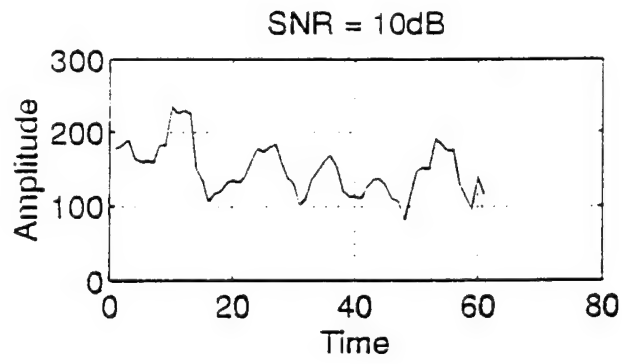
(1a)



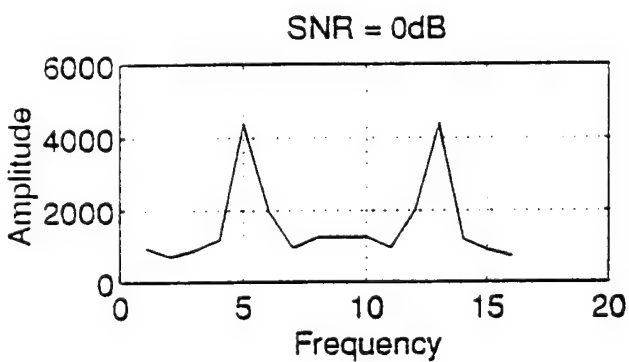
(1b)



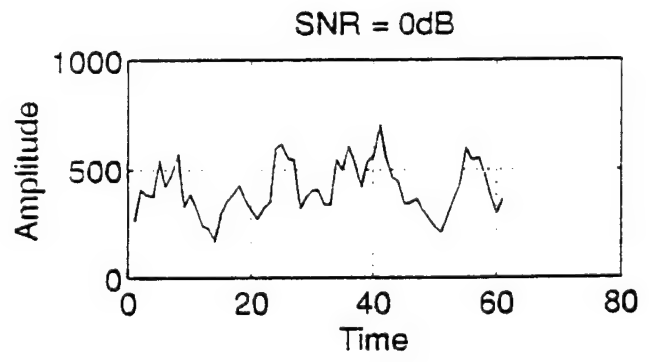
(2a)



(2b)



(3a)



(3b)

Figure 24: Averaged output of FFT detector for FSK signal at all SNR levels.

#### 4. QPSK

Figure 25a shows the output of the FFT detector driven by a noise-free QPSK signal. It shows that there is a modulated carrier. Figure 25b shows the corresponding contour plot, which allows bit rate estimation. Comparing this figure with Figure 6, we can identify a phase shift of  $180^\circ$  at locations 19, 39, 47, and 54, and phase shifts of plus or minus  $90^\circ$  at locations 2, 16, 24, 28, 32, 36, 44, 52, and 58. The carrier frequency at positions 5 and 13 can also be estimated.

Figure 26a shows the output of the detector at an SNR level of 10-dB. The estimation of the modulation is difficult since the carrier exhibits the characteristics of FSK, OOK, or BPSK. Figure 26b shows the corresponding contour plot. The modulation carrier is primarily at spectral positions 5 and 13. There is a possible carrier frequency shift at some locations (i.e., at delay 19 and 54). Transition points, probably due to phase shift, are present and can be used to estimate the bit rate.

Figures 27a and 27b show the output of the detector at an SNR level of 0-dB. It is impossible to identify the output as QPSK or any other modulated signals or to estimate any parameters due to the noise.

Figure 28 shows the output averaged over frequency and time. The time averaged output (see 1a, 2a, and 3a) shows that the signal is always present and the carrier frequency and bandwidth can be estimated. The frequency averaged output in the noise-free case shows constant carrier energy, while from the 10-dB and 0-dB SNR plots (see 2b and 3b) no information can be obtained.

### D. TIME-FREQUENCY DISTRIBUTION METHODS

#### 1. Method-1

As mentioned earlier (Eq. 4), this method is based on the Fourier transform of lagged products (over lag  $m$ ). The variable  $n$  is an independent argument here.

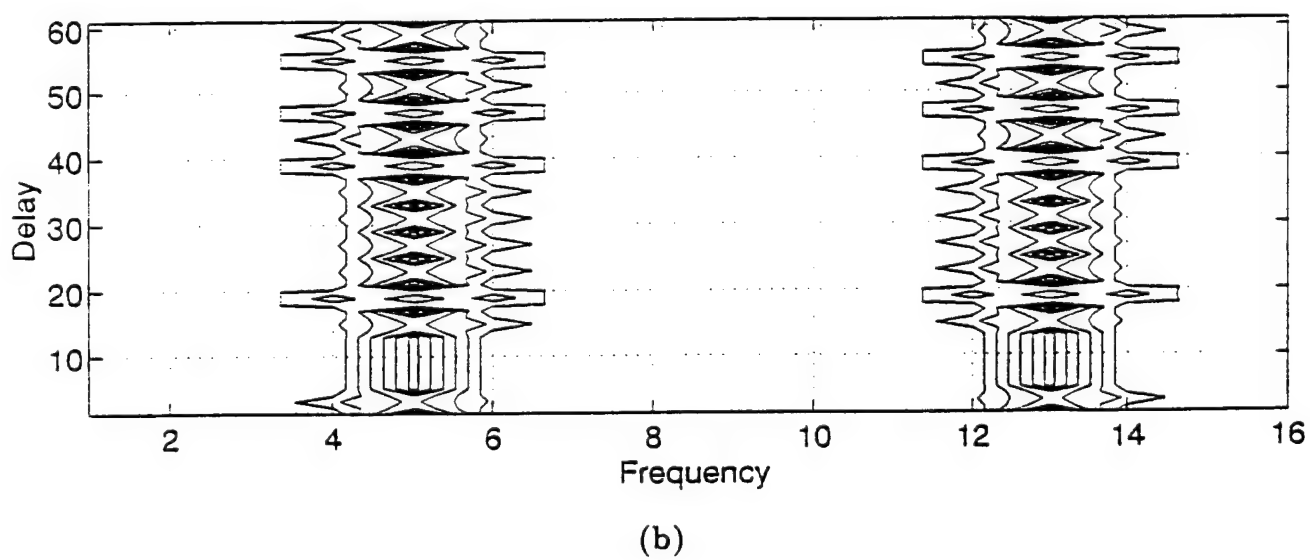
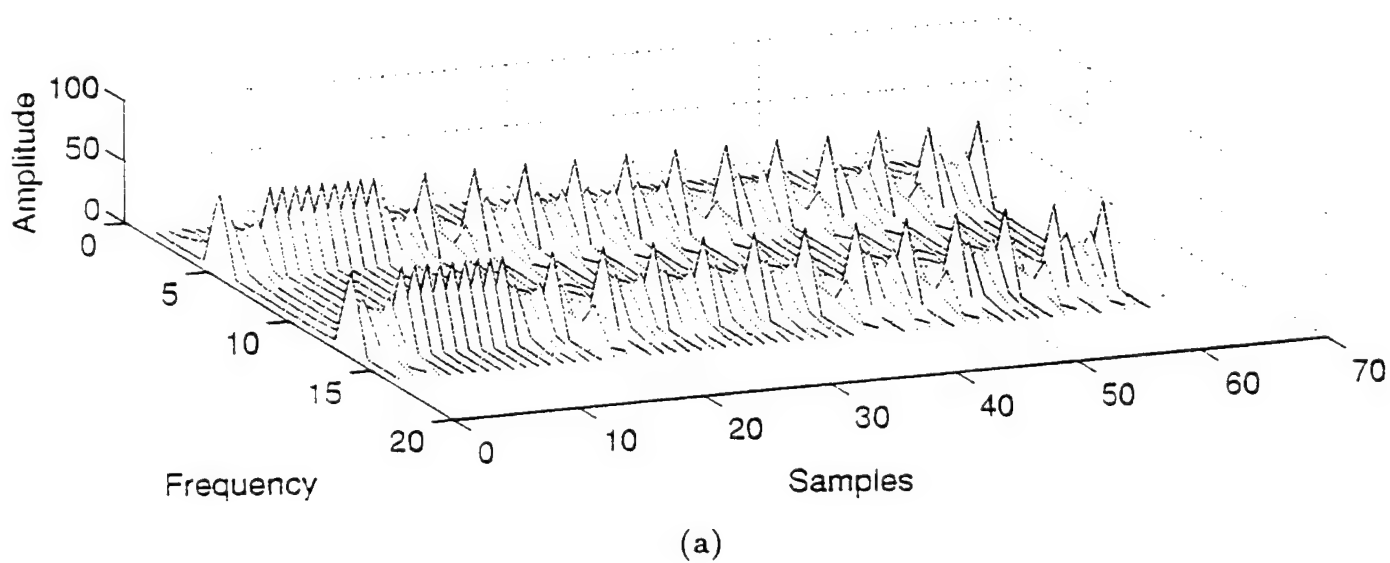
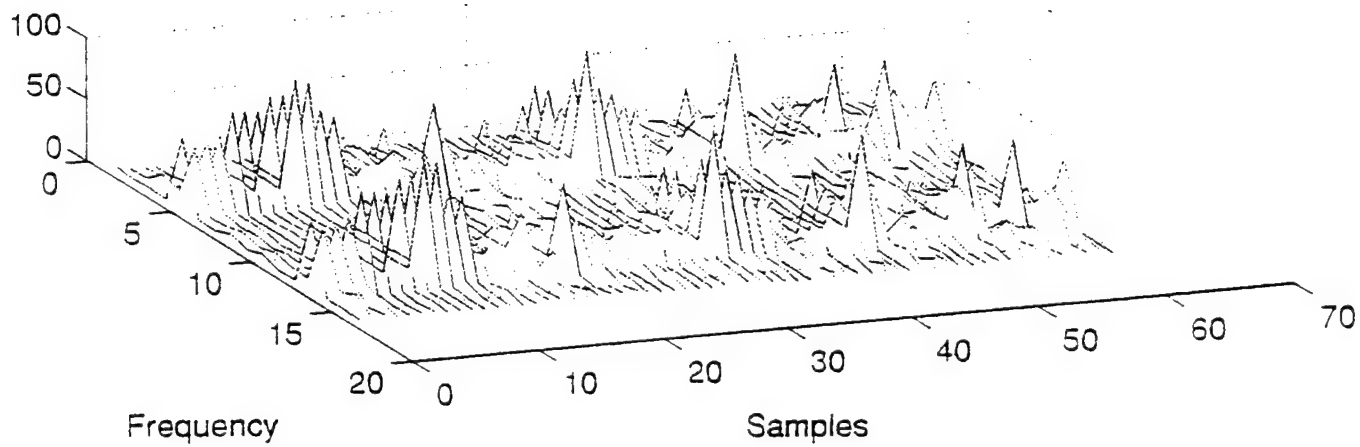
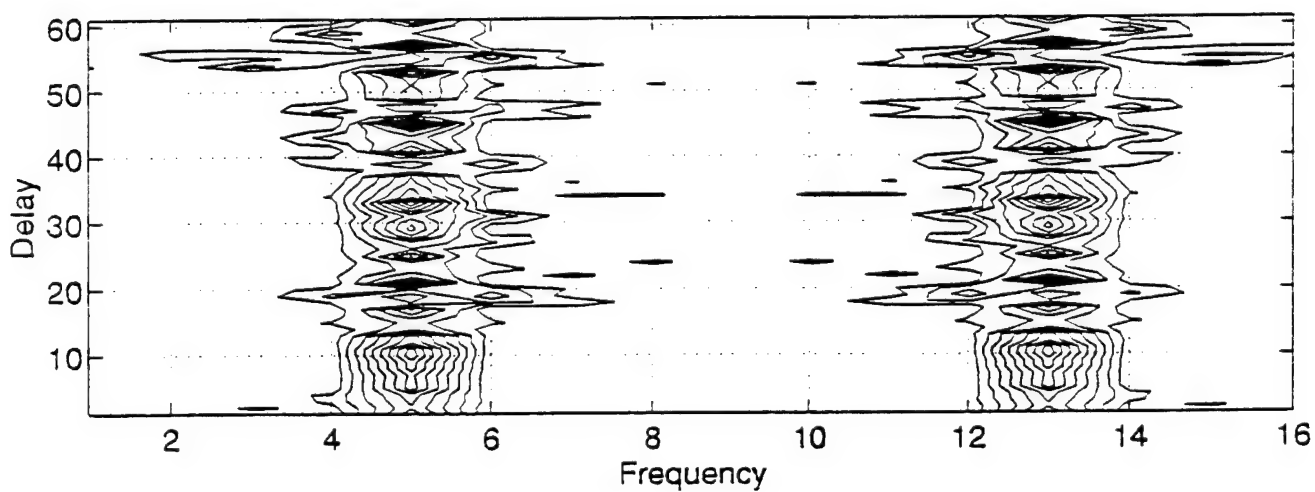


Figure 25: Output of FFT detector for QPSK signal, no noise; 75% overlap.



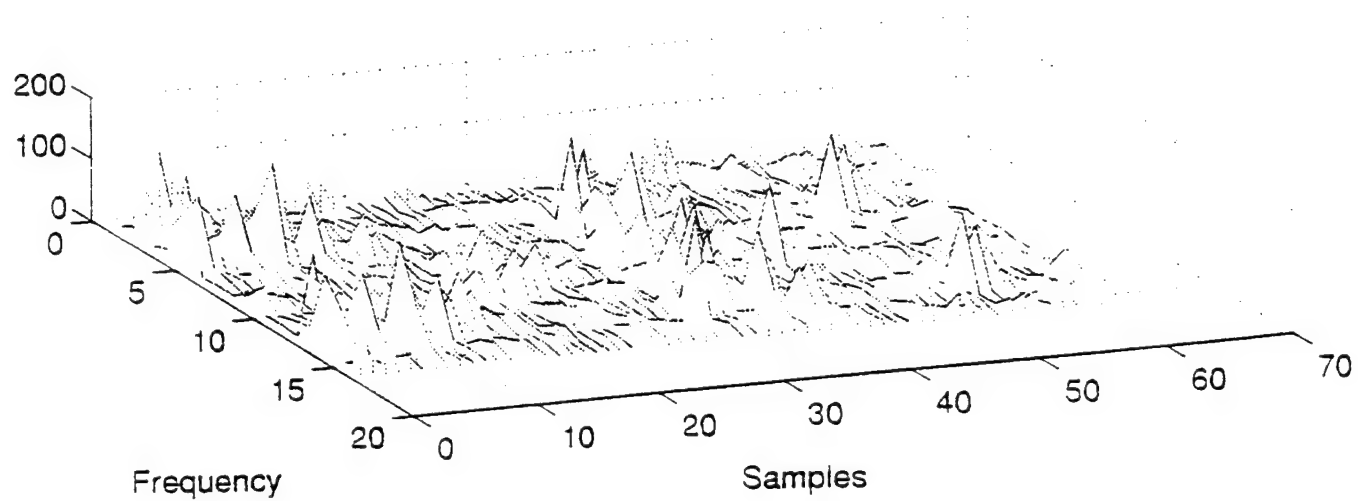


(a)

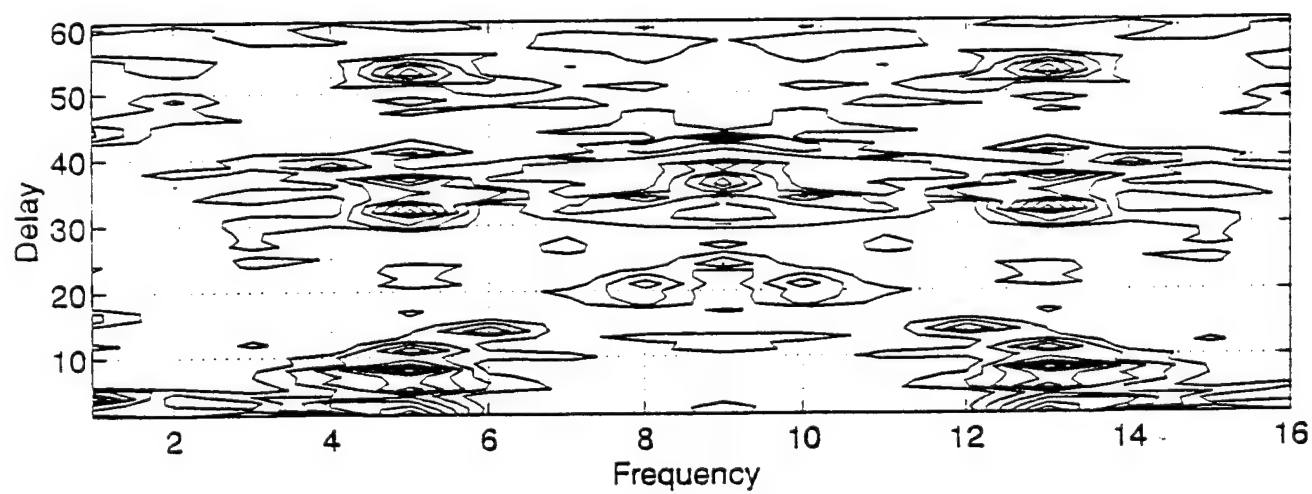


(b)

Figure 26: Output of FFT detector for QPSK signal, 10-dB SNR; 75% overlap.



(a)



(b)

**Figure 27:** Output of FFT detector for QPSK signal. 0-dB SNR: 75% overlap.

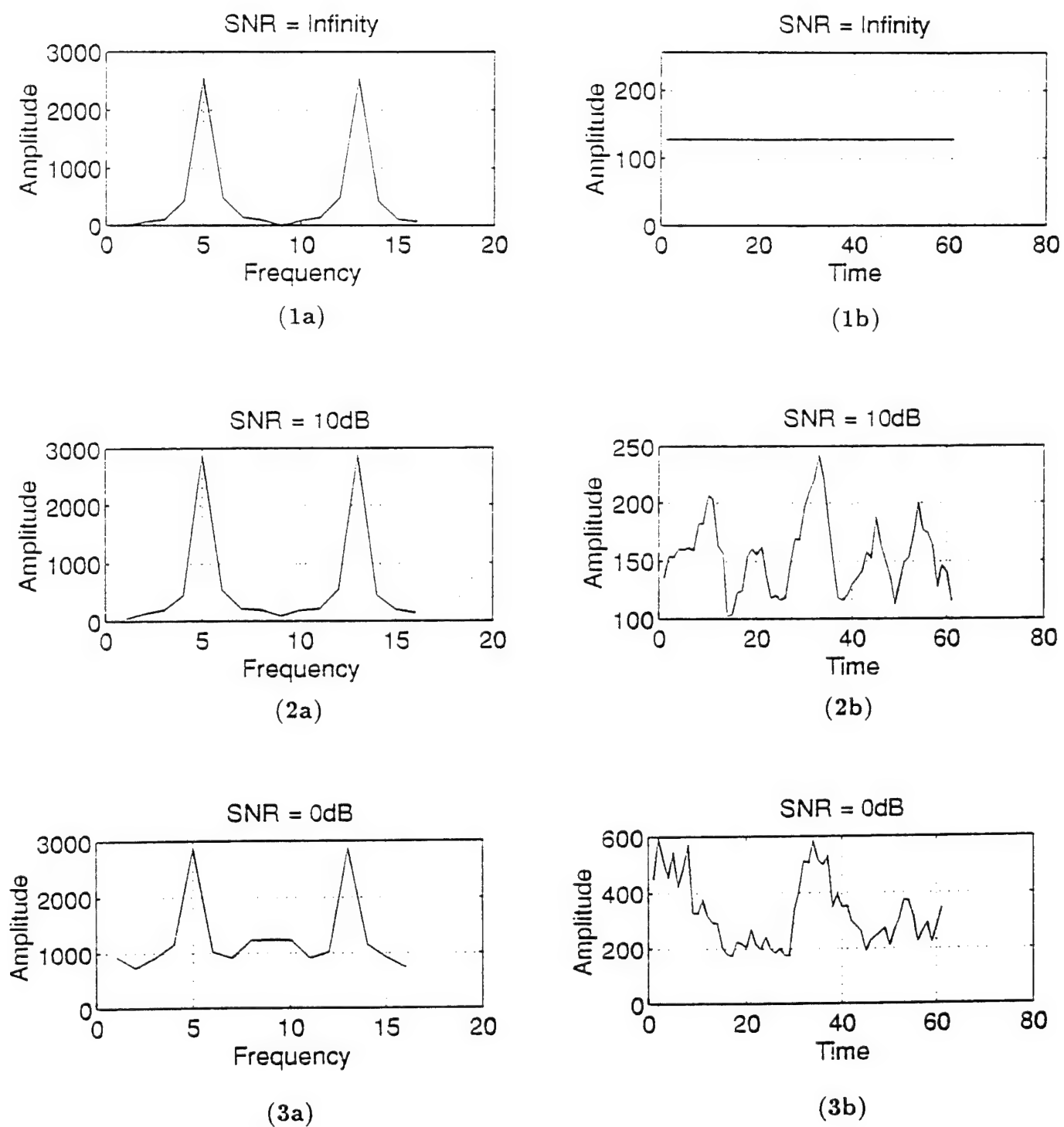


**Figure 28:** Averaged output of FFT detector for QPSK signal at all SNR levels.

A transform length of 16 is assumed and  $\overline{x(n)}$  is taken as the sample mean over these 16 points. The time axis (samples or delay) are scaled by 4, corresponding to a 75% overlap at a transform length of 16.

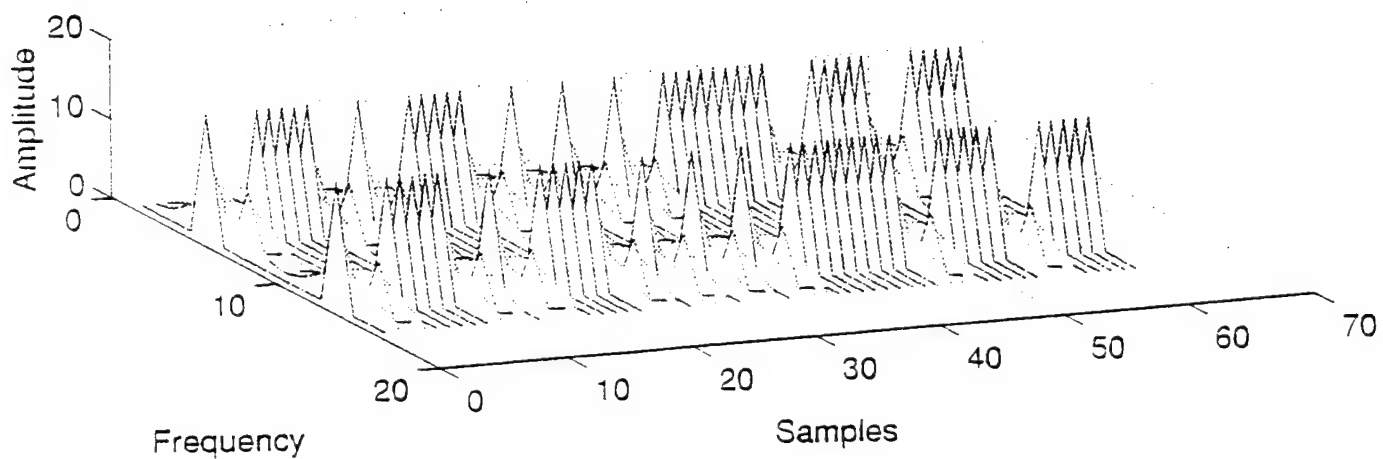
The outputs of the method-1 detector are shown using three types of plots. A three-dimensional output plot, similar to a spectrogram of the data shows power versus time and frequency (Figures 29a, 30a, 31a, 33a, 34a, 35a, 37a, 38a, 39a, 41a, 42a, and 43a). The outputs are also shown as contour plots for more analysis and extraction of parameters (Figures 29b, 30b, 31b, 33b, 34b, 35b, 37b, 38b, 39b, 41b, 42b, and 43b). Also, time averaged plots (see plots 1a, 2a, and 3a) and frequency averaged plots (see plots 1b, 2b, and 3b) are shown (Figures 32, 36, 40, and 44).

#### **a. BPSK**

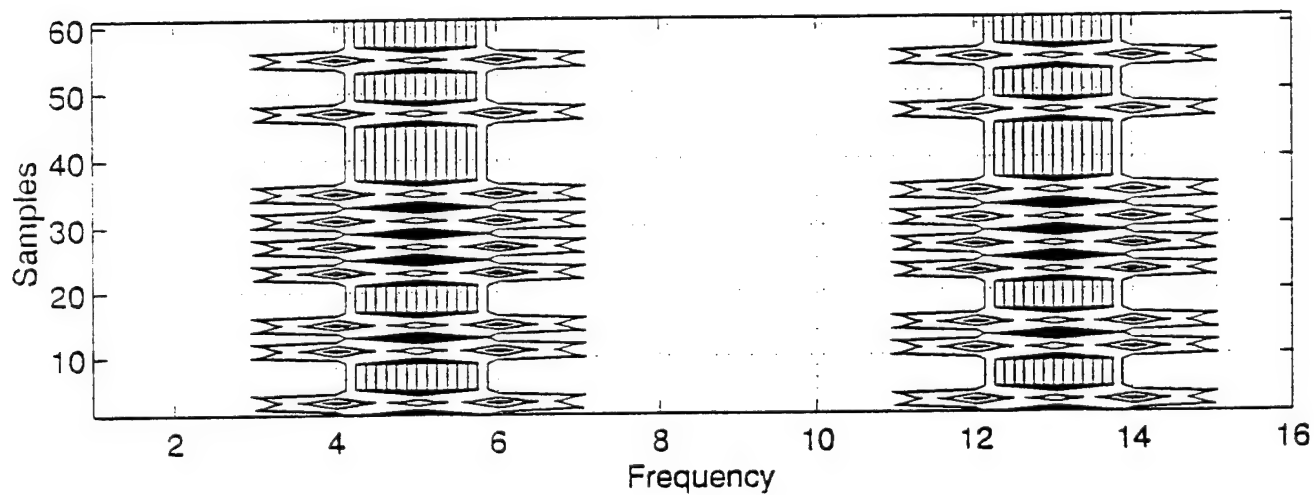
Figure 29a shows the output of the detector for a BPSK signal without noise. Note the appearance of the modulated carrier at some carrier frequency. Fluctuation in the magnitude of the output, may indicate the presence of phase modulation. The contour plot in Figure 29b allows the estimation of the carrier frequency at spectral positions 5 and 13, and the bit rate.

Figures 30a and 30b show the output of the detector for a signal with an SNR of 10-dB. Note that the features of the output are difficult to determine in both figures, which may lead to an improper identification of the type of modulation. It is obvious that the output of the detector at an SNR level of 0-dB (Figures 31a and 31b) will give worse results than those shown in Figures 30a and 30b.

Figure 32 shows the output averaged over frequency and time. The time averaged output (see plot 1a for noise-free, 2a for 10-dB SNR, and 3a for 0-dB SNR) shows that at each of the different noise levels, the carrier frequency and the bandwidth can be estimated. The frequency averaged output shows a constant output

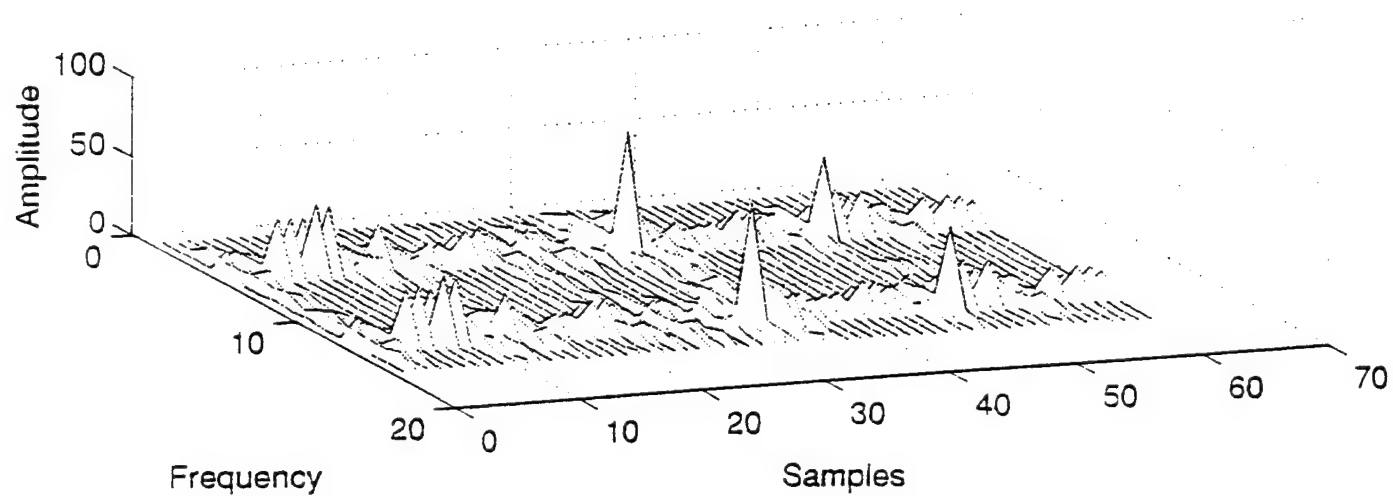


(a)

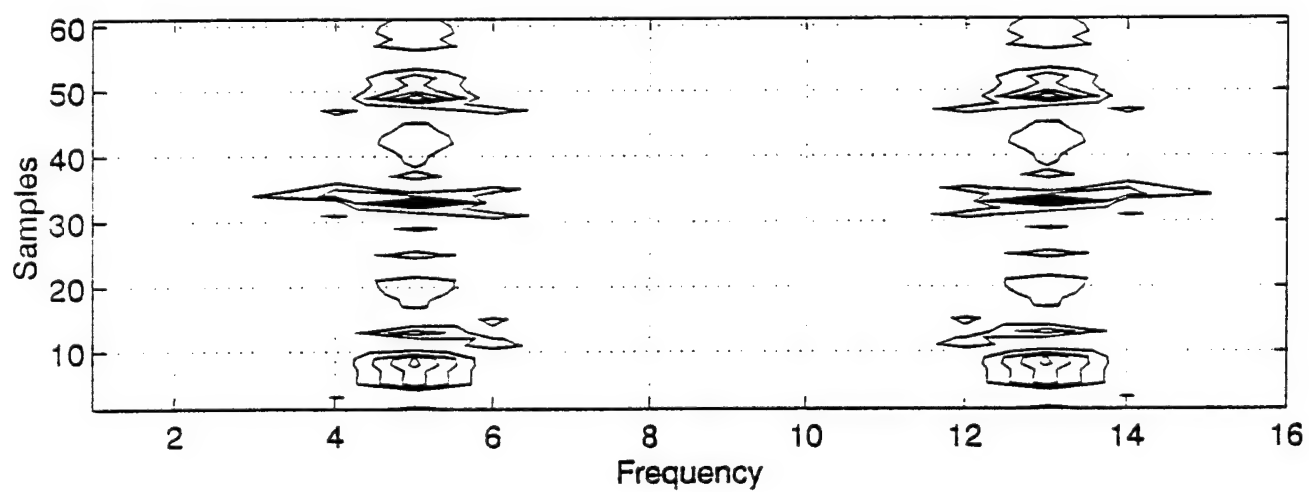


(b)

Figure 29: Output of Method-1 detector for BPSK signal, no noise.

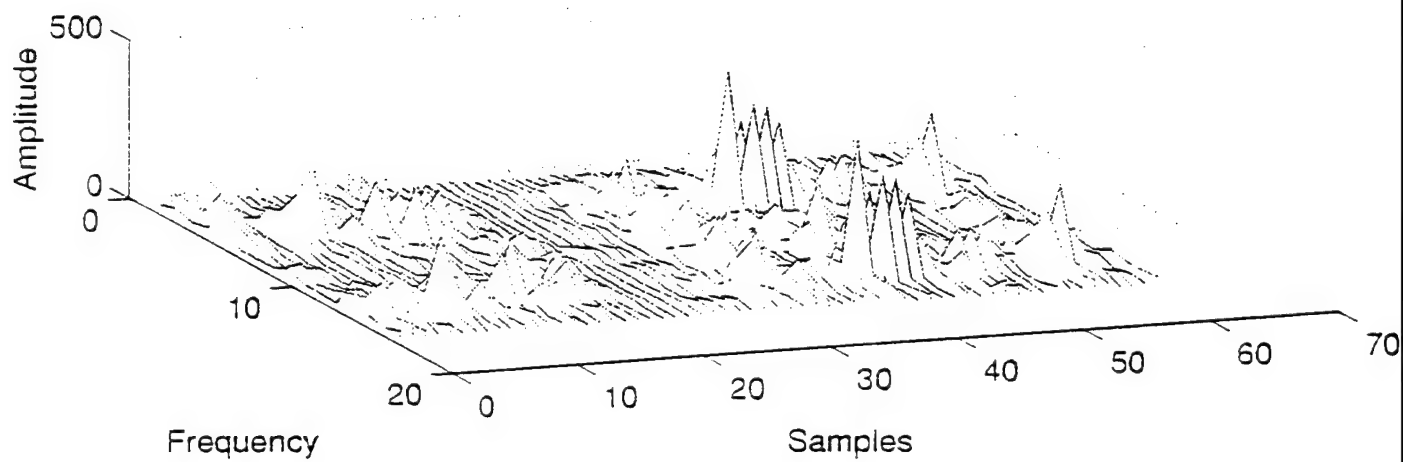


(a)

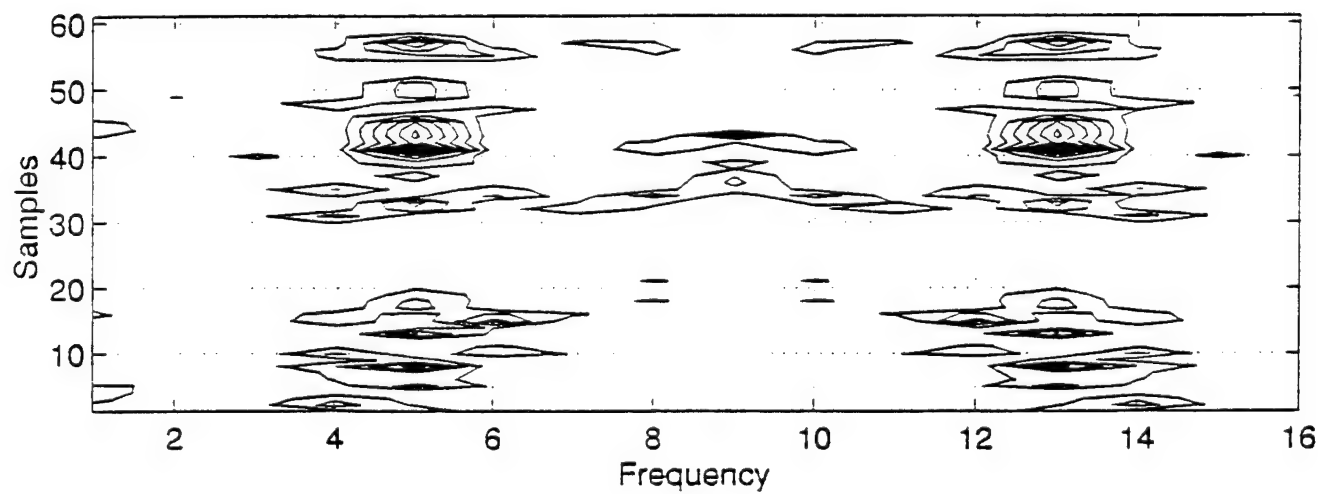


(b)

Figure 30: Output of Method-1 detector for BPSK signal, 10-dB SNR.

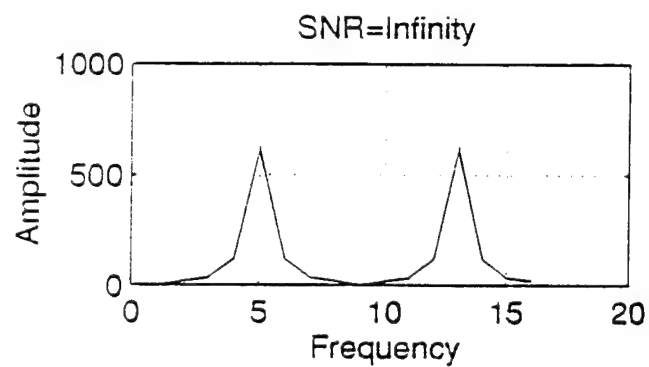


(a)

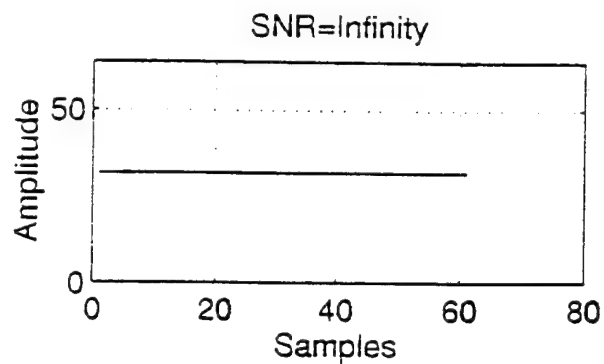


(b)

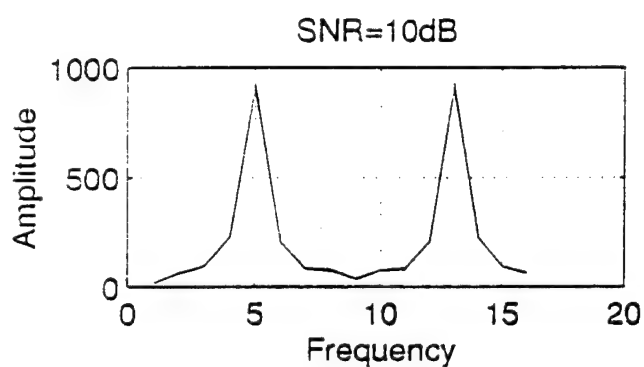
**Figure 31:** Output of Method-1 detector for BPSK signal, 0-dB SNR.



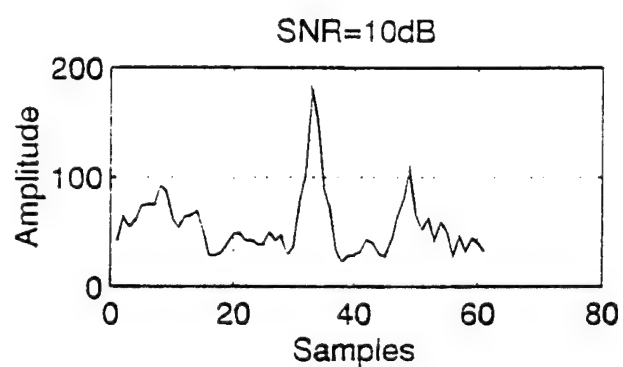
(1a)



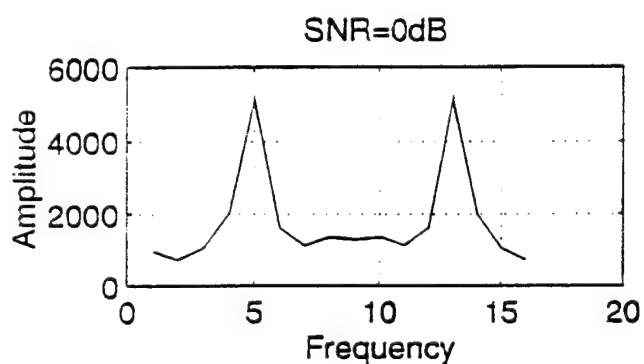
(1b)



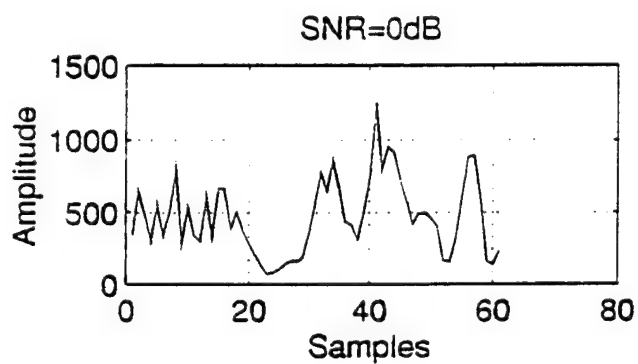
(2a)



(2b)



(3a)



(3b)

**Figure 32:** Averaged output of Method-1 detector for BPSK signal at all SNR levels.



for the noise-free case (see 1b). The output at an SNR of 10-dB (2b) and an SNR of 0-dB (3b) does not indicate the presence of a signal.

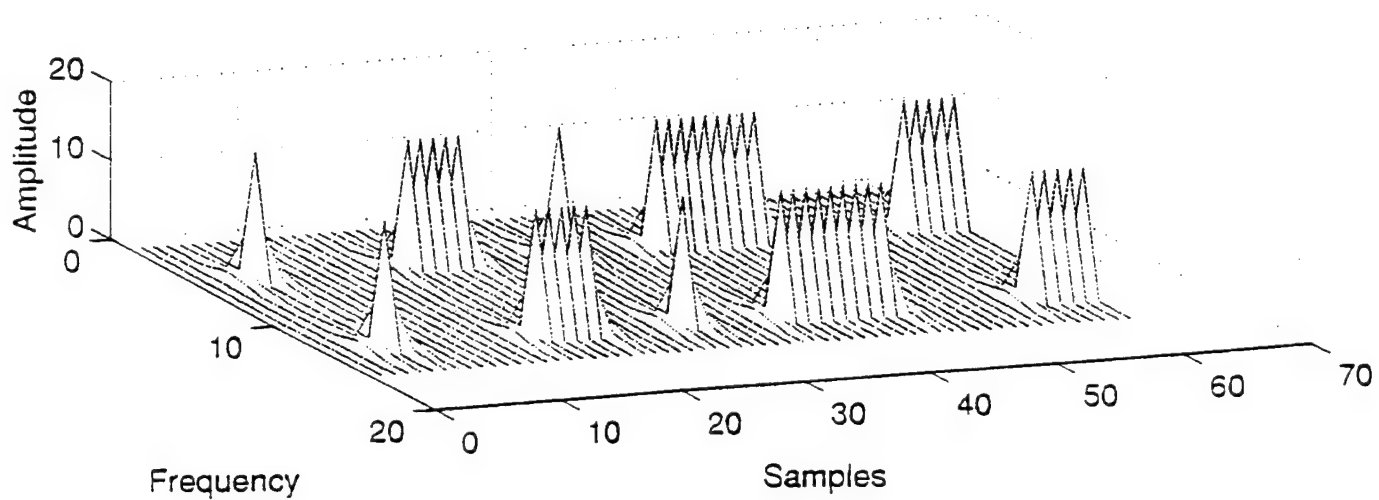
#### **b. OOK**

The output of the detector for the OOK signal without noise is shown in Figures 33a and 33b. In Figure 33a, an amplitude modulated carrier is present and the message code can be estimated. Figure 33b displays the corresponding output as a contour plot. The carrier frequency is easily verified at positions 5 and 13. The bit rate can be estimated.

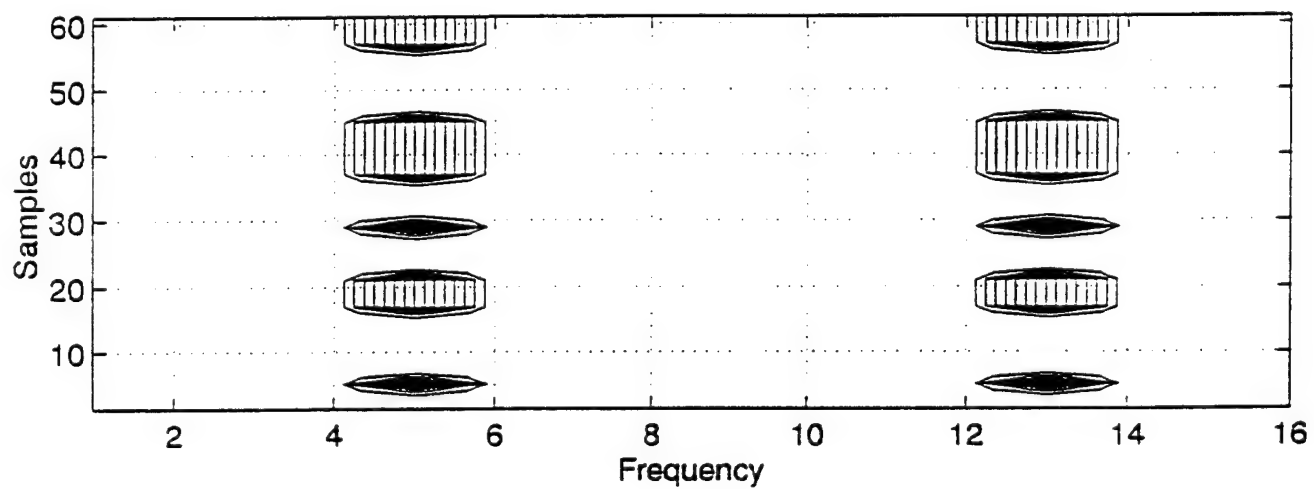
Figure 34a shows the detector output for an SNR level of 10-dB. Note that a amplitude modulation can be observed and the message code can still be estimated. Figure 34b allows carrier frequency and bit rate estimation.

The output of the detector at 0-dB SNR is shown in Figures 35a and 35b. Note that it is difficult to recognize features of an OOK signal due to the high noise level.

Figure 36 shows the output averaged over frequency and time. The time averaged output (see plot 1a for noise-free, 2a for 10-dB SNR, and 3a for 0-dB SNR) shows the presence of the signal, and the carrier frequency as well as the bandwidth can be estimated. The frequency averaged output is shown in plots 1b , 2b, and 3b. In 1b the output is noise-free and the message code can be estimated easily. The amplitude modulation can be recognized and the bit rate can be measured. In 2b, where the output has an SNR of 10-dB, OOK type modulation can still be recognized noting instants in time where the energy is minimal (i.e., no carrier). The bit rate can be estimated but the message code cannot be estimated. The frequency averaged output of the detector (3b) does not provide modulation clues under low SNR conditions (i.e., 0-dB).

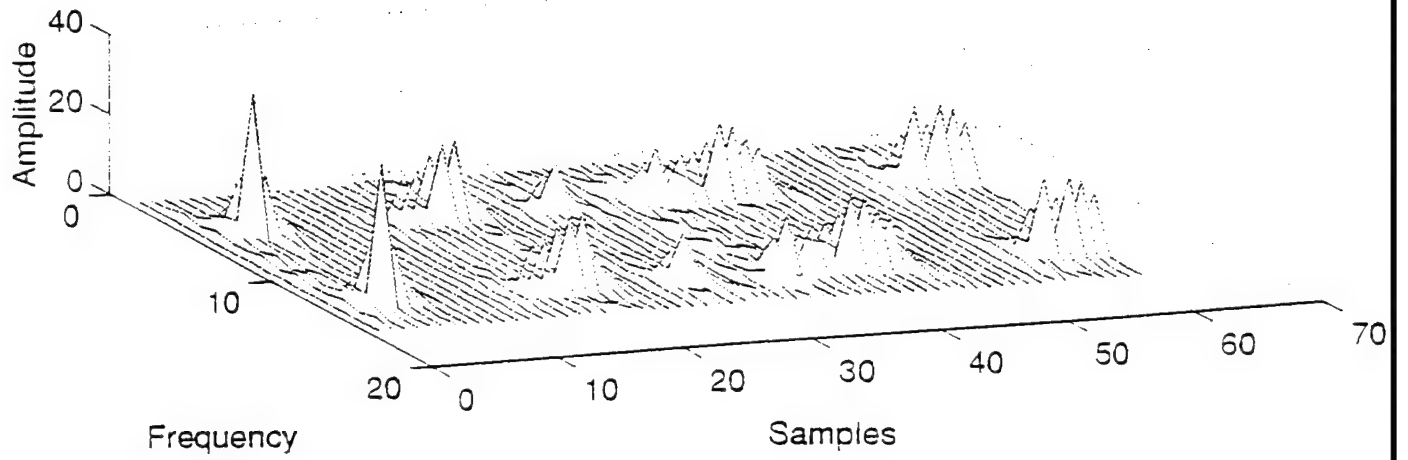


(a)

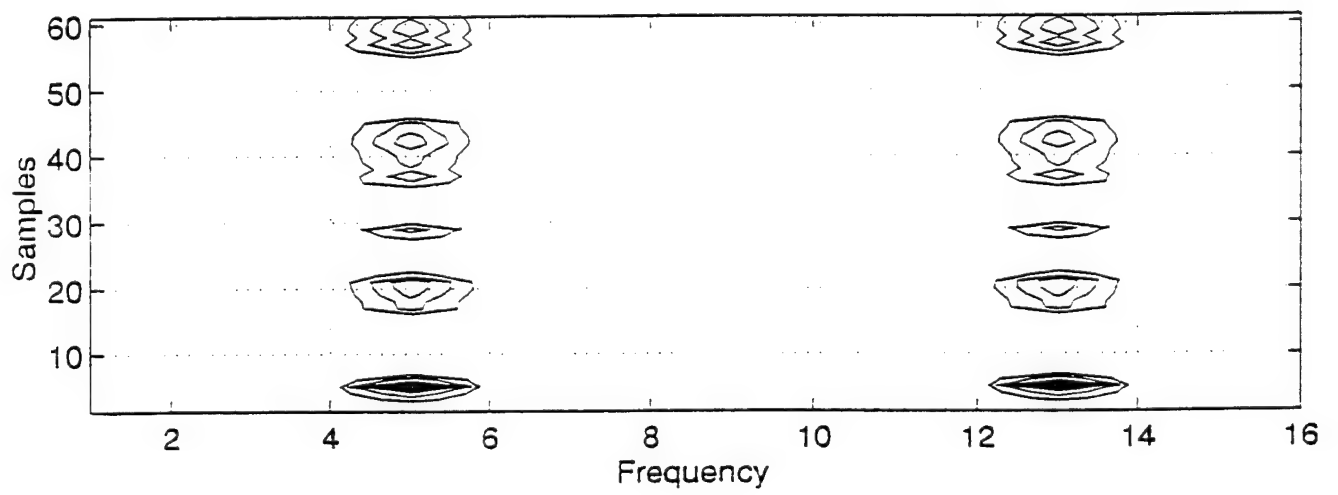


(b)

Figure 33: Output of Method-1 detector for OOK signal, no noise.

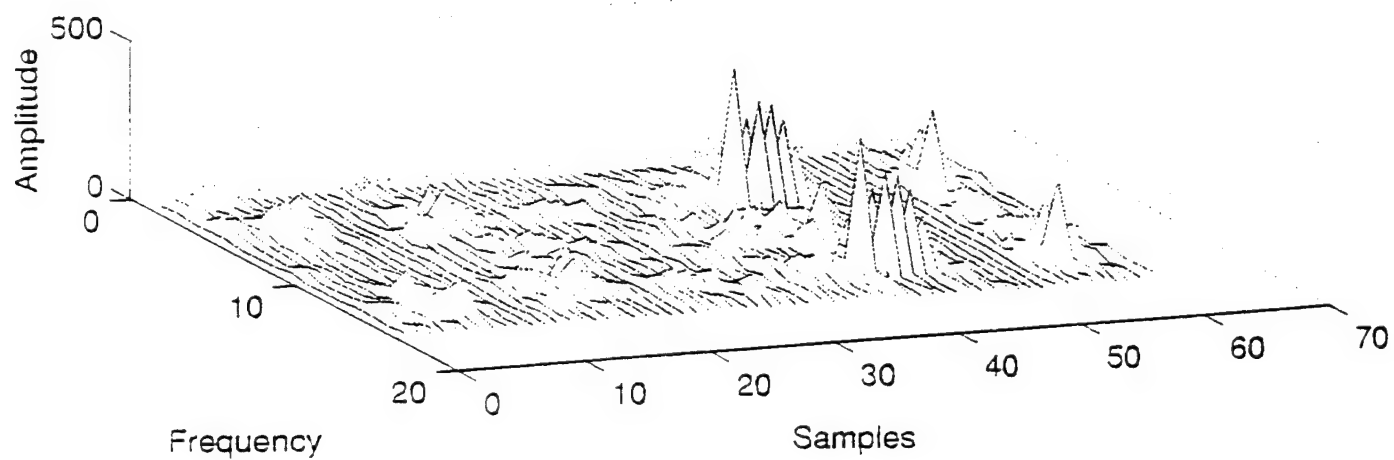


(a)

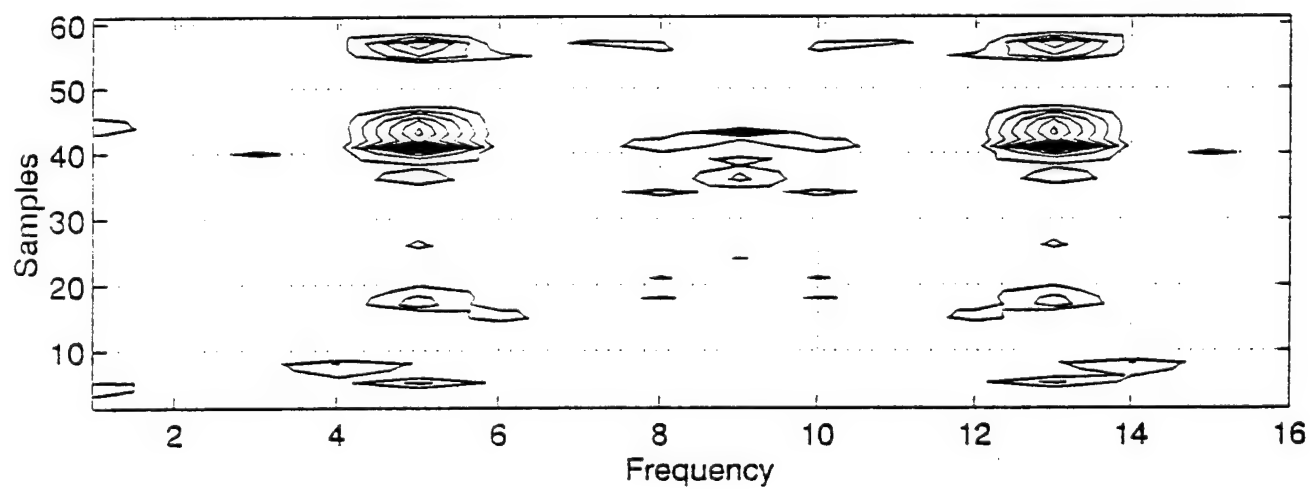


(b)

**Figure 34:** Output of Method-1 detector for OOK signal, 10-dB SNR.



(a)



(b)

Figure 35: Output of Method-1 detector for OOK signal, 0-dB SNR.

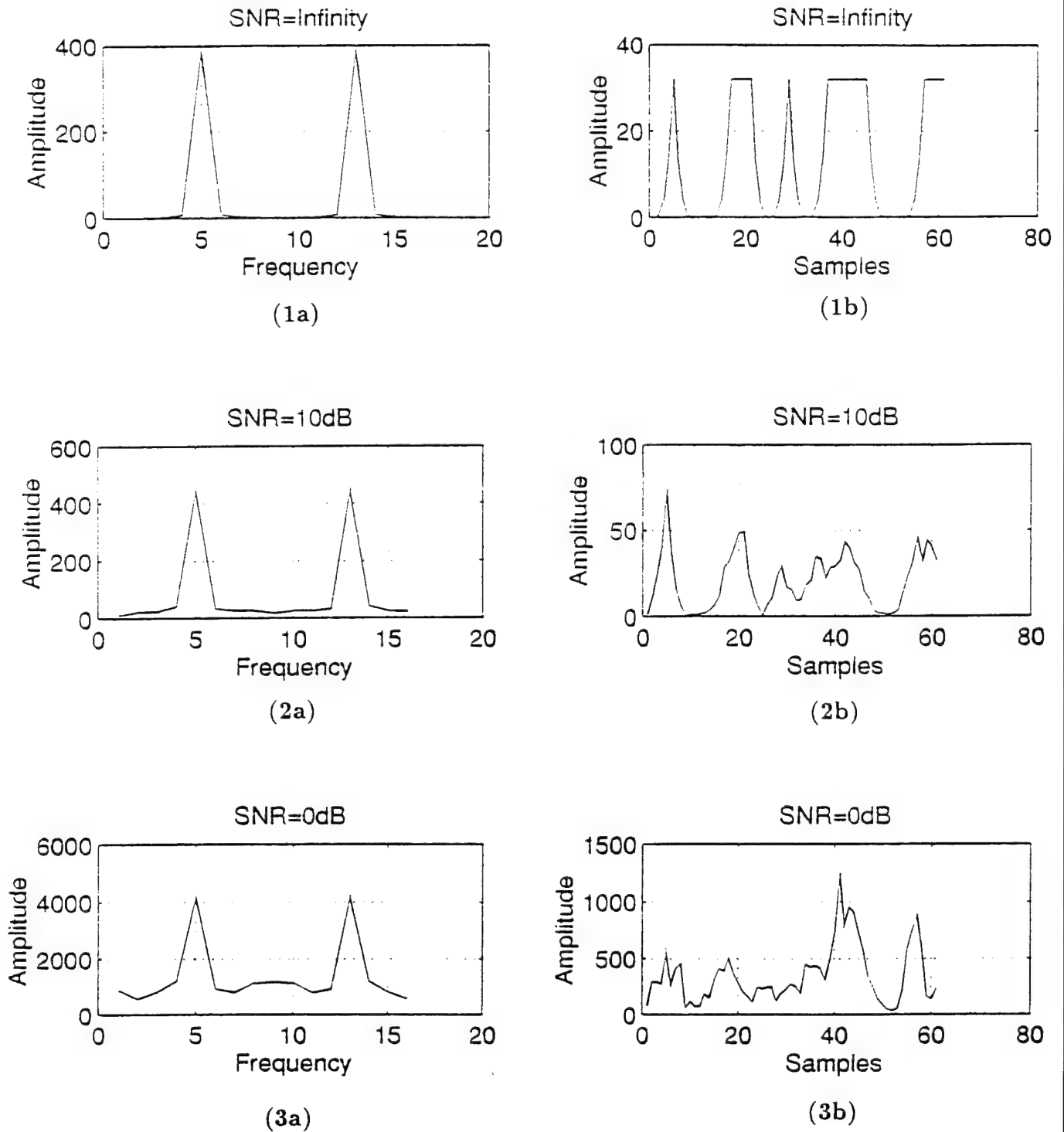


Figure 36: Averaged output of Method-1 detector for OOK signal at all SNR levels.

### c. FSK

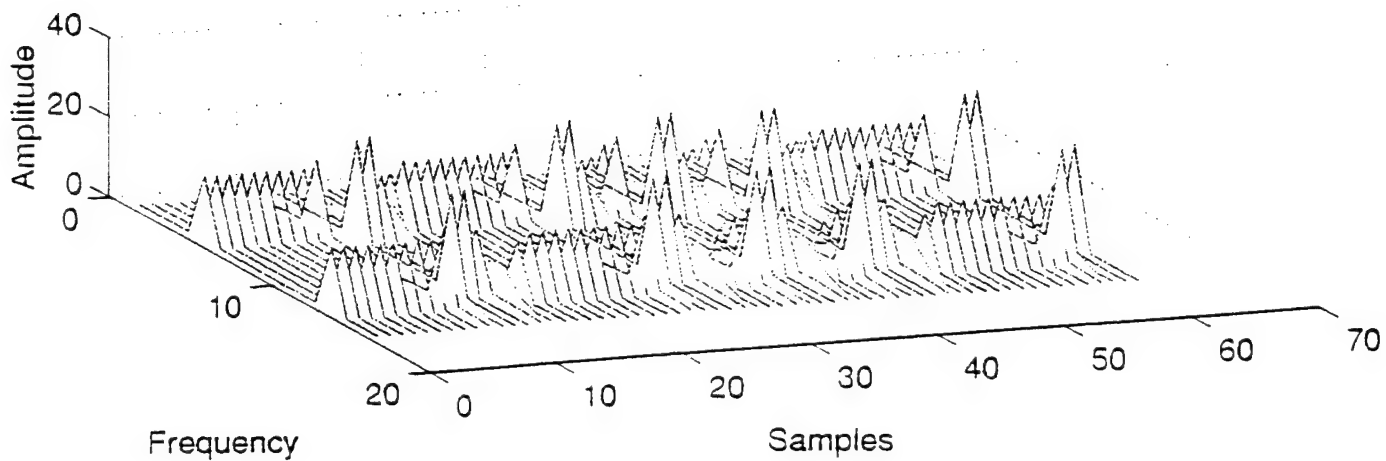
The output for the noise-free FSK signal is shown in Figure 37a. A modulated carrier with several levels of magnitude is present. Figure 37b shows the carrier frequency, shift frequency (positions 5 and 6, 12 and 13), and allows bit rate estimation. Figure 38a shows the output of the detector for an SNR of 10-dB. A modulated carrier is present. Figure 38b shows the FSK feature and allows carrier frequency estimation at spectral positions 5, 6, 12, and 13. The bit rate can still be estimated.

Figures 39a and 39b show the output for an SNR level of 0-dB. We cannot recognize the FSK modulation at this level of noise and this may lead to a misclassification of the modulation (i.e., OOK at carrier frequency spectral positions 5 and 13).

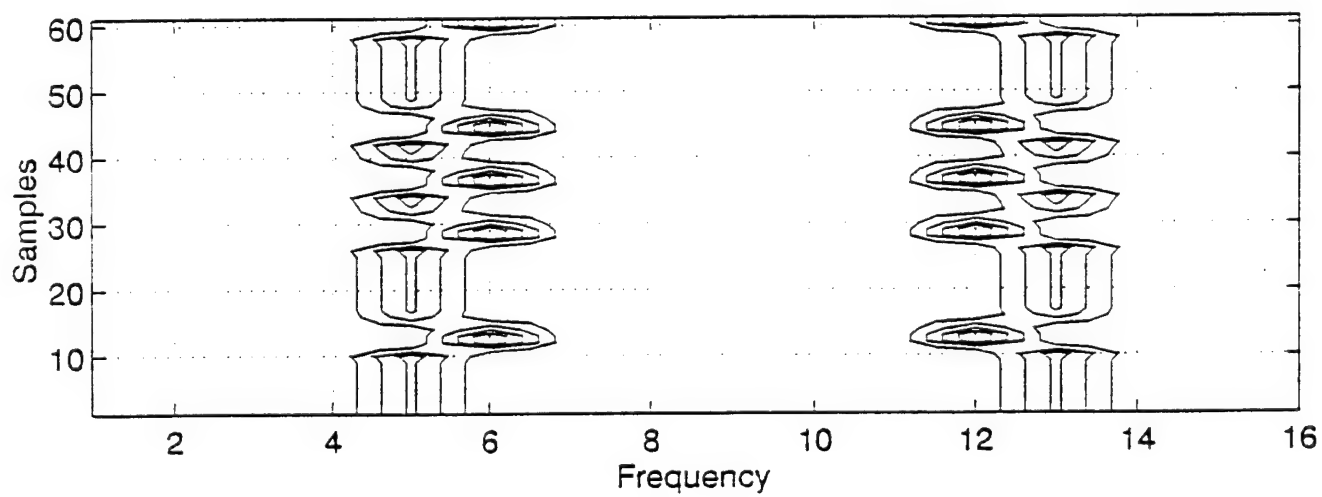
Figure 40 shows the output averaged over frequency and time. The time averaged output (see plot 1a for noise-free, 2a for 10-dB SNR, and 3a for 0-dB SNR) shows that at the different SNR considered, the carrier can be recognized having a non-symmetrical spectral shape. This indicates the presence of more than one spectral component, which is a feature of FSK. A measure of bandwidth can be obtained. The frequency averaged output (see 1b, 2b, and 3b) shows, in the noise-free case (1b), the points of the frequency shift. At 10 and 0-dB SNR even that clue disappears (see 2b for 10-dB and 3b for 0-dB).

### d. QPSK

Figure 41a shows the output of the detector for noise-free QPSK signal. It appears that there is a modulated carrier. Figure 41b shows that the bit rate estimation is possible and that transition points (i.e., phase shifts) can be identified as a  $180^\circ$  phase shift or as phase shifts of  $90^\circ$ . The carrier frequency can be estimated at spectral positions 5 and 13.

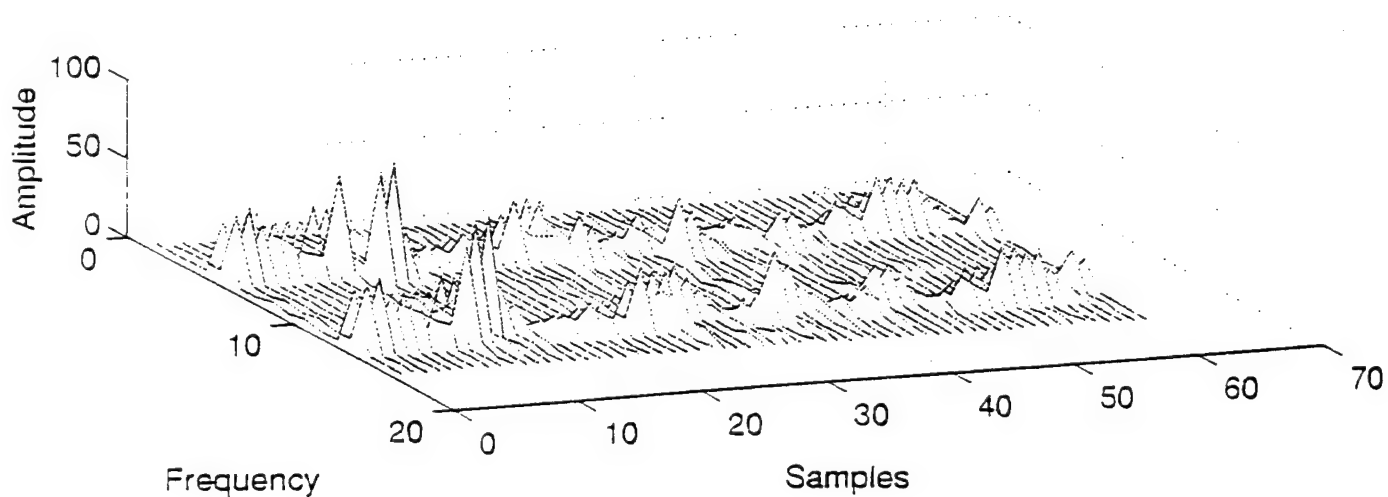


(a)

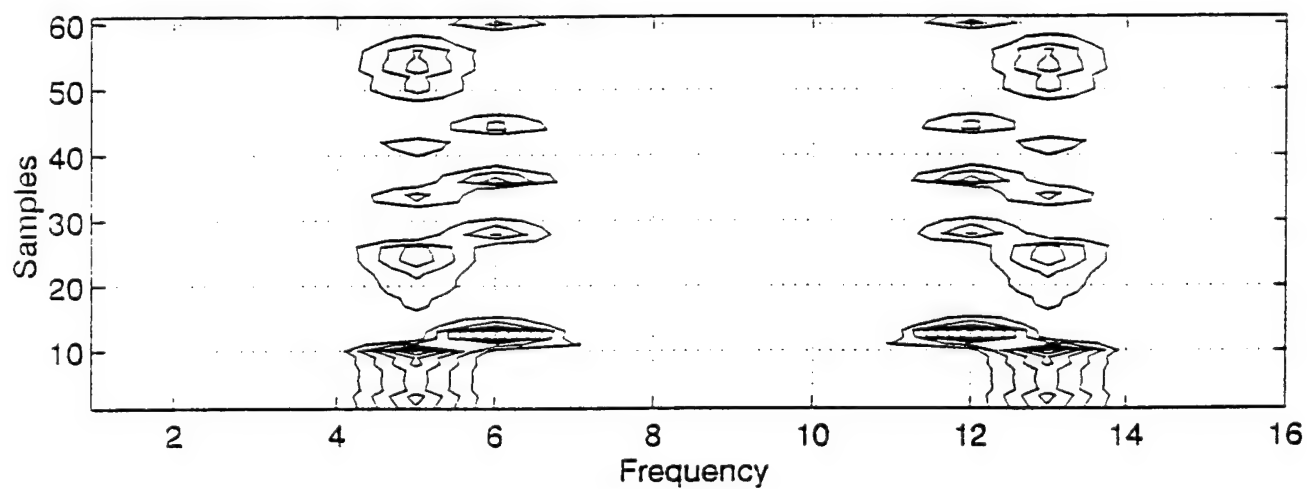


(b)

**Figure 37:** Output of Method-1 detector for FSK signal, no noise.



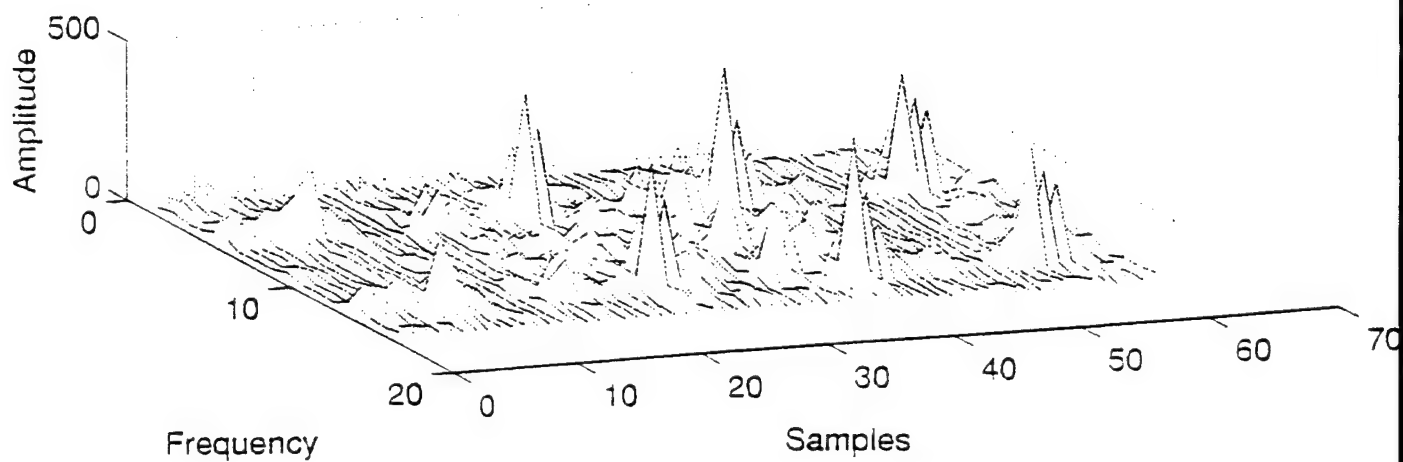
(a)



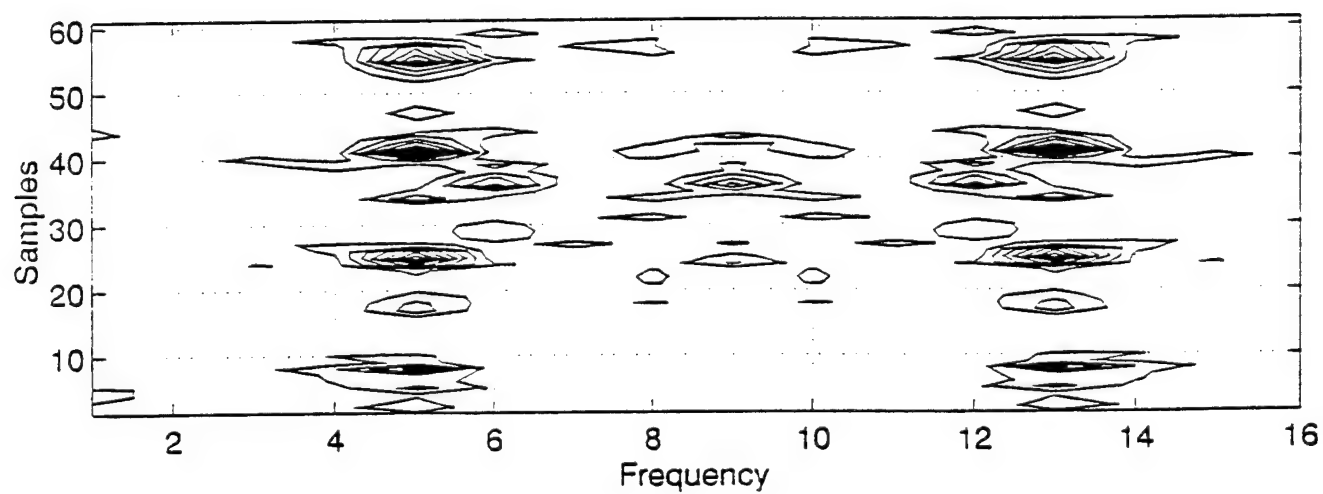
(b)

Figure 38: Output of Method-1 detector for FSK signal, 10-dB SNR.





(a)



(b)

**Figure 39:** Output of Method-1 detector for FSK signal, 0-dB SNR.

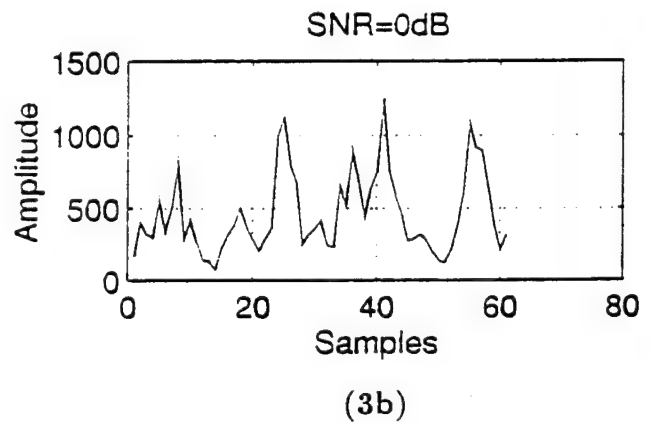
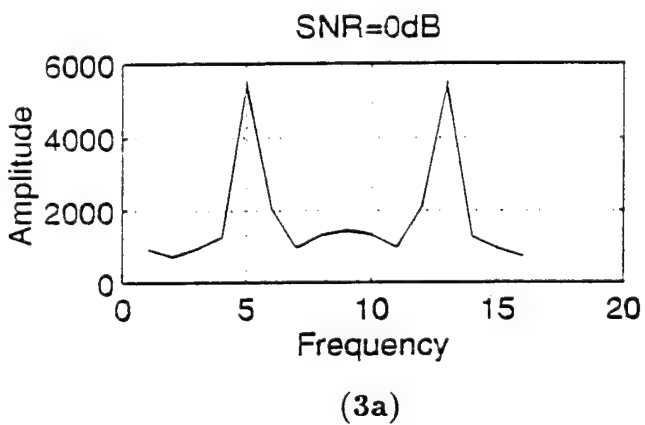
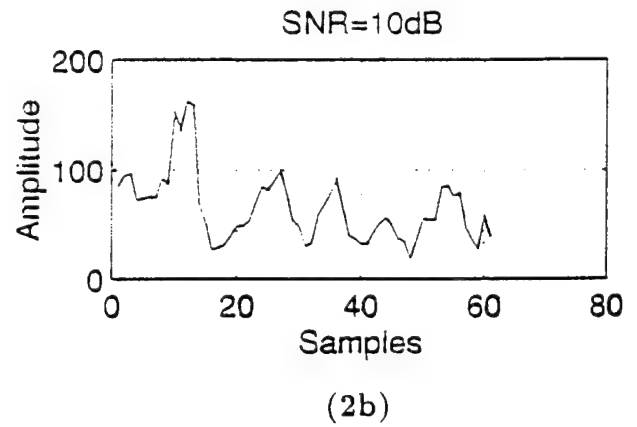
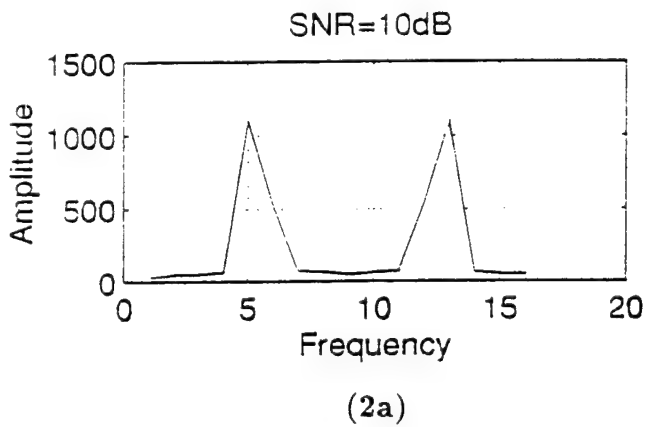
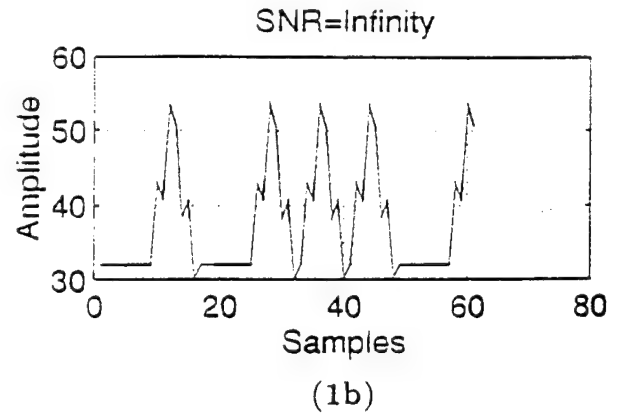
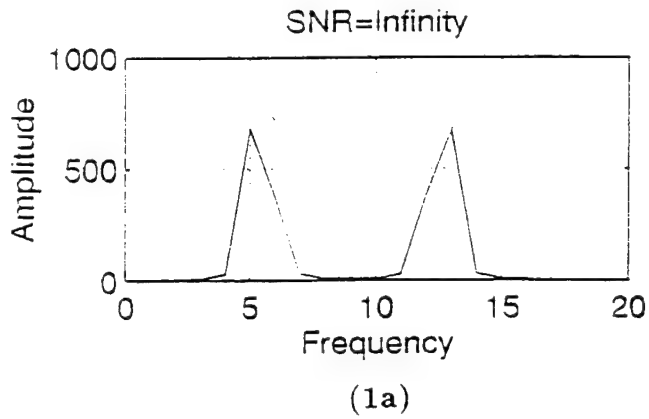
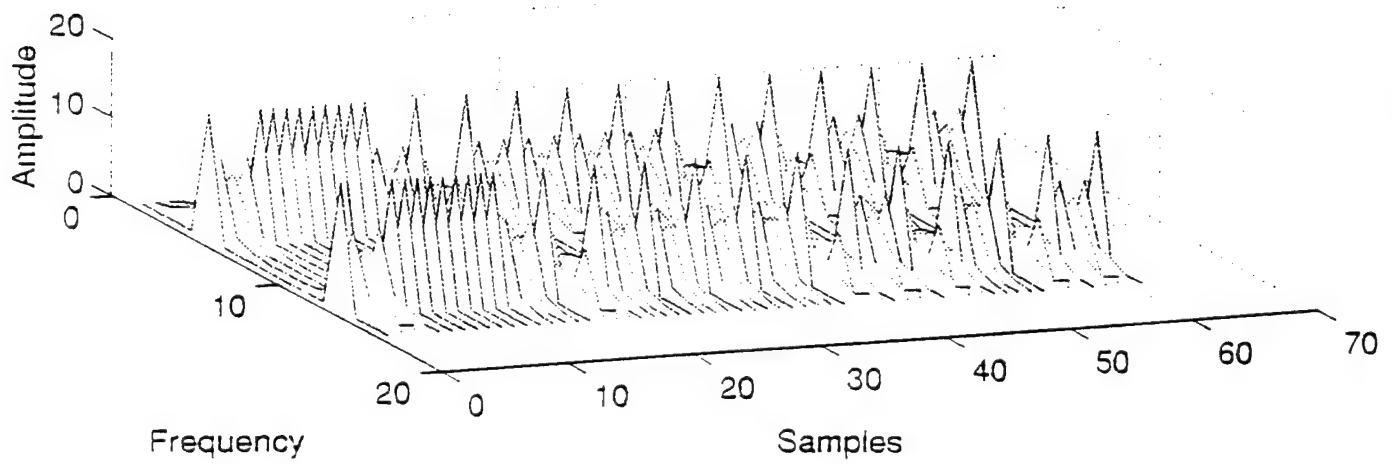
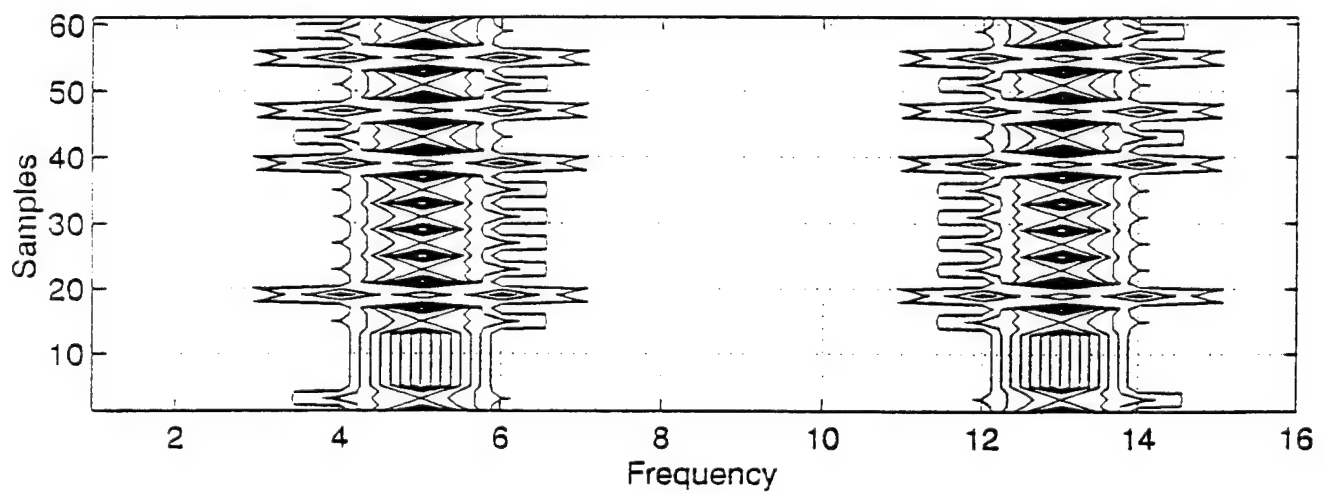


**Figure 40:** Averaged output of Method-1 detector for FSK signal at all SNR levels.



(a)



(b)

Figure 41: Output of Method-1 detector for QPSK signal, no noise.

The output of the detector for an SNR of 10-dB is shown in Figures 42a and 42b. A modulated carrier centered at spectral positions 5 and 13 is present. Figure 42b also allows an OOK interpretation at carrier frequency 5 and 13.

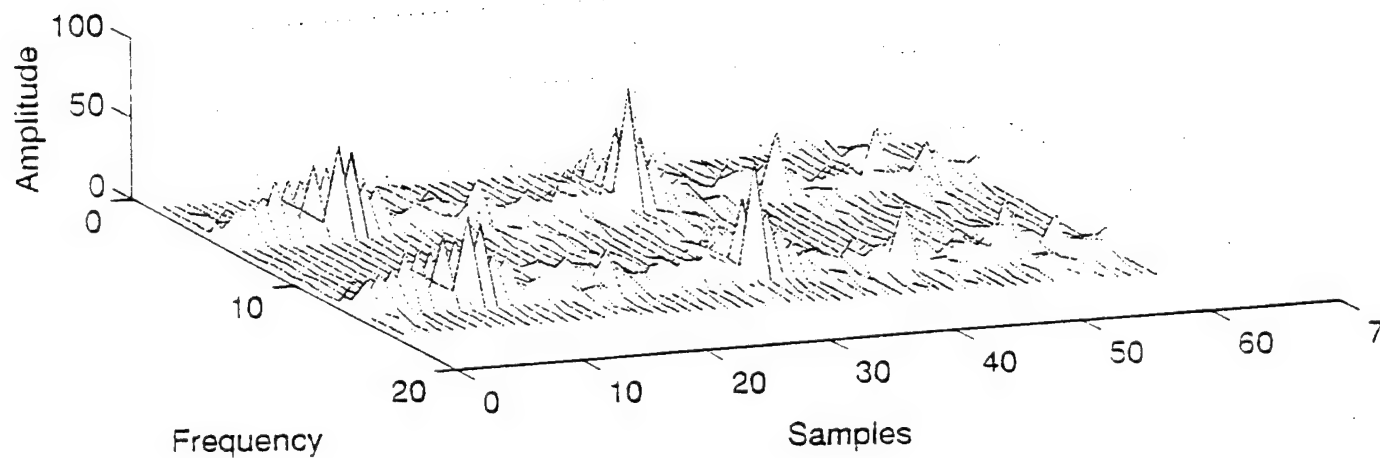
Figures 43a and 43b show the output of the detector for an SNR of 0-dB, indicating that it is difficult to recognize QPSK at this low SNR level.

Figure 44 shows the output averaged over frequency and time. The time averaged output (see plot 1a for noise-free, 2a for 10-dB, and 3a for 0-dB) shows that the carrier frequency can be identified and the bandwidth can be estimated. The frequency averaged output is shown in plots 1b, 2b, and 3b. For the noise-free signal (see 1b) a constant energy is shown. For 10 and 0-dB SNR output (see 2b, 3b, respectively), the signal completely vanishes and it appears that only noise is present.

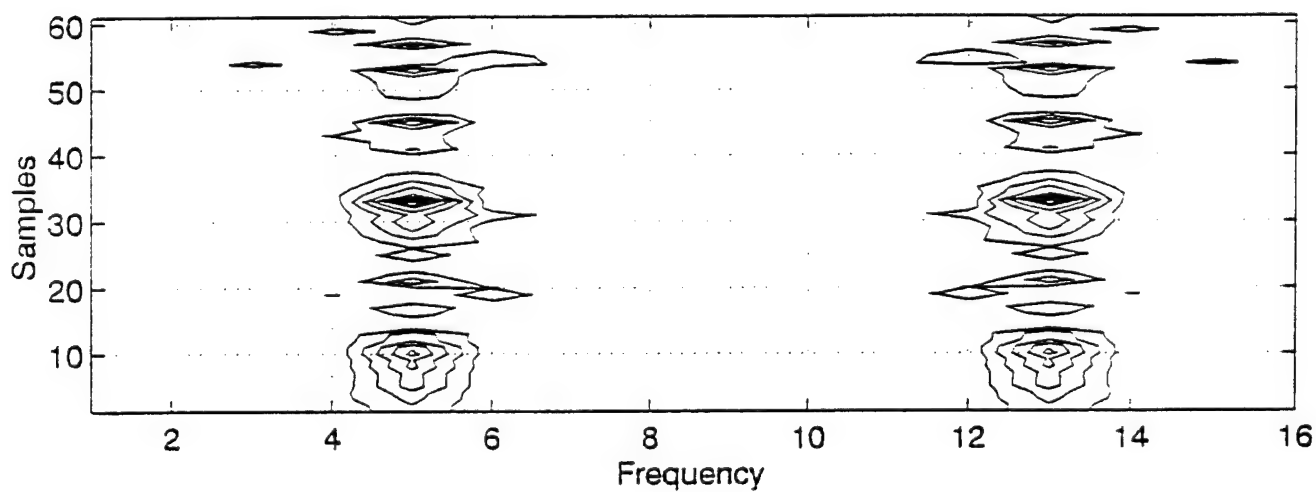
From the analysis of the magnitude of the method-1 outputs, we note that there is no apparent difference in performance between the FFT based detector and method-1 even though some estimated parameters differ slightly.

## **2. Method-2**

As mentioned earlier (Eq. 6), this method is related to WVD and is based on the Fourier transform of lagged products (over time  $n$ ). The most distracting property of WVD is that it can have spectral components in regions where one would expect none. These spurious values, which are due to the so-called cross terms, are particularly prevalent in multi-component signals. Noise, of course, is the superposition of many signals, hence causing recognition problems. We are not using any method to minimize or filter out this effect at this time. The Choi-Williams method is one approach to deal with this problem [10]. This problem will manifest itself in the detector output. To suppress the amplitude belonging to the negative frequency, complex envelopes of the signal are used in the program. Note that the reason the signal appears at twice the carrier frequency is that we use the product of two signals in the time

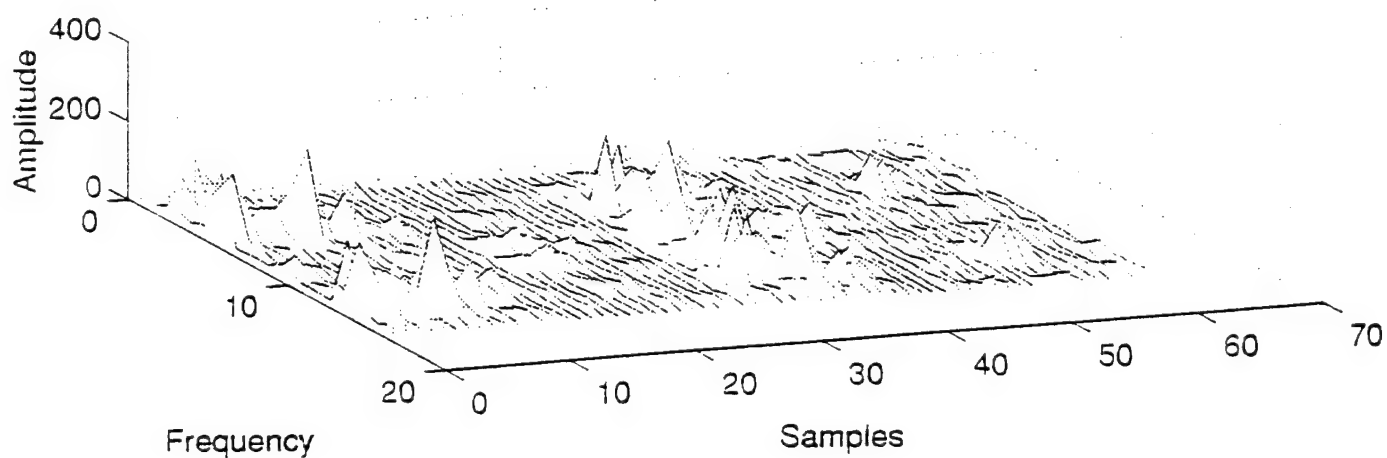


(a)

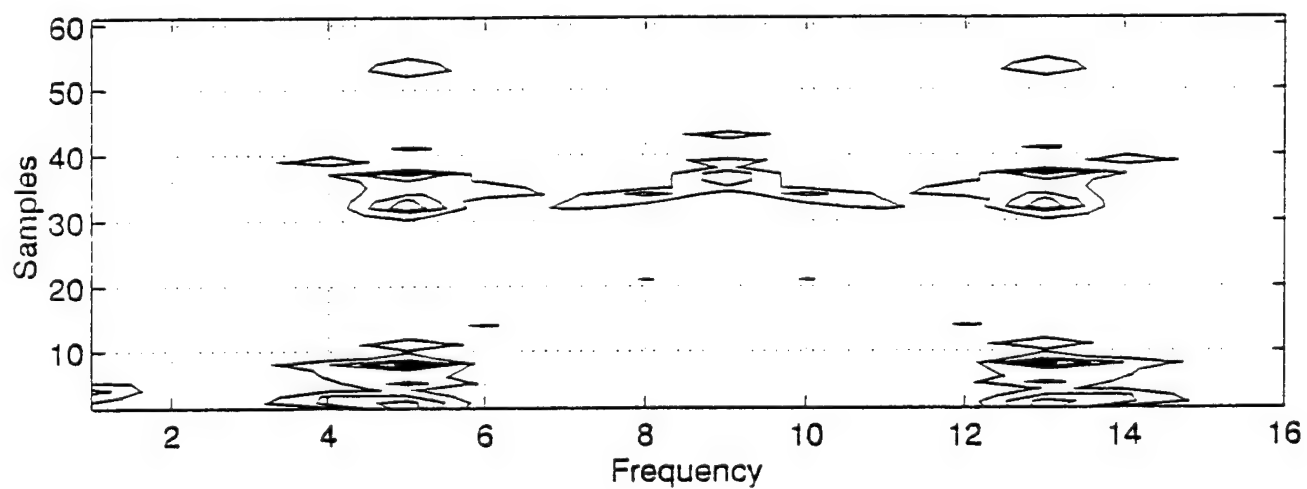


(b)

Figure 42: Output of Method-1 detector for QPSK signal, 10-dB SNR.



(a)



(b)

**Figure 43:** Output of Method-1 detector for QPSK signal, 0-dB SNR.

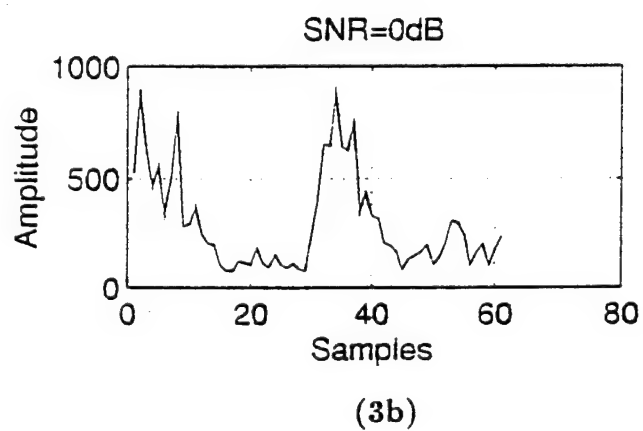
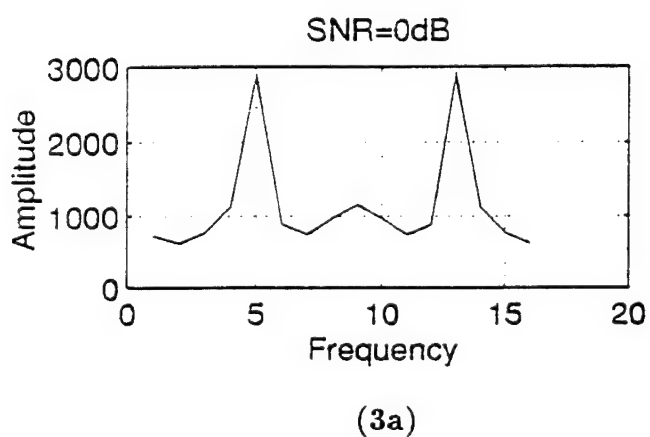
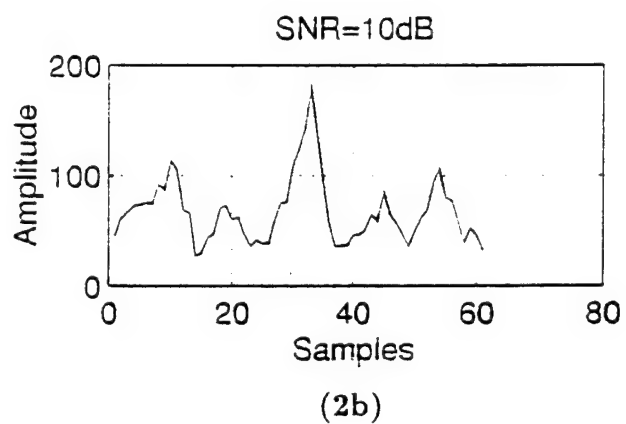
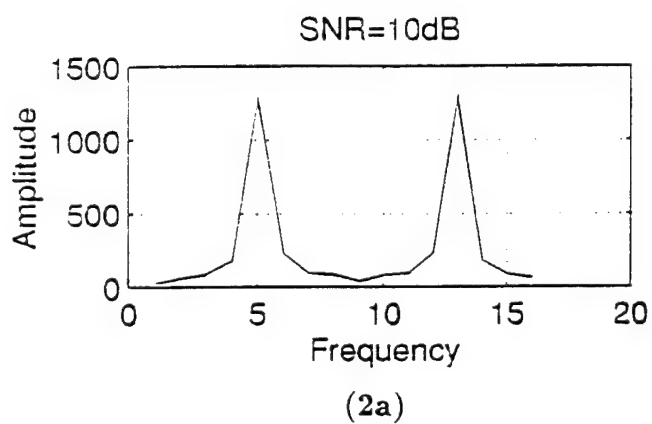
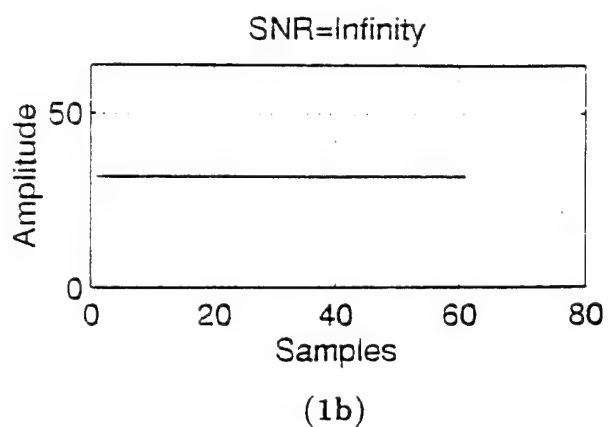
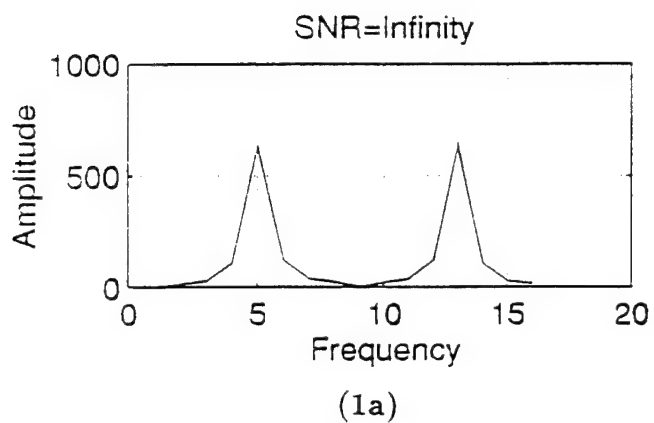


**Figure 44:** Averaged output of Method-1 detector for QPSK signal at all SNR levels.

domain and, as expected, in the frequency domain we have components at the DC value and at double the carrier frequency (i.e.,  $\sin^2(\omega t) = 1/2[1 - \cos(2\omega t)]$ ).

The output of this detector is presented using two types of plots. First, contour plots are shown in Figures 45 through 47, 49 through 51, 53 through 55, and 57 through 59. Second, outputs averaged over time (see plots 1a, 2a, and 3a) and over frequency (see plots 1b, 2b, and 3b), are given in Figures 48, 52, 56, and 60. Due to the selection of the values of the parameter  $m$ , the frequency averaged outputs display a non-symmetry and the number of computations reduce by a factor of 2, with delay, in the range  $-127$  to  $+127$  with a step size of 2.

#### a. BPSK

Figure 45 shows the output of the detector for a BPSK signal without noise. Note the presence of broadband energy between spectral positions 120 and 140, with a center frequency about 130. A symmetric pattern is present along the delay axis between the two limits on the frequency axis. This pattern consists of isolated high intensity segments. The size of the segment is not equal or uniform, possibly because of the selection size of variable  $m$ . Thus, it is difficult to relate this to the bit rate or phase shift.

Figure 46 shows the output of the detector for an SNR level of 10-dB. We note that the presence of broadband energy between the approximate limits. The symmetric pattern is still present.

Figure 47 shows the output at an input SNR level of 0-dB. Note that some of the pattern is still present and noise and cross terms are now dominant about the center frequency.

Figure 48 (see 1a, 2a, and 3a) represents the time averaged output for different levels of SNR. In 1a we note the presence of a carrier frequency and spectral spikes. The bandwidth can be estimated. The presence of discrete spectral



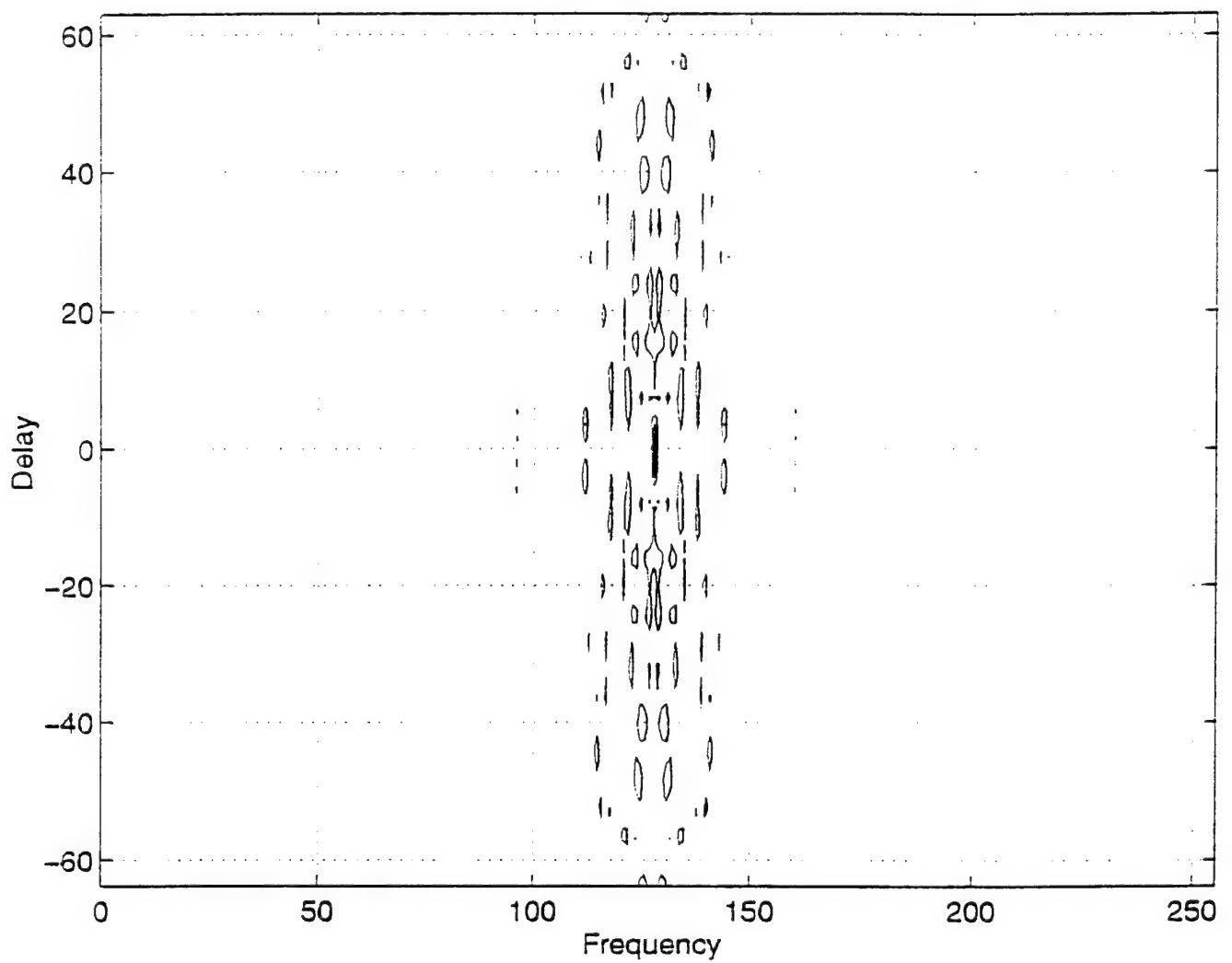
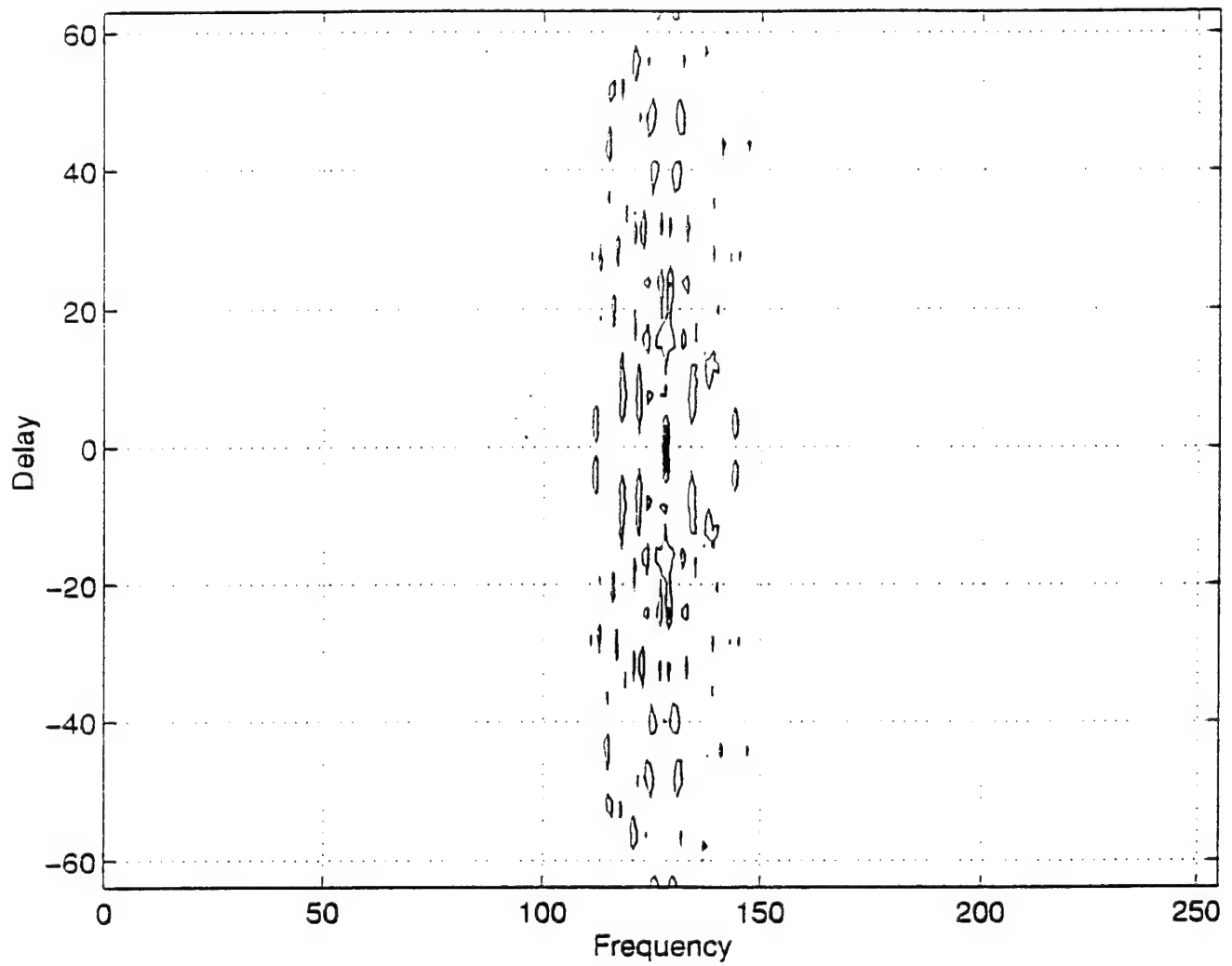


Figure 45: Output of Method-2 detector for BPSK signal, no noise.



**Figure 46:** Output of Method-2 detector for BPSK signal, 10-dB SNR.

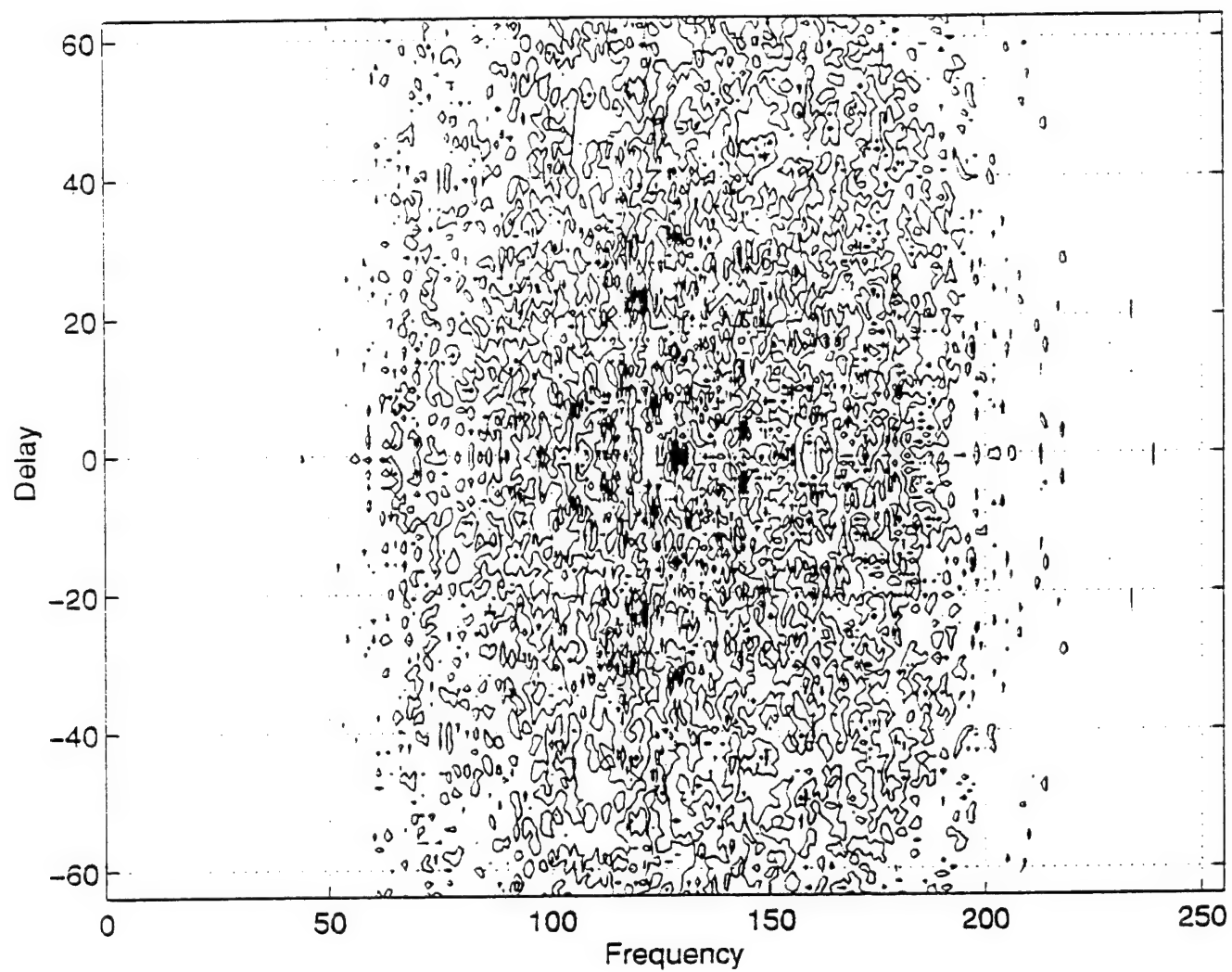
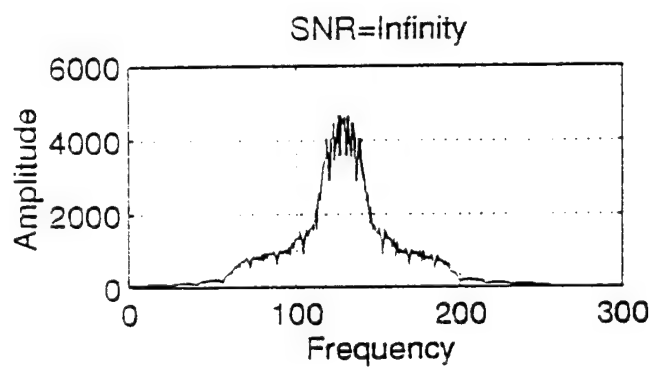
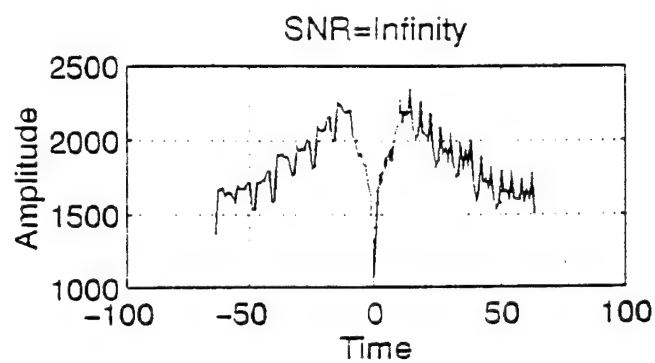


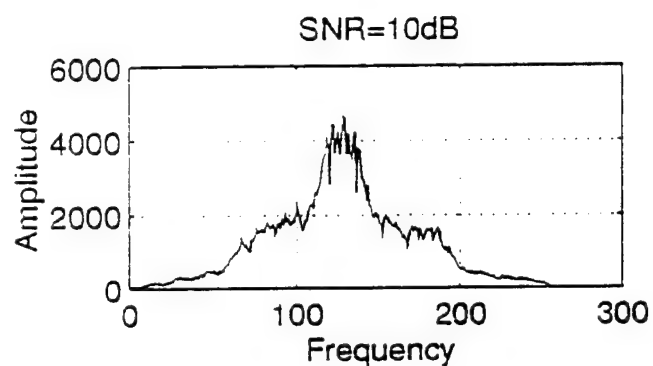
Figure 47: Output of Method-2 detector for BPSK signal, 0-dB SNR.



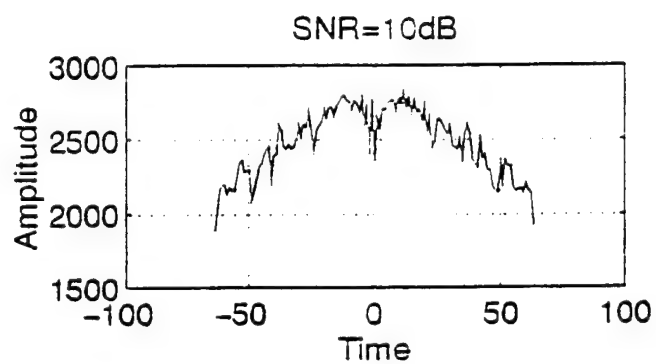
(1a)



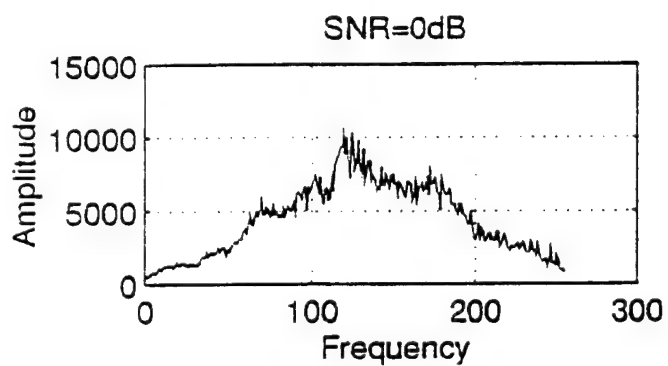
(1b)



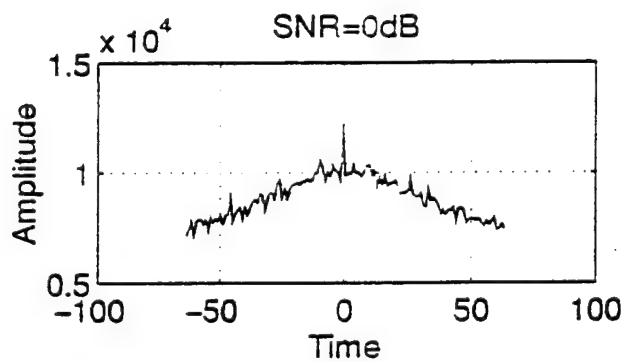
(2a)



(2b)



(3a)



(3b)

Figure 48: Averaged output of Method-2 detector for BPSK signal at all SNR levels.

components may be due to the cross terms of the WVD. In 2a we get a similar result as 1a, but, in 3a the level of noise masks the signal completely. The frequency averaged output (see 1b, 2b, and 3b) provides no information at any SNR level.

#### **b. OOK**

Figure 49 shows the output of the detector using an OOK input signal under noise-free conditions. Note the presence of broadband energy between positions 120 and 140 along the frequency axis, with the center frequency at spectral position 130. A symmetric pattern of high density segments of energy can be identified concentrated at the center frequency. Patterns of this form may indicate OOK type modulation.

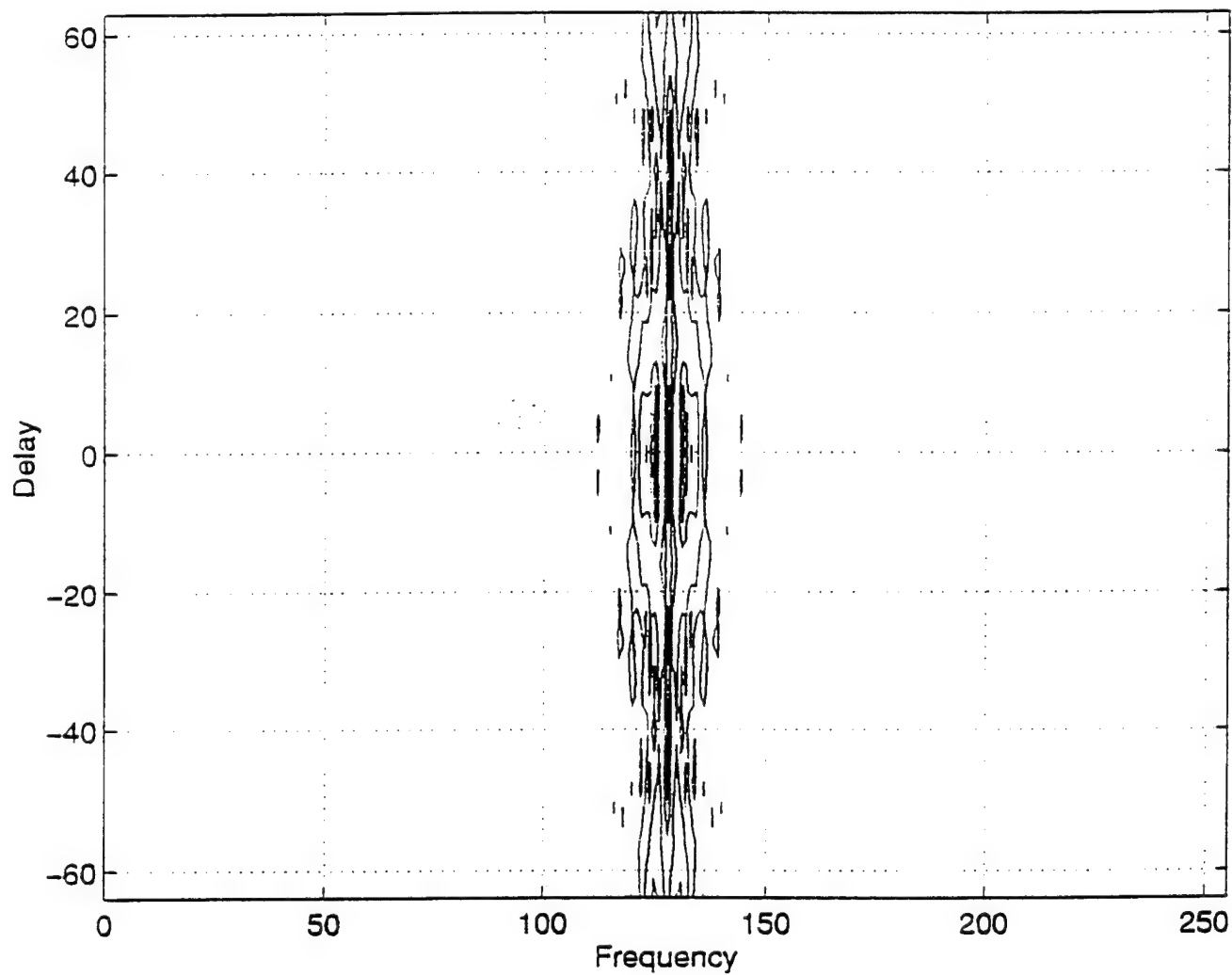
Figure 50 shows the output for an SNR level at 10-dB. Even at this level of noise, patterns similar to the ones obtained in Figure 49 can be obtained.

Figure 51 shows the output for an SNR level of 0-dB. Note that at this level of noise most of the signal is masked.

Figure 52 shows the output averaged over time and frequency. The time averaged output (see 1a) under noise-free condition shows a strong spectral component at location 130. The spectrum of the signal seems to be noisy, which may be due to cross terms. The bandwidth can be estimated. At an SNR of 10-dB (see 2a), the spectral component can be recognized with a peak at the appropriate center frequency. The strength of the cross terms are more evident. At an 0-dB SNR level there is no trace of a signal. The frequency averaged output (see 1b, 2b, and 3b) provide no useful clues.

#### **c. FSK**

Figure 53 shows the output of the detector for an FSK signal without noise. Broadband energy is present between spectral positions 120 and 170. Equidistant spectral components exist with spacing equal to six bins on the frequency



**Figure 49:** Output of Method-2 detector for OOK signal, no noise.

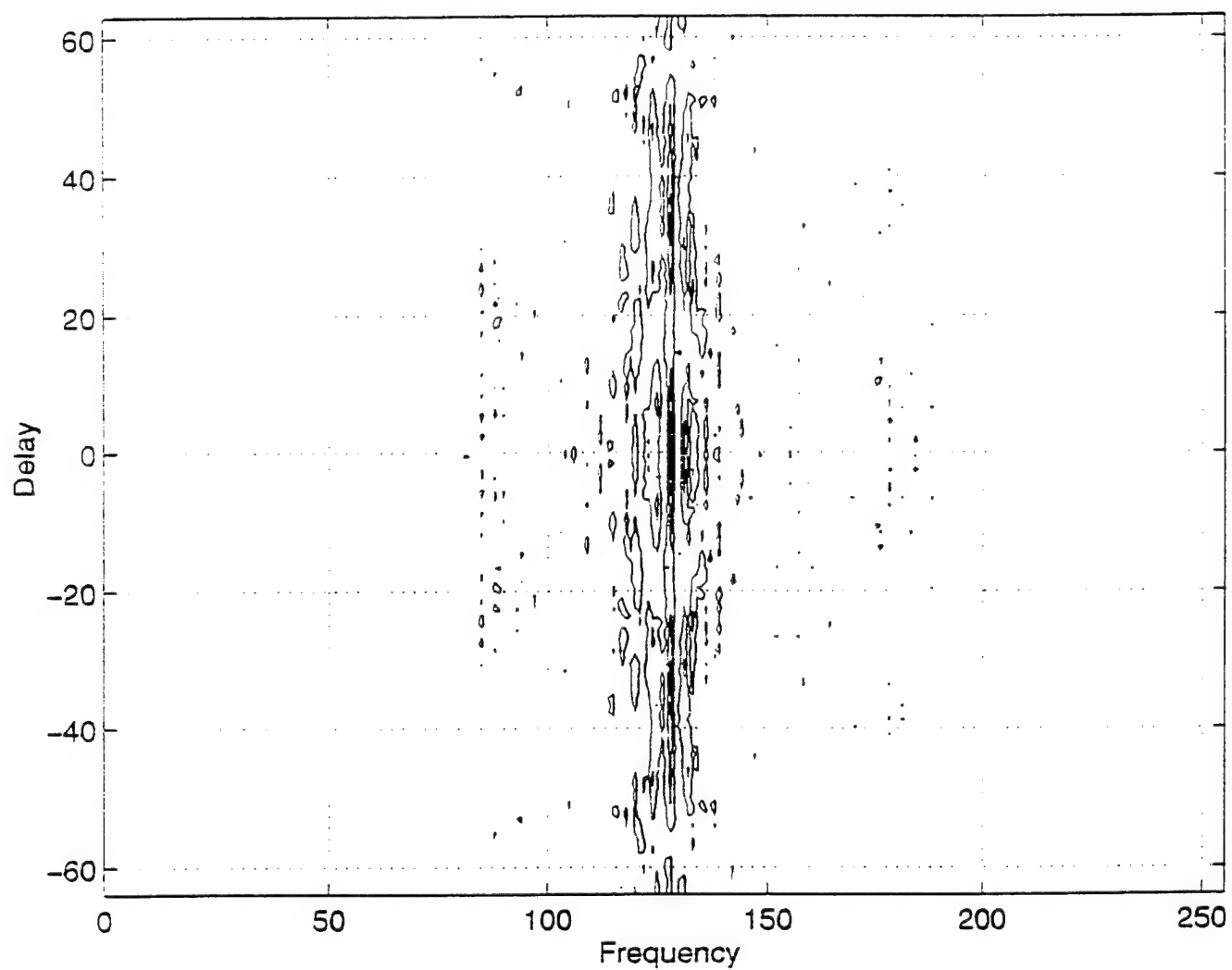


Figure 50: Output of Method-2 detector for OOK signal, 10-dB SNR.

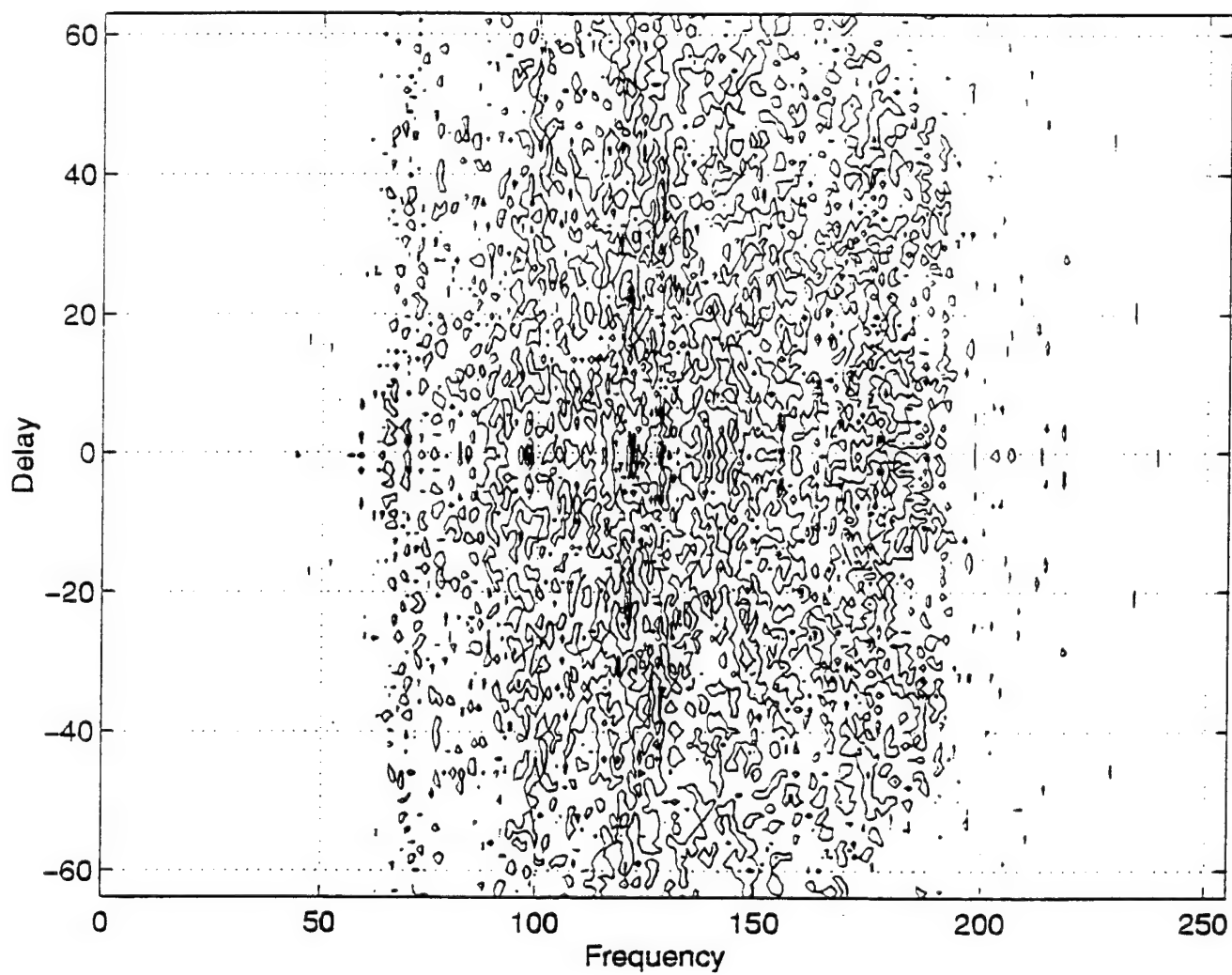
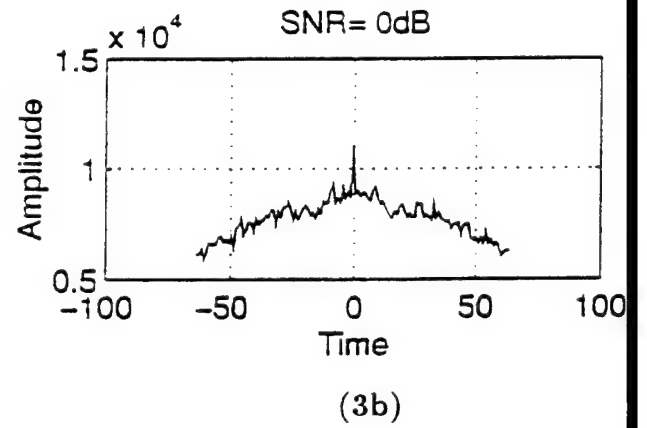
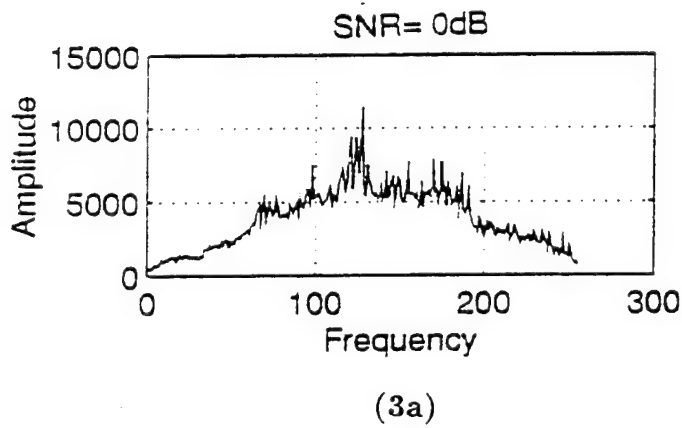
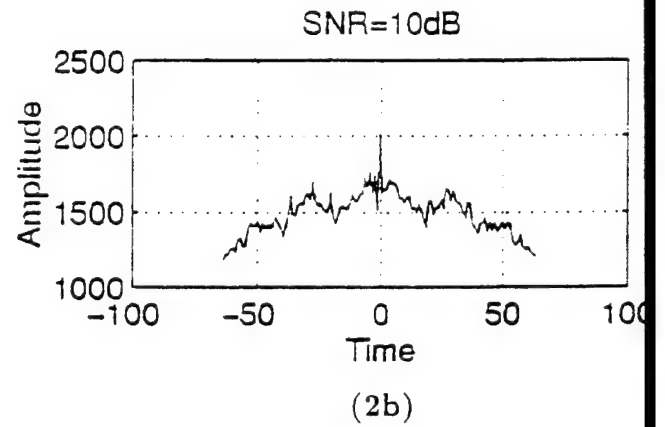
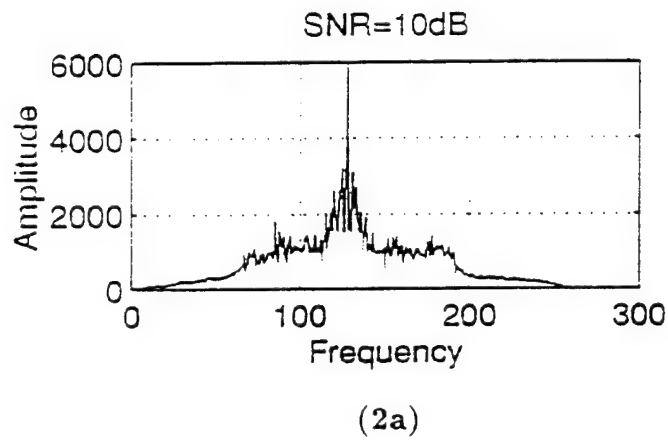
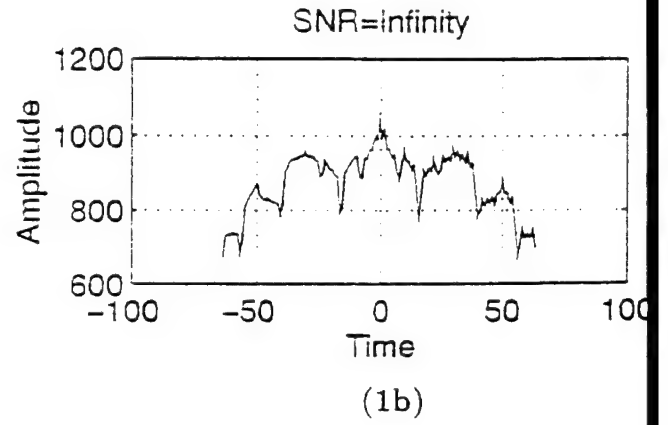
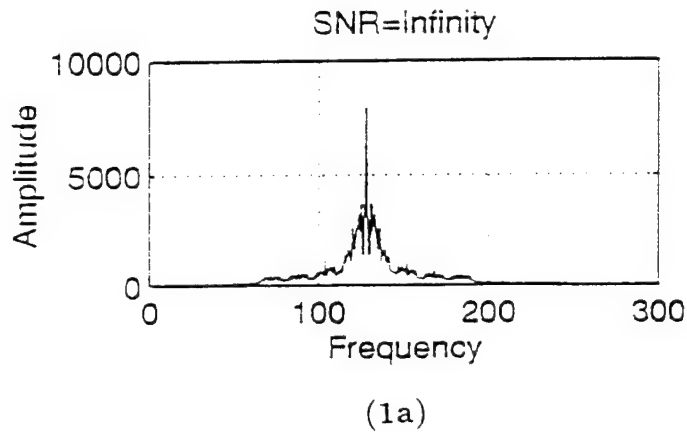


Figure 51: Output of Method-2 detector for OOK signal, 0-dB SNR.





**Figure 52:** Averaged output of Method-2 detector for OOK signal at all SNR levels.

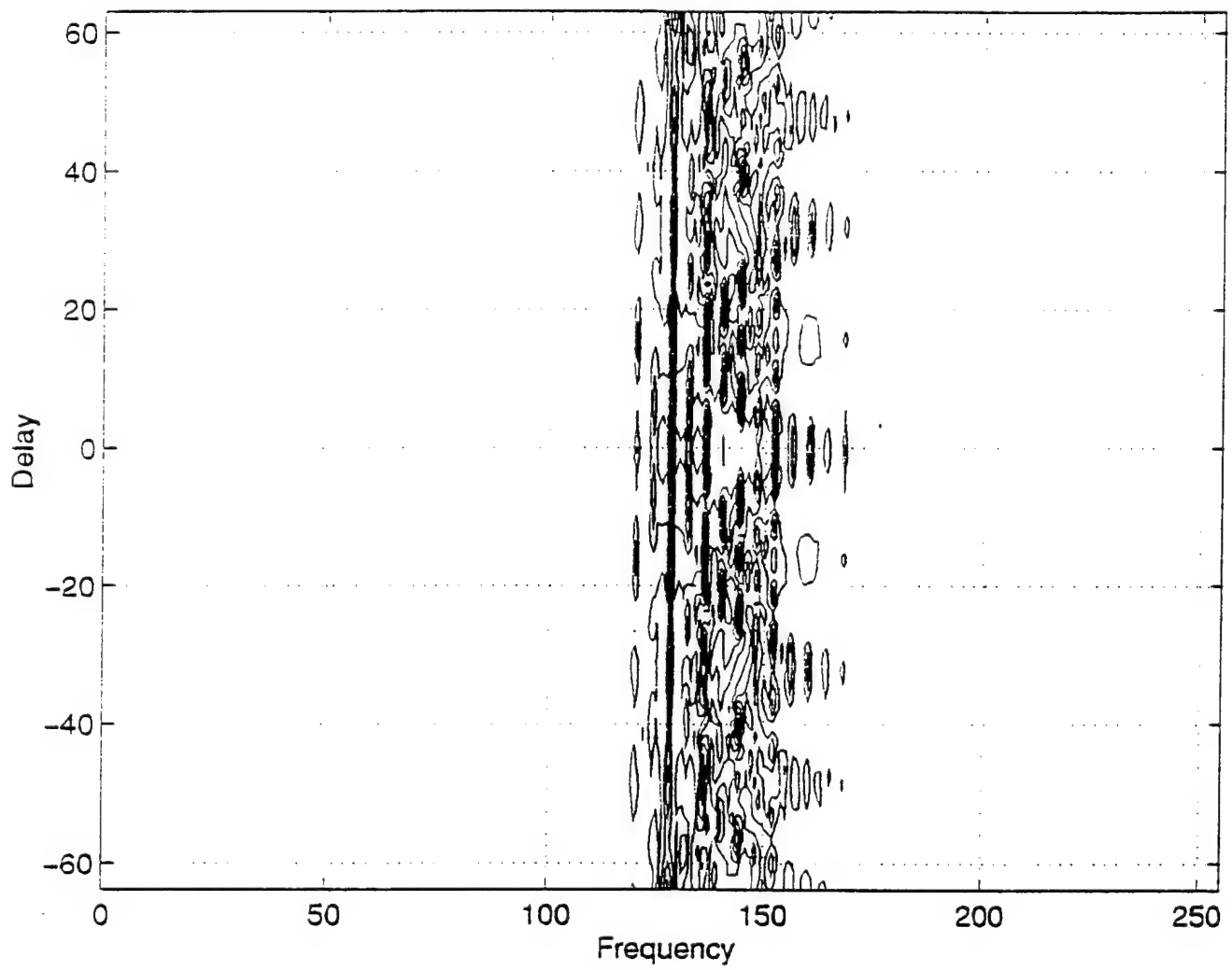


Figure 53: Output of Method-2 detector for FSK signal, no noise.

axis. This corresponds to the bit rate of the modulating signal. Simulation shows a strong sensitivity of these spectral peaks to the number of transitions in the original message (i.e., modulation index). Also, the cross terms seem to be present. Segment shapes between spectral positions 130 and 170 show a cosine squared behavior along the delay axis. Figure 54 shows the output of the detector at an SNR level of 10-dB. Results similar to those found in Figure 53 are evident. Figure 55 shows the output of the detector at 0-dB SNR. There are still some high energy segments of spectral components recognizable along the delay axis, which may be used for modulation identification.

Figure 56 shows the output averaged over time (see 1a, 2a, and 3a) and frequency (1b, 2b, and 3b) at different SNRs. At noise-free conditions, the time averaged output (see 1a) shows the presence of spectral components with constant spacing corresponding to the bit rate. At an SNR of 10-dB (2a), the spectral components can still be recognized and the bit rate can be estimated. At an SNR level of 0-dB some of the spectral components are still present and the bit rate can still be estimated. The averaged frequency plots (see 1b, 2b, and 3b) convey no information about the modulation.

#### **d. QPSK**

Figure 57 shows the output of the detector for a QPSK signal without noise. Broadband energy between spectral positions 100 and 170 is present. The dominant spectral components seem to be centered at location 125. A symmetric pattern along both axes and some high energy spots at the center frequency can be recognized. Figure 58 shows the output for a signal with 10-dB SNR. The signal related energy is concentrated between positions 120 and 140 and the noise is concentrated between positions 70 and 180. Figure 59 shows the detector output at an SNR level of 0-dB. The features of the signal have disappeared completely.

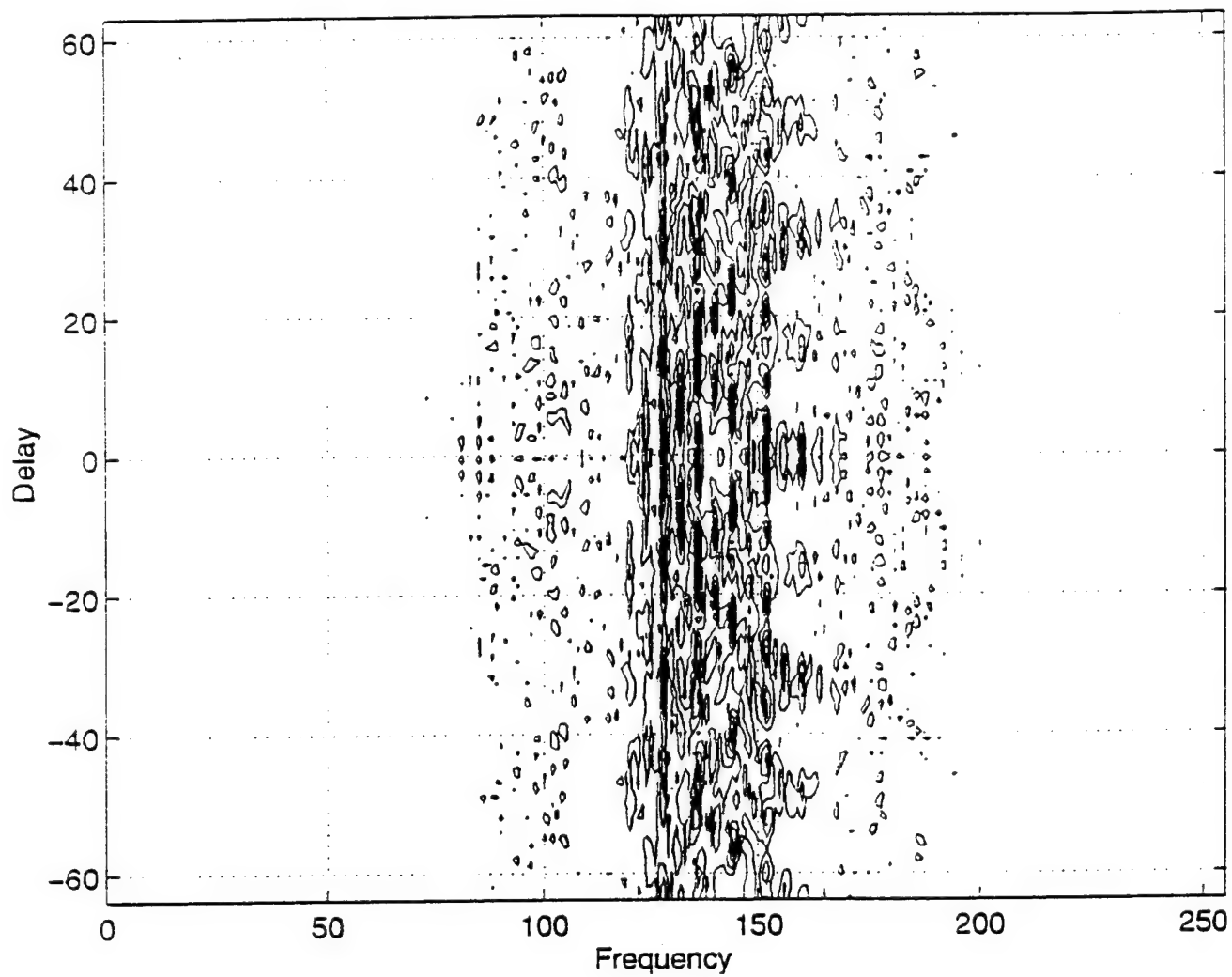


Figure 54: Output of Method-2 detector for FSK signal. 10-dB SNR.

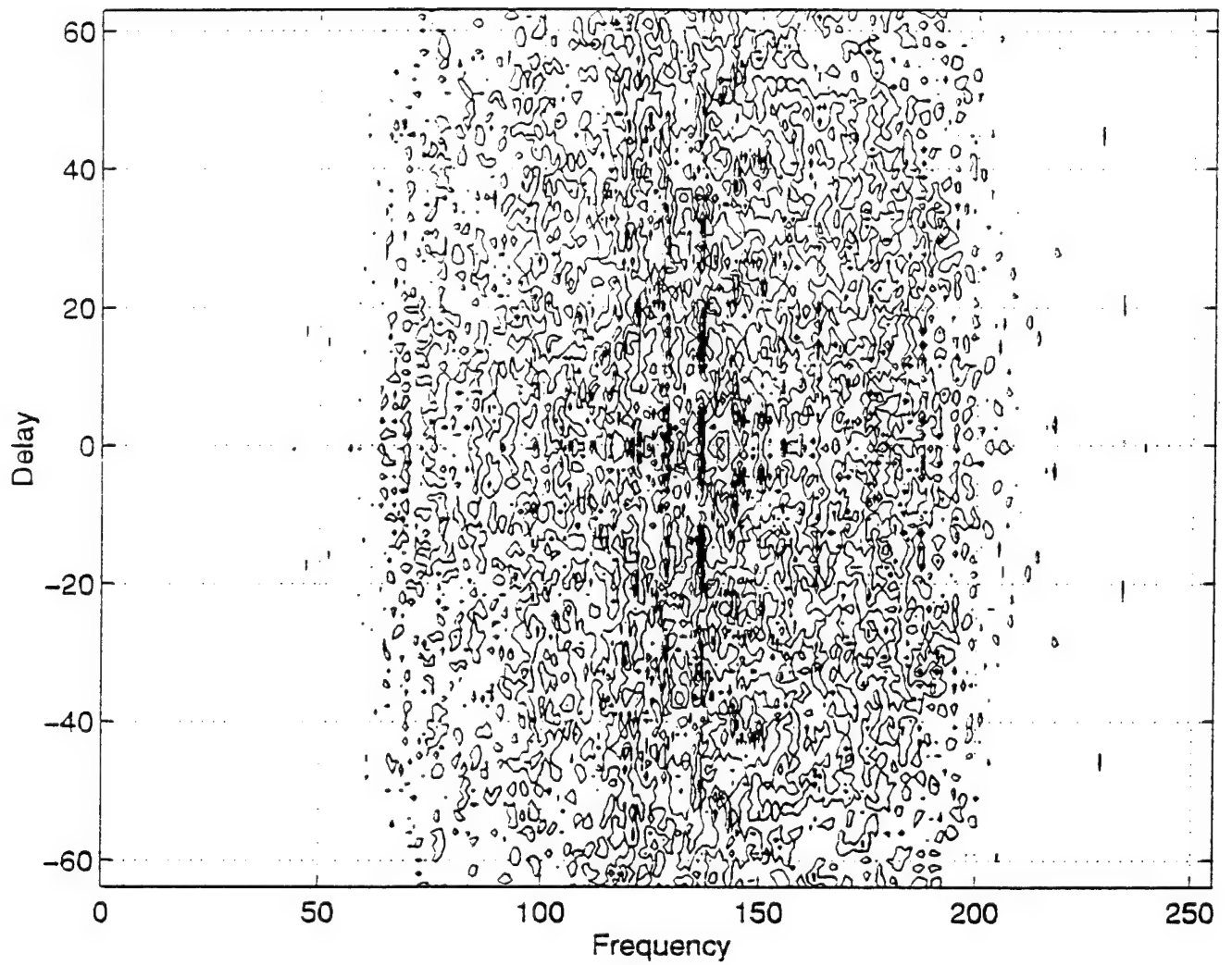
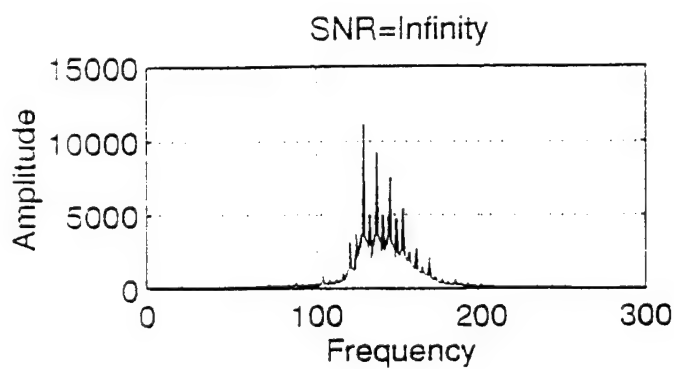
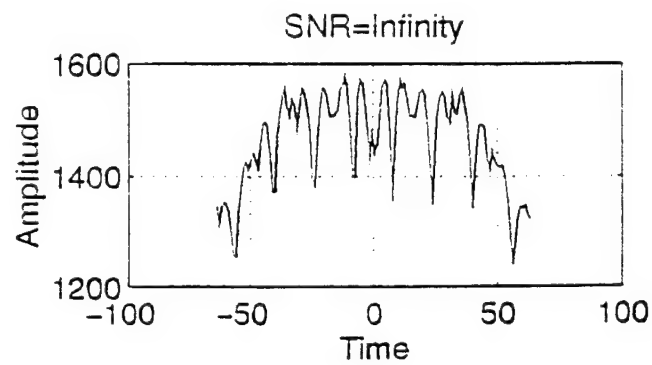


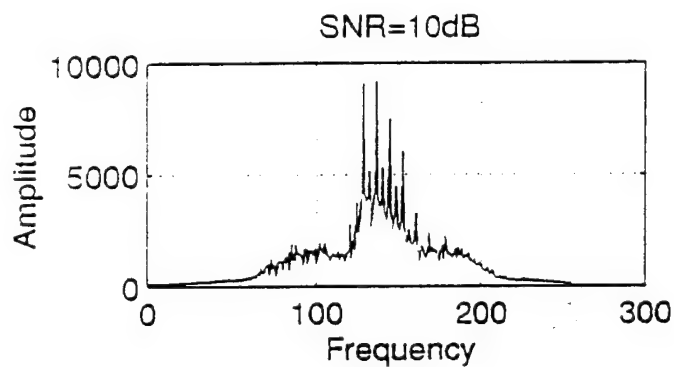
Figure 55: Output of Method-2 detector for FSK signal, 0-dB SNR.



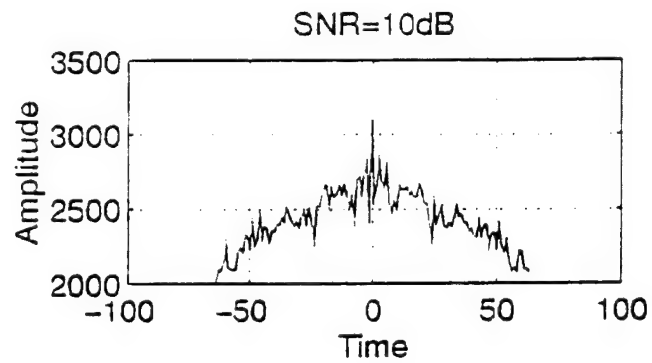
(1a)



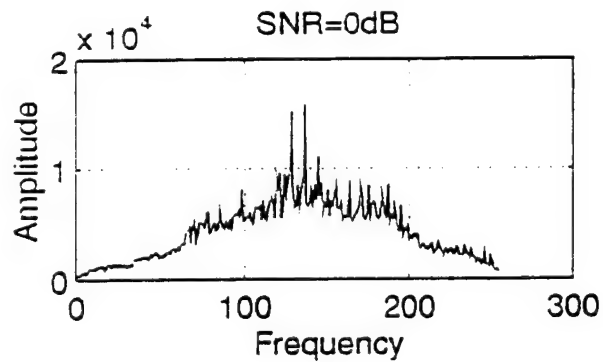
(1b)



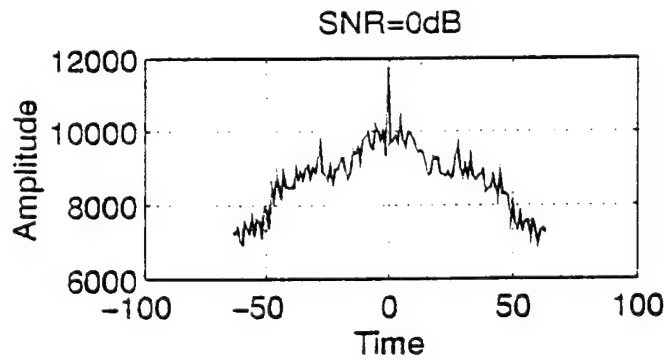
(2a)



(2b)



(3a)



(3b)

Figure 56: Averaged output of Method-2 detector for FSK signal at all SNR levels.

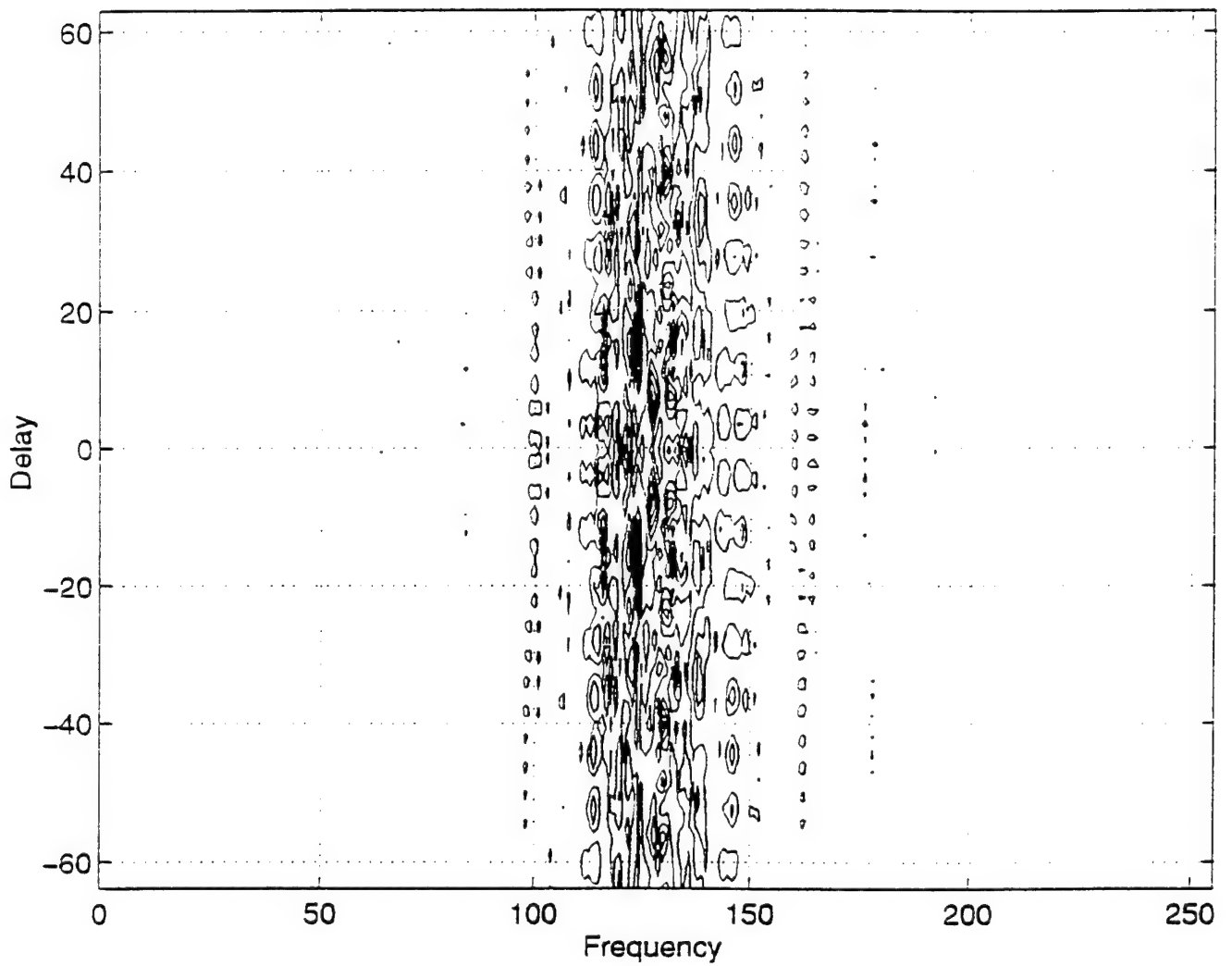
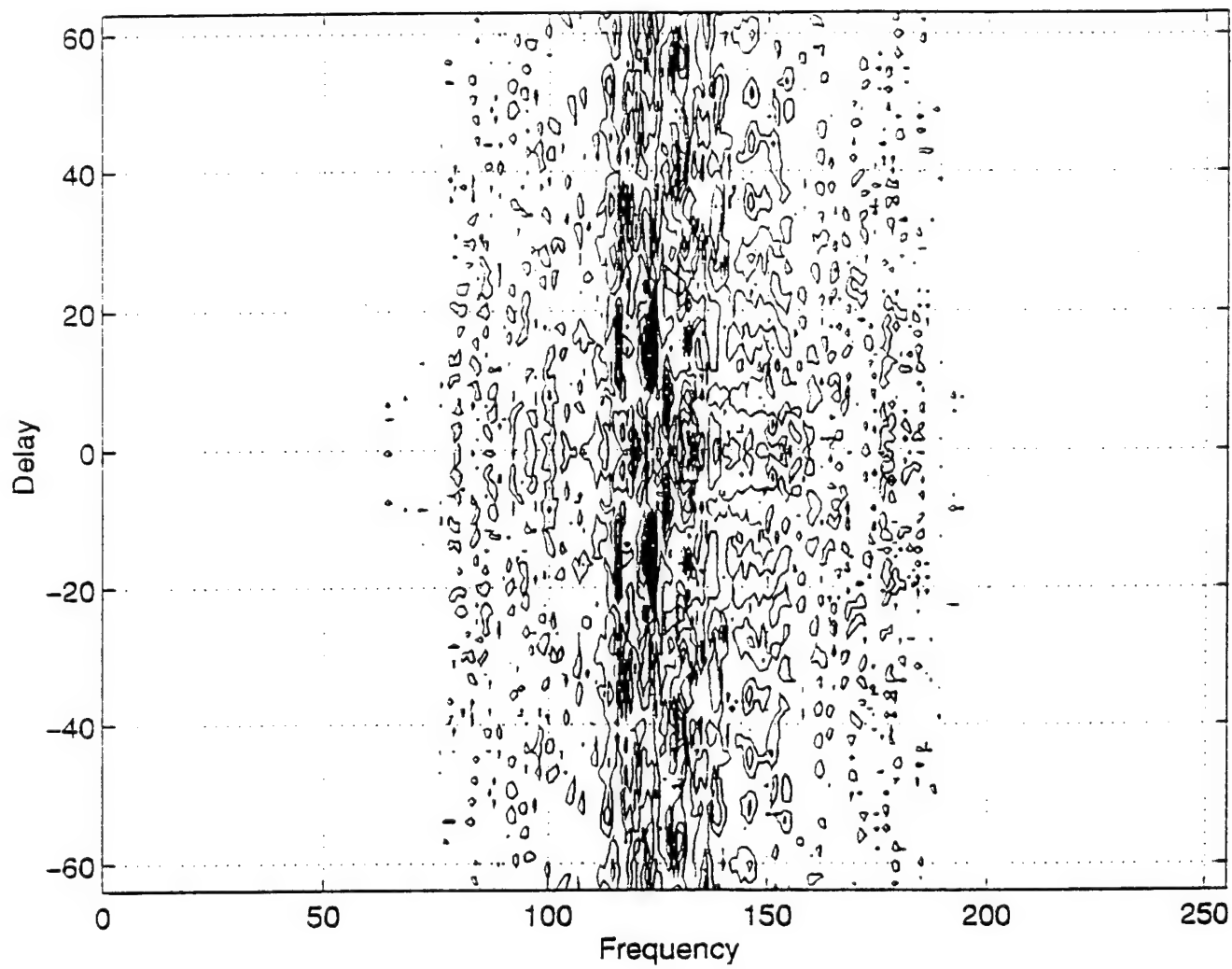


Figure 57: Output of Method-2 detector for QPSK signal, no noise.



**Figure 58:** Output of Method-2 detector for QPSK signal, 10-dB SNR.



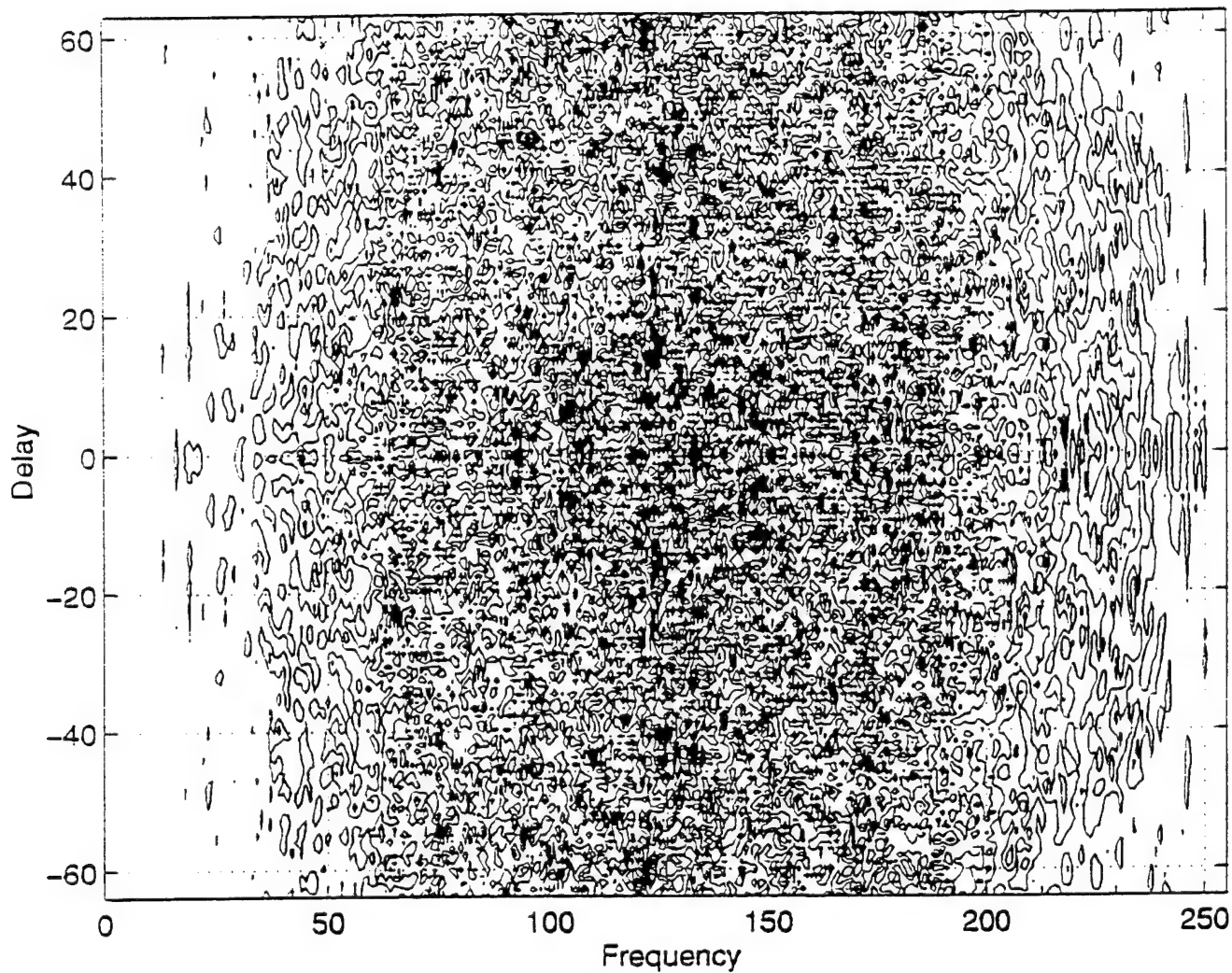
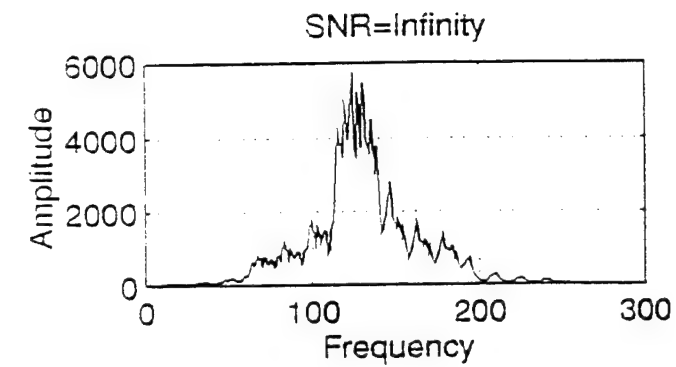


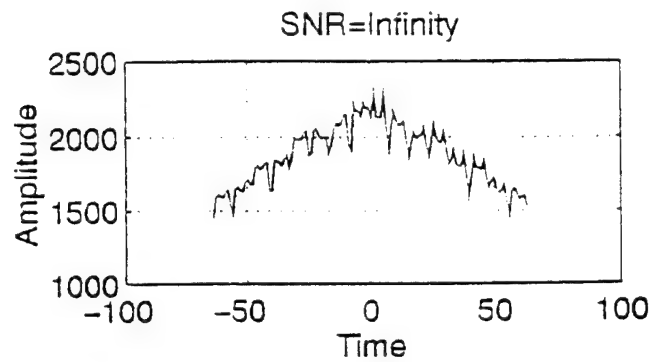
Figure 59: Output of Method-2 detector for QPSK signal, 0-dB SNR.

Figure 60 shows the output averaged over time and frequency at different levels of SNR. The time averaged output is shown in 1a, 2a, and 3a. In plot 1a (no noise condition) the center frequency and bandwidth can be estimated. The presence of spectral spikes can be recognized and may be related to cross terms. At an SNR level of 10-dB (see 2a) similar information as in 1a can be obtained. At an SNR level of 0-dB the detector output consists mainly of noise. The frequency averaged plots convey no useable information (see 1b, 2b, and 3b).

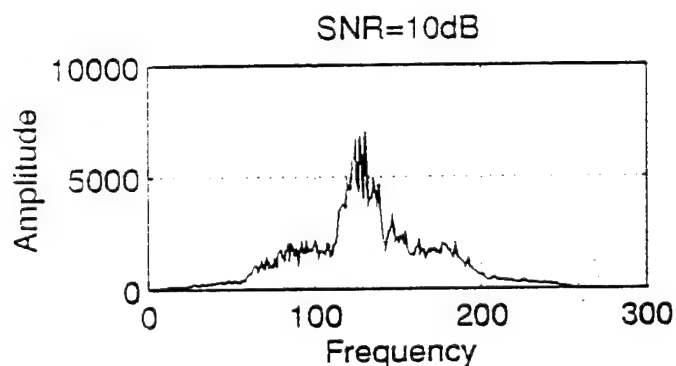
The method-2 output permits estimation of only the center frequency and the bandwidth (see plots averaged over time). Method-2, however, provides output patterns that are unique and distinct for each signal modulation at all SNRs tested. This may lead to fingerprint recognition for modulation identification and, if successfully implemented, could be automated to work in conjunction with a neural network trained to recognize (i.e., identify) typical modulation types. The SNR dependency can be improved by taking longer transforms, provided the data duration permits it.



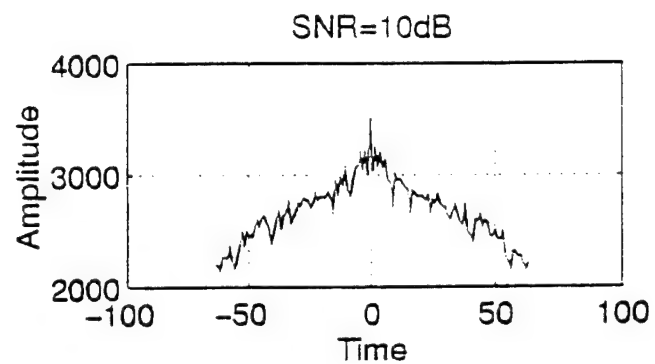
(1a)



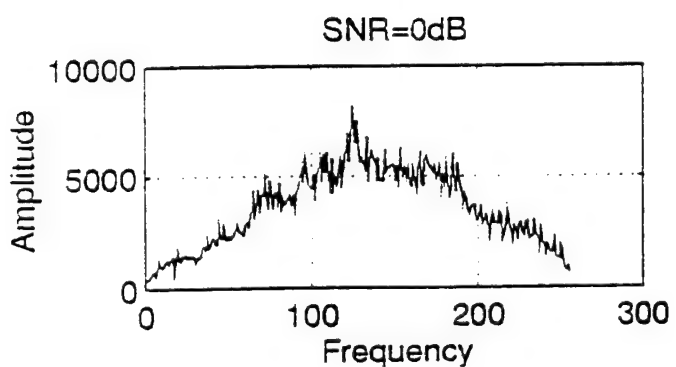
(1b)



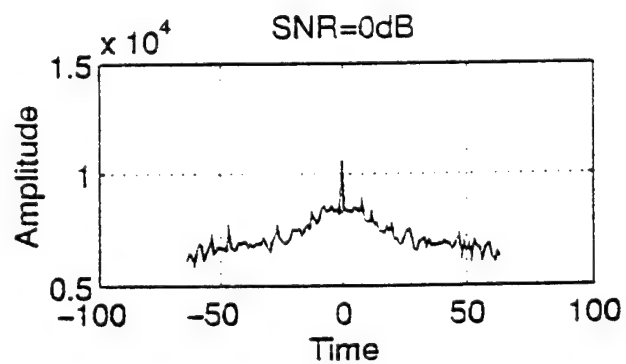
(2a)



(2b)



(3a)



(3b)

Figure 60: Averaged output of Method-2 detector for QPSK signal at all SNR levels.

## V. SUMMARY AND CONCLUSION

The signal collection capabilities of four types of receivers (interceptors) considered in this work are compared under three noise conditions: no noise, 0-dB SNR, and 10-dB SNR. Additionally, they are compared with respect to their response to signal modulation and their dependence on detector parameters (e.g., FFT size). The four receiver types are designated as broadband energy, FFT based, method-1, and method-2 detector.

The broadband energy detector can be used as a pulse-width detector for OOK at SNR levels greater or equal to 10-dB.

There is no apparent detection capability difference between the FFT based detector and the method-1 detector, even though some realizations differ slightly.

The application of method-2 can be equated with the operation of a circuit with a prefilter, delay, and multiplication as shown in Figure 61. In some sense, this arrangement is similar to the detector advocated in [3]. One of the main differences is due to the FFT taken over the product of the time series with a delayed version of itself.

Table 1 shows the confusion matrix. It shows that at free-noise conditions, all modulations can be identified by the three detectors. At a level of 10-dB SNR, method-2 seems to be more powerful than the other two detectors in identifying the modulation. The FFT fails to identify QPSK modulation at this level and method-1 fails to identify BPSK and QPSK modulation. At 0-dB SNR all detectors fail to identify the modulations. Table 2 shows which of the parameters can be extracted from the detectors as a function of SNR. The carrier frequency can be identified at all SNR levels considered. In the FSK case, only one of the carrier frequencies can be estimated and identified. The FFT based detector and method-1 allow estimation of

most parameters, provided the SNR is sufficiently large. Method-2 is more useful in estimating the type of modulation.

Recommended future research in this area:

1. More than one data realization should be tested to get statistical information.
2. The performance of the detectors should be investigated more thoroughly by using SNR levels in smaller steps between 0-dB and 20-dB.
3. All simulations are done with detectors synchronized with the signals. An area for future research is to evaluate performance of the detectors having different carrier synchronization, frequency offset, and/or phase offset.
4. All detection simulations are carried out on a signal, in addition to Gaussian noise. An area for further research is the extraction of parameters from one specific signal in the presence of an additional interfering signal.
5. The parameter extraction performance of method-2 should be investigated after filtering, that is, removal of cross terms.
6. The averaging procedure corresponds to the DC term of an FFT. The time averaged outputs should be computed by taking the Fourier transform rather than just the DC term. This approach may reveal modulation parameters as a function of time.

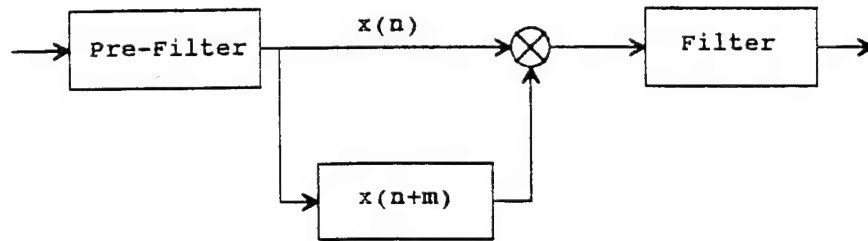


Figure 61: Method-2 block diagram.

Modulation (truth)	SNR (dB)	Modulation Identified											
		FFT Base Detector				Method-1 Detector				Method-2 Detector			
		B	O	F	Q	B	O	F	Q	B	O	F	Q
BPSK	$\infty$	1				1				1			
	10	1				*	*			1			
	0	*	*	*		*	*	*		0			
OOK	$\infty$		1				1				1		
	10		1				1				1		
	0		0				0				0		
FSK	$\infty$			1				1				1	
	10			1				1				1	
	0		*	*			*	*				0	
QPSK	$\infty$				1				1				1
	10	*	*	*	*		*		*				1
	0				0				0				0

Table 1: Confusion Matrix

Key to table:

B = BPSK modulation      1 = identified  
 O = OOK modulation      \* = multiple modulation  
 F = FSK modulation      identified  
 Q = QPSK modulation      0 = only noise

*Note :* An empty block indicates a modulation that cannot be recognized.

Detector Type	SNR (dB)	Modulation Type					
		BPSK					
		$f_c$	$B_w$	$B_R$	$f_{sh}$	$P_s$	$M_p$
FFT	$\infty$	1	1	1		1	1
	10	1	1	1		1	1
	0	1	1	0		*	*
Method-1	$\infty$	1	1	1		1	1
	10	1	1	0		0	0
	0	1	1	0		0	0
Method-2	$\infty$	1	1	0		0	0
	10	1	1	0		0	0
	0	0	0	0		0	0

Detector Type	SNR (dB)	Modulation Type						
		OOK						
		$f_c$	$B_w$	$B_R$	$f_{sh}$	$P_s$	$M_p$	$P_w$
FFT	$\infty$	1	1	1			1	1
	10	1	1	1			1	1
	0	1	1	0			0	0
Method-1	$\infty$	1	1	1			1	1
	10	1	1	1			1	1
	0	1	1	0			0	0
Method-2	$\infty$	1	1	0			0	0
	10	1	1	0			0	0
	0	0	0	0			0	0

**Table 2:** Parameters Extracted from the Modulations after Identification

Key to table:

$f_c$ = carrier frequency	1 = identified
$B_w$ = bandwidth	* = multiple modulation identified
$B_R$ = bit rate	0 = only noise
$f_{sh}$ = frequency shift	
$P_s$ = phase shift	
$M_p$ = message pattern estimation	
$P_w$ = pulse width	

**Note :** An empty block indicates that modulation parameters cannot be recognized.

Detector Type	SNR (dB)	Modulation Type					
		FSK					
		$f_c$	$B_w$	$B_R$	$f_{sh}$	$P_s$	$M_p$
FFT	$\infty$	1	1	1	1		1
	10	1	1	1	1		1
	0	1	1	0	0		*
Method-1	$\infty$	1	1	1	1		1
	10	1	1	1	1		1
	0	1	1	0	0		*
Method-2	$\infty$	1	1	1	0		0
	10	1	1	1	0		0
	0	0	0	1	0		0

Detector Type	SNR (dB)	Modulation Type					
		QPSK					
		$f_c$	$B_w$	$B_R$	$f_{sh}$	$P_s$	$M_p$
FFT	$\infty$	1	1	1		1	1
	10	1	1	1	*	0	*
	0	1	1	0		0	0
Method-1	$\infty$	1	1	1		1	1
	10	1	1	*		0	*
	0	1	1	0		0	0
Method-2	$\infty$	1	1	0		0	0
	10	1	1	0		0	0
	0	0	0	0		0	0

Table 2: Continued





## APPENDIX

### BPSK Signal Generation Function (bpsk.m)

```
% Up date 9.2.94
% LCDR ANWAR AL-JOWDER.

% This function generates an bpsk signal from a uniformly-distributed
% random sequence{-1,1}.
%
clc
clear
N=input('ENTER THE NUMBER OF SAMPLES...=');
fs = input('ENTER THE SAMPLING FREQUENCY..=');

x=rand(1,N);

for i=1:N;
    if x(i)>.5
        x(i)=1;
    else
        x(i)=-1;
    end
end
end
    y=boxcar(N);
    a1=(y*x);
    a1=reshape(a1,1,((N).^2));
    s=a1.*sin((2*pi*fs/N).*(1:((N).^2)));

save bpsk s
```

## OOK Signal Generation Function (ook.m)

```
% Up date 9.2.94
% LCDR ANWAR AL-JOWDER.

% This function generates an bpsk signal from a uniformly-distributed
% random sequence{-1,1}.
%
clc
clear
N=input('ENTER THE NUMBER OF SAMPLES...=');
fs = input('ENTER THE SAMPLING FREQUENCY..=');

x=rand(1,N);

for i=1:N;
    if x(i)>.5
        x(i)=1;
    else
        x(i)=0;
    end
end
y=boxcar(N);
a1=y*x;
a1=reshape(a1,1,((N).^2));
s=a1.*sin((2*pi*fs/N).*(1:((N).^2)));

save ook s a1
```

### FSK Signal Generation Function (fsk.m)

```
% Up date 9.2.94
% LCDR ANWAR AL-JOWDER.

% This function generates an bpsk signal from a uniformly-distributed
% random sequence{-1,1}.
%

clear
N=input('ENTER THE NUMBER OF SAMPLES...=');
fs = input('ENTER THE SAMPLING FREQUENCY..=');
x=randn(1,N);
a=ones(1:N);
for i=1:N;
    if x(i)>.5
        x(i)=1;
    else
        x(i)=0;
    end
end
y=boxcar(N);
l=N^2;
a1=y*x;
a2=reshape(a1,1,l);
f=a2+fs;
%for i=1:length(a1);
    s=sin(2*pi*(f./length(a)).*(1:l));

% end

save fsk s
```

### QPSK Signal Generation Function (QPSK.m)

```
% Up date 9.2.94
% LCDR ANWAR AL-JOWDER.
% This function generates a QPSK signal waveform. Uniformly-distributed
% random sequence{-1,1}. The difference between the four levels set to
% values equal to {.25, .5, .75, 1.0}.
clear
N=input('ENTER THE NUMBER OF SAMPLES...=');
fs = input('ENTER THE SAMPLING FREQUENCY..=');
%
b=N;
x=rand(1,b);
for i=1:b;
if x(i)<.25
    x(i)=2*pi;
%
end
end
for i=1:b;
if x(i)<.5
    x(i)=pi/2;
%
end
end
for i=1:b;
if x(i)<.75
    x(i)=pi;
%
end
end
for i=1:b;
if x(i)<=1.0
    x(i)=3*pi/2;
%
end
end
y=boxcar(b);
a2=y*x;
a1=reshape(a2,1,(b).^2));
s1=sin((2*pi*fs/N).*(0:length(a1)-1));
s=sin(((2*pi*fs/N).*(0:length(a1)-1))+a1);
save qpsk s a1
```

## Broadband Energy Detector (Energy.m)

```
% Up date 10.2.94
% LCDR ANWAR AL-JOWDER
%
% This program calculates the signal energy, within a sliding window, starting
% from any sample point I within finite length of 256 samples.
%
%
%
% List of variables/parameters for the energy program
%   U= Numbers of the window samples points to be selected by the user.
%   P= Size of the window (in sample periods).
%   I= Starting Window(in sample periods relative to beginning of record).
% YEN = Null matrix.
%
%
load ook
load noise10
sn=s+W;
% Set the input maximum SNR in dB.

YEN=[];

U=input('ENTER THE SIZE OF N..[8,16,32,64..],U= ');
    F=zeros(256,U);
    for P=1:U;
        for I=1:256-P+1;
            F(I,P)=0;
            for i=I:I+P-1;
                F(I,P)= F(I,P)+sn(i)^2;
            end
        end
    end
    YEN=[YEN;F];
end
save energy YEN
```

## FFT Method Detector (shift2.m)

```
% Up date 10.12.94
% LCDR ANWAR AL-JOWDER

% This program will input any signal generation function and will display
% the FFT detector output for purposes of evaluations.
%
%
% List of variables/parameters for the shift2 program
% G= Null matrix
% V= Size of the window shift
%
clear
%clg
load bpsk

%load noise
%sn=s+W;
% The parameter V is the size of the FFT window selected by the user
% and it should be a power of 2 with a maximum length of 256.

V=input('select the shift point[16,32,128,256],V= ');
y=[s zeros (1:V)];
G=[];
S=input('Do you need overlap..?Y/N [Y]:','s');
if S=='Y';
    OL=input('Enter the Value in % ,OL=');
    shift=((100-OL)/100)*(256/V);
else
    shift=(256/V);
end;
for i=1:shift:256-V+1
    G=[G;(fft(y(i:V+i-1))).^2];
end;

save shift G
```

## Correlation Method 1 Detector (Corr1.m)

```
% Up date 10.2.94.
% LCDR ANWAR ALJOWDR.
%
% This program input any signal generation function
% and will display the spectral correlation
% detector output, based on delay time n, for purposes evaluation.
%

% List the variables/parameters for the corr1 program.

% Ycor1 = Null matrix used for storing the data signal.
% sn     = The corrupted signal with noise.
% s      = The signal without noise.
% S2     = The correlated signal using method two (delay - m).
% av     = Simple main.
clear

load fsk
%load noise10
%sn=s+W;
Ycor1=[];

    S2=zeros(16);
    for i=1:4:225;
        av=(s(i)+s(i+15))/16;
        S2=(abs(av*fft(s(i:i+15)))).^2;

        Ycor1=[Ycor1;S2];

    end

save corr1 Ycor1
```



## Correlation Method 2 Detector (corr2.m)

```
% Up date 10.2.94
% LCDR ANWAR AL-JOWDER
%
% This program will input any of signal generation function
% and will display the spectral correlation detector output
% for purposes of evaluation.
% This equation related to Wigner-Ville Distribution.
%
% List the variables/parameters for the Corri program.
% Ycor2 = Null matrix used for storing the signal data.
% sig   = Input signal to-noise power ratio in dB.
% xp1   = Received signal (with dely)plus noise.
% xp2   = Received signal (without delay) plus noise.
% xp3   = The correlation function between the signal and the delyed
%         signal.

clear
load qpsk

load noise0
sn=s+W;
s1=hilbert(sn);

Ycor2=[];

nn=max(size(s1));

S1=[];

for m=1-(255/2):2:(255/2)-1;
    if m<0;
        xp1=[s1(1,1-m:nn) zeros(1,-m)];
    else
        xp1=[zeros(1,m) s1(1,1:nn-m)];
    end
    xp2=s1;
    xp3=xp2.*xp1;

    S1=fft(xp3);
    Ycor2=[Ycor2;S1];
```

```
end
    save corr2 Ycor2
x=linspace(-64,63,127);
y=linspace(0,255,256);
```



## LIST OF REFERENCES

1. Notes for EC 4590 (Digital Satellite Communication), and EC 2410 (Fourier Transformation), Naval Postgraduate School, 1992 (unpublished).
2. Johnson, V. K., "Detection of Spread Spectrum Signals in the Presence of Noise and Narrowband Interface," Master's Thesis, Naval Postgraduate School, Monterey, CA, Sep. 1986.
3. Kuehls, J. F., and Evaggelos, G., "Presence Detection of Binary-Phase-Shift-Keyed and Direct-Sequence Spread Signals Using a Prefilter Delay and Multiply Device," *IEEE J. on Selected Areas in Communication*, Vol. 8, No. 5, June 1990.
4. Ziemer, R. E. and Peterson, R. L., *Introduction to Digital Communications*, Macmillan, New York, 1992.
5. Roden, M. S., *Digital Communication System Design*, Prentice Hall, New York, 1988.
6. Spooner, S. G., "An Energy Analysis of the Pseudo Wigner-Ville Distribution in Support of Machinery Monitoring and Diagnostics," Master's Thesis, Naval Postgraduate School, Monterey, CA, June 1992.
7. Torrieri, D. J., *Principles of Secure Communications Systems*, 2nd ed., Artech House, New York, 1992.
8. Proakis, J. G., *Digital Communications*, McGraw-Hill, New York, 1983.
9. Couch, L. W., II, *Digital and Communication Systems*, 4th ed., Macmillan, New York, 1993.
10. Cohen, L., "Time-Frequency Distributions — A Review," *Proc. of the IEEE*, Vol. 77, No. 7, July 1989.



## INITIAL DISTRIBUTION LIST

		No. Copies
1.	Defense Information Center Cameron Station Alexandria, VA 22304-6145	2
2.	Library Code 52 Naval Postgraduate School Monterey, CA 93943-5101	2
3.	Chairman, Code EC/Mw Department of Electrical and Computer Engineering Naval Postgraduate School Monterey, CA 93943-5121	1
4.	Professor Ralph Hippenstiel, Code EC/Hi Department of Electrical and Computer Engineering Naval Postgraduate School Monterey, CA 93943-5121	2
5.	Professor Donald Wadsworth, Code EC/Wd Department of Electrical and Computer Engineering Naval Postgraduate School Monterey, CA 93943-5121	2
6.	Professor H. H. Loomis, Jr., Code EC/Lm Department of Electrical and Computer Engineering Naval Postgraduate School Monterey, CA 93943-5121	1
7.	LTCOL Yusuf Mallalah Commander, Bahrain Amiry Navy BDF, P.O. Box 245 Naval Base State of Bahrain	2
8.	LTCOL Abdullatif Al-Zayani BDF, P.O. Box 245 HQ, Organization & Planning Department State of Bahrain	1

	No. Copies
9. LCDR Anwar Al-Jowder BDF, P.O. Box 245 Naval Base, Electrical Flotila Office State of Bahrain	2